THE UNIVERSITY OF MICHIGAN

INDUSTRY PROGRAM OF THE COLLEGE OF ENGINEERING

THE EFFECT OF COMPRESSION RATIO ON THE ABILITY TO BURN LEAN FUEL-AIR MIXTURES IN A SPARK-IGNITION ENGINE

David H. Holkeboer

A dissertation submitted in partial fulfillment
of the requirements for the degree of
Doctor of Philosophy in The
University of Michigan
1960

March, 1961

IP-500

Doctoral Committee:

Professor Jay A. Bolt, Chairman
Professor John A. Clark
Doctor Craig Marks
Professor William Mirsky
Professor Donald E. Rogers
Professor J. Louis York

PREFACE

In this study, the term lean mixtures refers to fuel-air mixtures containing air in excess of that required to form a stoichiometric mixture. Two aspects of engine operation with lean mixtures were studied: 1) the effect of engine variables on the lean limit or minimum fuel-air ratio for steady firing, and 2) the performance of the engine operating with lean mixtures.

An analytical study of the factors determining the lean limit was made. On the basis of published data on lean limits it was concluded that in a mixture of fuel and air, the minimum fraction of fuel necessary for flame propagation was a linear function of the temperature of the reactants and independent of the pressure.

Measurements of the lean limit were made in a single-cylinder CFR Engine operating at compression ratios of 7, 10, 13, and 16 with propane gas as the fuel. The intake pressure was varied from seven psia. to 19.4 psia., and the intake temperature from 100°F to 300°F. It was found that for steady firing to occur, the minimum fraction of fuel required in the charge in the engine cylinder was a linear function of the compression temperature and was independent of the compression pressure of the engine. The lean limit predicted in the analytical study was about 35 percent leaner than the minimum fuel-air ratio for steady firing.

The performance of the engine operating with propane-air mixtures ranging from stoichiometric to the lean limit was also investigated. The engine was operated at part throttle at compression ratios of 5.5, 7, 10, 13, and 14.9 and at a speed of 1200 rpm. with m.b.t.

ignition timing. It was found that the ignition had to be advanced as the mixture was made leaner. The thermal efficiency of the engine increased gradually as the mixture was made leaner over most of the fuel-air ratio range. The maximum thermal efficiency was about five percent greater than the efficiency obtainable with a stoichiometric mixture. The fuel-air ratio at which maximum efficiency was reached varied from 80 percent theoretical fuel at a compression ratio of 5.5 to 70 percent theoretical fuel at a compression ratio of 14.9.

Pressure-time diagrams were obtained for use in studying the combustion characteristics of lean mixtures in the engine. Two phases of the combustion process were distinguished: a delay period and a pressure rise period. The delay period, an interval of one to seven milliseconds duration between the occurrence of the spark and the first noticeable pressure rise, was found to increase as the mixture was made leaner and as the compression ratio was decreased. The duration of the pressure rise period was five to seven milliseconds, increasing as the mixture was made leaner, but nearly independent of the compression ratio

Conclusions to be drawn from this investigation are:

1. The minimum fraction of fuel in the charge is a linear function of the compression temperature but is independent of the compression pressure.
2. The maximum thermal efficiency obtained with the engine and fuel used in this study was realized when the mixture contained 70 to 80 percent theoretical fuel, depending on the compression ratio. The maximum thermal efficiency was about five percent greater than the thermal efficiency obtained with a stoichiometric mixture.

3. The pressure rise resulting from combustion of a lean fuel-air mixture is preceded by a delay period varying from one to seven milliseconds, depending on compression ratio and fuel-air ratio. The increase of the delay period makes it necessary to advance the ignition timing substantially as the mixture is made leaner.

The author wishes to express his appreciation to all members of the Doctoral Committee for their counsel and guidance. Particular thanks is due to Professor Jay Bolt and Professor William Mirsky for their assistance and advice rendered throughout this investigation.

Acknowledgement is also made of the financial assistance given by the Shell Oil Company and by Texaco, Incorporated in the form of Fellowships to the author. Thanks is also due to the Zenith Carburetor Division, Bendix Aviation Corporation for equipment for handling propane fuel. The assistance of the Mechanical Engineering Department of the University in providing material and equipment for this investigation is gratefully acknowledged.

Thanks is also due to my wife, Marilyn, for preparation of the original manuscript and to the Industry Program of the College of Engineering for the reproduction of this dissertation.

TABLE OF CONTENTS

TABLE OF CONTENTS (cont'd)

TABLE OF CONTENTS (cont'd)

LIST OF TABLES

LIST OF ILLUSTRATIONS

LIST OF ILLUSTRATIONS (cont'd)

LIST OF ILLUSTRATIONS (cont'd)

NOMENCLATURE

Symbols

C_P	local specific heat at constant pressure
e	base of natural logarithms
f	function of
f	weight fraction of residual exhaust gas in the charge
F	weight fraction of fuel in the charge
F_L	weight fraction of fuel in the charge at the lean limit
FA	fuel-air ratio, by weight
FA_S	fuel-air ratio, by weight, in a stoichiometric mixture
$\overline{g}$	molar free energy (Gibbs' function)
$\overline{g}^o$	molar free energy of formation at 25°C and 1 atm.
h	pressure drop across fuel orifice, inches of water
h	enthalpy per unit mass
h_{RP}	enthalpy of combustion per unit mass of fuel
$\mathcal{H}$	Enthalpy Parameter, $\frac{-Fh_{RP}}{C_P T_T}$ (see page 10)
k	ratio of specific heats
K_N	nozzle constant (see page 31)
K_O	orifice constant (see page 36)
L	length of piston stroke, inches
m	mass, pounds
$\dot{m}$	mass rate of flow, pounds per hour
m_r	mass of residual exhaust gas
M	molecular weight
MR	reading on cylinder head micrometer, inches
n	number of moles

Symbols

n	polytropic exponent
p	partial pressure
P	pressure
r_P	pressure ratio, P_e/P_i
r_V	compression ratio
r_T	temperature ratio, T_e/T_i
$\overline{R}$	universal gas constant
T	absolute temperature
T_c	absolute temperature of the charge in the engine cylinder before compression
T_r	absolute temperature of the residual exhaust gas after expansion to intake pressure
T_T	threshold temperature
s	entropy per unit mass
V	volume
V_r	volume of residual gas at T_r, P_i
$\overline{V}$	velocity
$\overline{V}_s$	flame speed, relative to unburned gas
$\mathscr{V}$	velocity parameter (see page 10)
x	mole fraction
x	distance normal to flame front, measured from point where $T = T_T$
x_b	effective thickness of burning zone
y	parameter (see page 125)
α	thermal diffusivity

NOMENCLATURE (cont'd)

Symbol

Λ	fraction of chemical reaction completed
ϕ	fraction of theoretical fuel, $F \div \frac{FA_S}{FA_S+1}$
λ	thermal conductivity
Θ	crankshaft angle, degrees; negative sign - B.T.C., positive sign - A.T.C.
Θ_1	crank angle at point of four percent pressure rise
Θ_2	crank angle at point of 96 percent pressure rise
Θ_D	duration of delay period, degrees of crank rotation
Θ_R	duration of pressure rise period, degrees of crank rotation
ρ	mass density
τ	time
η_H	thermal efficiency based on enthalpy of combustion
η_G	thermal efficiency based on free energy of combustion

Subscripts

a	air
c	charge
e	exhaust
f	fuel
i	intake
I	ignition
n	nth component of mixture
P	products of combustion
R	reactants

Abbreviations

A.T.C.	after top center
atm.	atmosphere
BHP.	brake horsepower
B.T.C.	before top center
BTU.	British thermal unit
CFR	Cooperative Fuel Research (engine)
CR	compression ratio
FHP.	friction (motoring) horsepower
IGN.	ignition
IHP.	indicated horsepower
kcal.	kilocalorie
ln	natural logarithm, base e
log	common logarithm, base 10
psi.	pressure, pounds per square inch
psia.	absolute pressure, pounds per square inch
rpm.	revolutions per minute

INTRODUCTION

The spark-ignition engine has been under constant and intensive development for nearly 60 years. Today there remains wide interest in modification of the design of spark-ignition engines to improve their performance. Increasing the compression ratio is one effective way to increase the power and efficiency of engines[3,11,18] provided suitable fuel is available. Since the maximum compression ratio of current commercial gasoline engines is approximately ten, information concerning the operating characteristics of spark-ignition engines with compression ratios greater than ten should be of immediate interest.

In this study the use of lean fuel-air mixtures in high compression ratio engines was investigated. The term "lean" is applied to fuel-air mixtures containing air in excess of that theoretically required. The term "lean limit" is used to refer to the fuel-air ratio of the leanest mixture which would fire steadily in the engine. In reference to work of other investigators in combustion bombs or tubes, "lean limit" means the leanest mixture through which flame propagation is possible. Two aspects of the use of lean mixtures in an engine have been studied:

(1) the effect of changes in the compression ratio on the minimum fuel-air ratio for steady firing, and

(2) engine efficiency and performance with lean mixtures.

A rational explanation for the effect of compression ratio on the minimum fuel-air ratio or lean limit was sought in the known effects of the compression ratio on the state of the charge in the engine cylinder at the time of ignition. The effects of the compression ratio and inlet conditions on the state of the charge have been determined quantitatively by several investigators.[14,17,23,24,96,98,99] In addition,

raising the compression ratio results in increasing the surface-volume ratio of the combustion chamber, thereby changing the flame quenching and heat transfer properties of the chamber. Changing the compression ratio may also have some effect on the amount of turbulence of the mixture. Finally, the amount of residual exhaust gas remaining in the cylinder is reduced as the compression ratio is raised[17,23]. The residual exhaust gas has at least two effects on the charge: namely, the charge is diluted and the temperature of the charge is raised.

An analysis of the effect of temperature, pressure, and dilution on the lean limit is discussed in Chapter I. This analysis is based on a thermal theory of flame propagation; it is postulated that flame propagation is possible only if the adiabatic flame temperature of the mixture exceeds a threshold temperature of about 3100°R. On the basis of this postulate, the minimum percentage of fuel in the charge is shown to be a function of the temperature of the mixture but not a function of the pressure of the mixture. Published data of other investigators supporting these conclusions are presented.

The lean limit for steady firing of propane-air mixtures was measured in a CFR engine. A variety of tests, discussed in Chapter III, were designed and carried out to show the separate effects of the ignition system, the charge pressure, the charge temperature, and finally, other important factors arising from increasing the compression ratio. In analyzing the results of these tests the residual exhaust gas was treated as an inert diluent having the measured exhaust temperature before dilution with the fresh fuel-air mixture. The amount of residual exhaust gas was not measured, but calculated on the basis of an idealized

mixing process. The results of the tests are compared with the lean limit equation developed in Chapter I.

In general, lean mixtures may be expected to have unfavorable combustion characteristics in that the flame speed is lessened as the mixture is made leaner[58,59,70]. However, it is also true that the temperature of the charge after combustion is lower when a lean mixture is used and the heat loss to the combustion chamber walls is therefore reduced. In addition, the deleterious effects of dissociation and variable specific heats are reduced by the lower temperature of the combustion products. Several investigators[4,6,7,12,24] have attempted to calculate the thermal efficiency of an engine on the basis of an Otto cycle carried out with real gases. David and Leah[4] made allowance for heat transfer in calculating thermal efficiency. In all cases, the thermal efficiency was shown to increase as the mixture was made leaner. However, it was assumed that combustion took place at constant volume in all cases, an assumption that was found to be invalid when lean mixtures are considered, particularly at high compression ratios. Consequently, it is not immediately evident from the above studies whether the thermal efficiency of the engine will increase or decrease when the mixture is made leaner.

It would therefore be desirable to make an analytical study which would include the effects of actual combustion rates on the efficiency of internal combustion engines. The necessary data for making such a study are not available at the present time, however. First, it has been shown that combustion in an engine is promoted considerably by turbulence of the charge, but little information as to the turbulence

in a high-compression CFR engine is available. It is not known if the residual exhaust gas from the previous cycle is homogeneously distributed in the charge at the time of ignition. In addition, data on combustion rates at engine pressures and temperatures are lacking and variations in combustion rate from cycle to cycle have not been explained. This lack of information essentially precludes a more detailed analytical study of the effect of lean mixtures on engine performance.

Engine tests with lean mixtures, reported by Hopkinson[7] in 1908 and by Ricardo[20] in 1923, have shown that by making the mixture leaner than the stoichiometric ratio, a small increase in thermal efficiency can be obtained. Burstall[1,2] has reported that further tests with the Ricardo E-35 engine operating at several compression ratios from four to eight with a variety of fuels showed that the maximum efficiency was reached at a fuel-air ratio appreciably leaner than stoichiometric and was about seven percent higher than the efficiency obtained with a stoichiometric mixture. Additional data by Paul and Humphreys[18], obtained with a CFR engine at compression ratios of six to twelve, also showed that the maximum thermal efficiency was attained with a lean mixture and that the optimum fuel-air ratio became leaner as the compression ratio of the engine was increased.

In Chapter IV, experimental data are given concerning the effect of fuel-air ratio on engine performance factors, such as power output, ignition timing, exhaust temperatures, and efficiency. These data cover compression ratios from 5.5 to 14.9 with the engine operating at part throttle at a speed of 1200 rpm., using a commercial propane fuel.

In Chapter V, a discussion of some combustion characteristics of lean mixtures is given. Pressure-volume diagrams obtained from the engine are used as a basis for this discussion.

CHAPTER I

THEORY OF THE LEAN LIMIT

A. Basis for Lean Limit Equation

It has been observed that many fuels possess a lean limit, that is, a minimum fraction of fuel in a fuel-oxidizer mixture for which self-sustaining flame propagation is possible. One of the earliest measurements of the lean limit of a hydrocarbon burning in air was made by Davy[35] in 1816. At this time Davy advanced the theory that flame propagation is possible only in those mixtures having a heating value sufficient to produce a flame temperature at least equal to the "ignition temperature". This theory was supported by the observation that addition of inert diluents or cold metal plates narrowed the range of fuel-oxygen ratios that formed combustible mixtures. Subsequently, LeChatelier and Boudouard[40,41] observed that in the case of light hydrocarbons burning in air, the heating values of all lean limit mixtures were approximately the same. They also observed that this lean-limit heating value decreased as the initial temperature was raised. Burgess and Wheeler[31] observed a similar constancy of mixture heating value in 1911, and made an attempt to calculate the lean limit on the basis of a measured ignition temperature. The calculated lean limit was found to be far leaner than that actually observed, however.

In 1948, Egerton and Powling[38] pointed out that the adiabatic flame temperature for a given hydrocarbon was very nearly constant at the lean limit, regardless of dilution with inert diluents or elevation of initial mixture temperature. This conclusion is compatible, or course, with the previously observed constancy of heating value of lean limit

mixtures. In the case of methane, the adiabatic flame temperature at the lean limit was found to be 2700-2800°R when the flame propagated upward.

On the basis of the work of the above investigators it appears that the important factor determining the lean limit is a temperature threshold which must be reached in the flame zone. For the oxidation of methane and similar light paraffins, this threshold seems to be located at about 3000°R as will be shown later.

B. Development of Lean Limit Equation

In order to evaluate the effect of changes in the physical properties of the mixture of reactants on flame propagation, recourse was taken to the thermal theory of deflagrations developed originally by Mallard and Le Chatelier[59,63,66]. Briefly stated, this theory postulates that a threshold temperature, at which combustion begins, exists for any combustible mixture and that the mechanism of flame propagation involves heating the mixture just ahead of the flame, by thermal conduction, from its original temperature to the threshold temperature, after which the material so heated burns and heats more of the mixture. This theory permits a calculation of the laminar flame speed if the physical properties of the mixture, such as specific heat, calorific value, thermal conductivity, and density are known. Considering that the physical properties of the mixture of reactants must be such that the flame speed is greater than zero, the flame speed equation can be used to determine the flame propagation limits.

In the discussion which follows, the development of the flame speed equation will be outlined briefly and this equation will be applied to the problem of determining the lean limit.

1. The Flame Model

It is convenient, for purposes of analysis, to consider a stationary flame burning in a flowing stream of gas, in the manner of a Bunsen burner flame. Unlike the Bunsen burner flame, however, the flame considered here is flat and perpendicular to the gas stream, and the cross-sectional area of the gas stream is constant (see Figure 1.1). A mixture of reactants is supplied from the left at an initial velocity corresponding to the normal flame propagation velocity, the products flow away to the right. There is no heat transfer between the gas stream and the surroundings.

The flame consists of two important zones: the preheat zone and the burning zone. The conversion of chemical energy to sensible form by combustion is confined to the burning zone. In the preheat zone, just ahead of the burning zone, the mixture is heated by thermal conduction only. The boundary between the zones, called the flame front, is taken as the reference point for measuring distances.

The temperature at the flame front is called the "threshold temperature" or "ignition temperature". In general, thermal theories of flame propagation are predicated on the existence of a definite "threshold temperature" which is assumed to be a constant for combustion of a given fuel. Flame propagation is, theroetically, dependent on the ability of the flame to preheat the reactants to the "threshold temperature".

It is also assumed that the gases involved in the combustion process are ideal and have constant specific heats and constant thermal conductivities. Pressure variations are neglected.

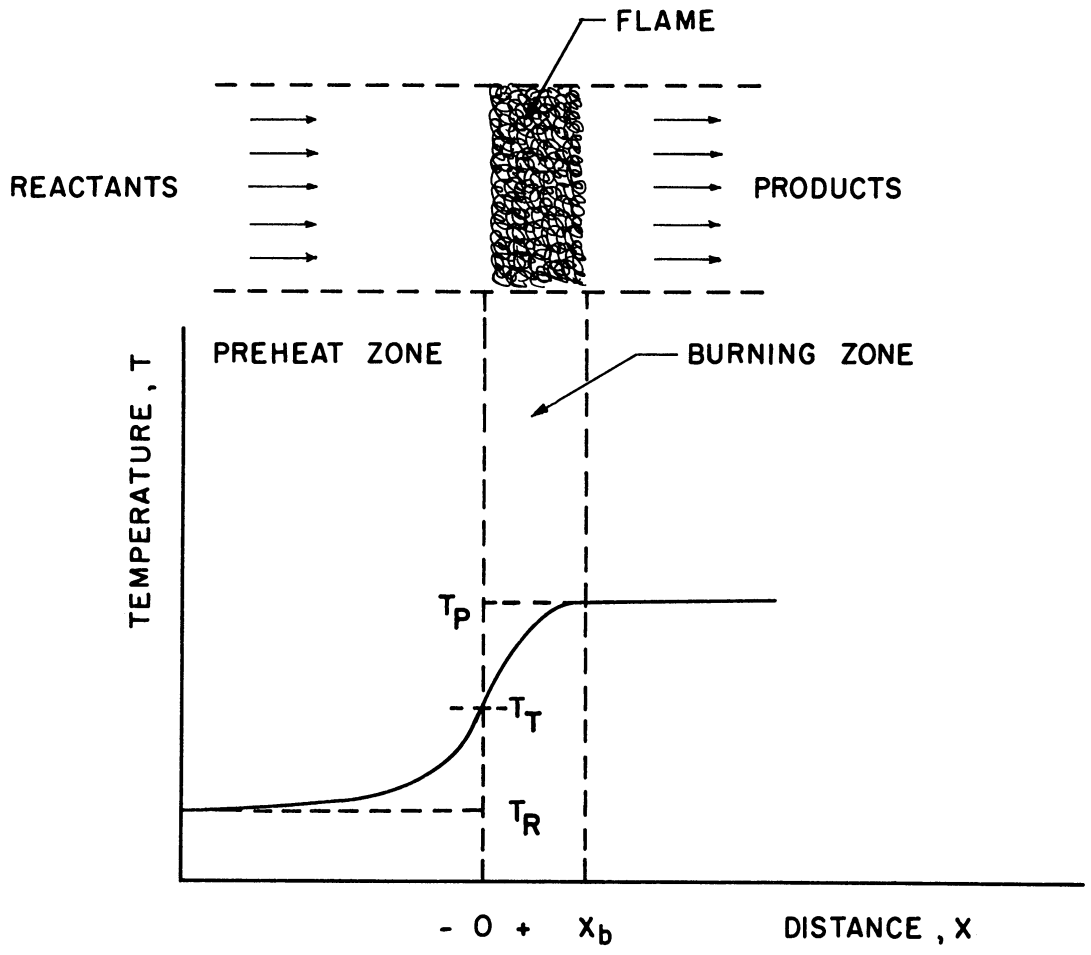

Figure 1.1 Flame Model. Including Schematic Diagram of Temperature Profile.

2. Development and Solution of Flame Propagation Equations

a. General Equations

Under the assumptions outlined above, continuity of mass can be expressed as:

$$\rho \bar{V} = \rho_R \bar{V}_S \tag{1.1}$$

Furthermore, conservation of energy occurs in each element of the mixture passing through the flame front, so that

$$\frac{d}{dx}\left(\lambda \frac{dT}{dx}\right) + \rho \bar{V} F(-h_{RP}) \frac{d\Lambda}{dx} = \rho \bar{V} C_P \frac{dT}{dx} \tag{1.2}$$

[Net rate of energy gain by conduction of heat] + [Rate of sensible energy increase due to chemical reaction] = [Rate of increase in enthalpy of element]

By combining Equations (1.1) and (1.2), and taking λ and C_P to be constant, the following general equation, to be applied with proper boundary conditions, is obtained:

$$\frac{d^2T}{dx^2} - \frac{\bar{V}_S}{\alpha}\frac{dT}{dx} - \frac{\bar{V}_S}{\alpha}\left(\frac{F h_{RP}}{C_P}\right)\frac{d\Lambda}{dx} = 0 \tag{1.3}$$

A solution to this equation will relate the flame speed to the properties of the fuel-air mixture, and can be used to determine the range of conditions under which the flame speed will be positive and flame propagation therefore possible. Such a solution can conveniently be expressed in terms of two parameters, the velocity parameter $\mathcal{V}$ and the enthalpy parameter $\mathcal{H}$, which are given as follows:

$$\mathcal{V} = \frac{\bar{V}_S x_b}{\alpha} \qquad \mathcal{H} = \frac{-F h_{RP}}{C_P (T_T - T_R)} \tag{1.4}$$

A limited amount of physical significance can be ascribed to these parameters. The velocity parameter $\mathcal{V}$ is a dimensionless expression relating the flame speed to the thermal diffusivity of the gas mixture. In essence, the velocity parameter is a ratio of the rate of absorption of heat by the reactants prior to combustion to the rate of conduction of heat to the reactants.

The enthalpy parameter $\mathcal{H}$ is a ratio of the enthalpy of combustion per unit mass of mixture to the heat absorbed by a unit mass of reactants in passing through the preheat zone. The physical significance of these parameters is not important to the solution of the flame propagation equation; these parameters are introduced here mainly as a matter of convenience.

In obtaining a solution to Equation (1.4), it is necessary to express the reaction rate $\frac{d\Lambda}{d\tau}$ in terms of the distance x and the local temperature T. At the present state of knowledge, it is not possible to represent the reaction rate in a form which will permit an analytical solution to be obtained, and various approximations are therefore used.

b. Solution 1 --Mallard and Le Chatelier[63,66]

This solution is based on the assumption that the temperature gradient at the flame front is proportional to the difference between the threshold temperature T_T and the final temperature T_P, that is

$$\left.\frac{dT}{dx}\right|_{x=0} = \frac{T_P - T_T}{x_b}$$

where x_b includes a constant of proportionality. In addition,

$$\lim_{x \to -\infty} T = T_R$$

$$\lim_{x \to -\infty} \frac{dT}{dx} = 0$$

Under these boundary conditions, a solution can be obtained in the following form:

$$\mathcal{H} = \mathcal{V} + 1 \tag{1.5}$$

c. Solution 2 --Tanford and Pease[24]

This solution represents a limiting case where the reaction rate $\frac{d\Lambda}{d\tau}$ increases rapidly with temperature. The basic assumption here is

$$\frac{d\Lambda}{d\tau} = 0 \quad \text{when} \quad x < x_b,$$

that is, the amount of heat release is negligible except when the final temperature T_P is approached. Additional boundary conditions are

$$\lim_{x \to -\infty} T = T_R$$

$$\lim_{x \to -\infty} \frac{dT}{dx} = 0$$

$$\lim_{x \to x_b} T = T_P$$

In the region $x < x_b$, Equation (1.3) becomes

$$\frac{d^2T}{dx^2} = \frac{\bar{V}_s}{\alpha} \frac{dT}{dx}$$

Under the boundary conditions given, the solution to this equation, in dimensionless form, is

$$\mathcal{H} = e^{\mathcal{V}} \tag{1.6}$$

d. Solution 3 -- Tanford and Pease[24]

This solution represents a limiting case in which the reaction rate is independent of temperature:

$$\frac{d\Lambda}{dx} = 0 \qquad \text{when} \quad x \leq 0$$

$$\frac{d\Lambda}{dx} = \frac{1}{x_b} \qquad \text{when} \quad 0 \leq x \leq x_b$$

In addition

$$\lim_{x \to -\infty} T = T_R$$

$$\lim_{x \to -\infty} \frac{dT}{dx} = 0$$

$$T = T_P \text{ when } x = x_b$$

The solution obtained in this case is

$$\mathcal{H} = \frac{\mathcal{V}}{1 - e^{\mathcal{V}}} \tag{1.7}$$

Three solutions to the general thermal equation for flame propagation have been presented above. These solutions all represent approximations to the real situation. It will be noted that these solutions result in flame speed equations which are quite similar in form and which can be summarized as follows:

$$\mathcal{H} = f(\mathcal{V}) \tag{1.8}$$

where $f(\mathcal{V})$ is the appropriate function of $\mathcal{V}$.

The relationship between $\mathcal{V}$ and $\mathcal{H}$ is shown in Figure 1.2, where the three solutions obtained above are plotted separately. It will be observed that the parameter $\mathcal{H}$ increases when $\mathcal{V}$ is increased in all cases, the rate of change of $\mathcal{H}$ being somewhat dependent on the form of the solution. The curve corresponding to Solution 1 lies between the curves corresponding to the bracketing solutions 2 and 3 respectively.

3. Lean Limit Equation

The relationship between $\mathcal{V}$ and $\mathcal{H}$, shown in Figure 1.2, may be examined for evidence of a lean limit, that is, a minimum value of $\mathcal{H}$. If it is assumed that the true curve relating $\mathcal{V}$ and $\mathcal{H}$, though not precisely known, falls between Solutions 2 and 3, it is seen that $\mathcal{H}$ decreases continuously with decreasing $\mathcal{V}$.

The actual minimum value of the parameter $\mathcal{V}$ is not known. However, $\mathcal{V}$ cannot be negative since it is a product of the factors $\bar{V}_s$, x_b, ρ, C_P, and $1/\lambda$, all of which are inherently positive. The fact that $\mathcal{V}$ is restricted to positive values means that the lowest possible limit of the enthalpy parameter $\mathcal{H}$ is one (see Figure 1.2) and therefore an absolute lower limit for the mixture strength is determined. From Equation (1.4) the mixture strength F_L corresponding to $\mathcal{H} = 1$ is given as

$$F_L = C_P \frac{T_T - T_R}{-h_{RP}}$$

or (1.9)

$$\frac{F_L\,(-h_{RP})}{C_P\,T_T} = 1 - \frac{T_R}{T_T}$$

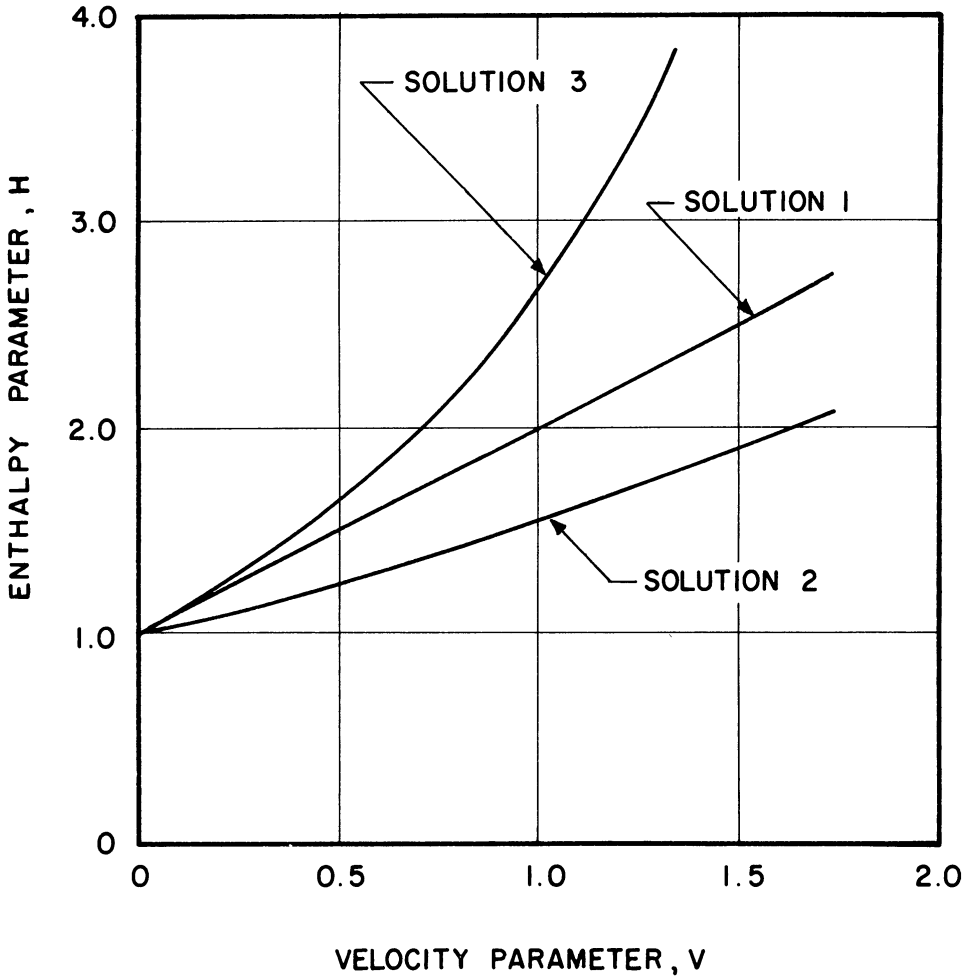

Figure 1.2 Enthalpy Parameter as a Function of Velocity Parameter for Three Approximate Solutions to the Flame Propagation Equation

Equation (1.9) indicates a linear relationship between the initial temperature T_R and the minimum mixture strength F_L.

It should be made clear that the above development is intended to show that flame propagation is not possible in mixtures leaner than the limiting mixture strength F_L. It does not necessarily follow from the above discussion that flame propagation is possible in all mixtures richer than F_L.

C. Supporting Evidence for Lean Limit Equation

The lean limit Equation (1.9) has been developed from very elementary flame propagation theory. It is well known that the mechanism of the propane-oxygen reaction is very complex and not fully understood. In view of the simplifications which were made, it remains to be demonstrated that Equation (1.9) is an adequate representation of the behavior of the physical system.

1. The Threshold Temperature

The threshold temperature indicates a point of transition from the preheat zone to the burning zone. Since the temperature rise in the burning zone is due primarily to combustion, rather than thermal conduction, a change in the temperature profile of the flame should occur at the point where the threshold temperature is reached. In addition, it will be seen from Equation (1.9) that the adiabatic flame temperature of a lean limit mixture will be equal to the threshold temperature. The magnitude of the threshold temperature can be judged from several sources of published data:

a) Temperature profiles of flames have been measured with very fine thermocouples, as well as by optical and spectroscopic means[49,53,55,56,57,60]. The point where combustion begins is not clear upon

direct examination of the measured temperature profiles, and two methods of analysis for determining this point have been used. In both cases, the general Equation (1.3), has been integrated to the form

$$\frac{dT}{dx} = \frac{\bar{V}_s}{\alpha}(T-T_R) + \frac{\bar{V}_s}{\alpha}\left(\frac{F h_{RP}}{C_p}\right)\Lambda \qquad (1.10)$$

In one method of analysis[49,53,55,56], $\frac{dT}{dx}$ and T were taken from the measured temperature profile and $\bar{V}_s$ was separately measured. The value of the last term, indicating the extent of chemical reaction, was then calculated as a function of x.

In the second method of analysis[57,60], Equation (1.10) was rearranged and integrated once more:

$$\frac{dT}{T-T_R} = \frac{\bar{V}_s}{\alpha}dx + \frac{\bar{V}_s}{\alpha}\frac{F h_{RP}\Lambda}{C_p(T-T_R)}dx$$

$$\ln(T-T_R) = \frac{\bar{V}_s}{\alpha}x + \frac{\bar{V}_s F h_{RP}}{\alpha C_p}\int\frac{\Lambda\, dx}{T-T_R}$$

The preheat zone was thus shown to be characterized by a linear relationship between x and the logarithm of $(T - T_R)$, and the temperature profiles were plotted in these coordinates. The point of deviation of the profile from the predicted linear relationship was taken as the beginning of combustion.

Both methods of analysis yielded essentially the same result: combustion begins at 2550° to 2700°R for light hydrocarbons burning in air. It has been pointed out that the accuracy of the first method of analysis is strongly dependent on the accurate determination of the ratio $\frac{\bar{V}_s}{\alpha}$ [56]. An error in this constant can

result in an apparent very gradual beginning of combustion at a temperature several hundred degrees lower than that given above. Such gradual beginnings in combustion shown by the data of earlier investigators are therefore ignored in arriving at the temperatures 2550° to 2700°R.

b) According to the lean limit Equation (1.9), the enthalpy of combustion of a unit mass of mixture at the lean limit is just equal to the heat absorbed in preheating a unit mass of reactants to the threshold temperature. Since there is no excess of enthalpy, the products of combustion leave the combustion zone at the threshold temperature. It follows, therefore, that the adiabatic flame temperature of a lean limit mixture may be taken as a measure of the threshold temperature. Data obtained by several investigators[32,39,48] is shown in Table I. The temperatures found here are about 2800° to 3000°R. In addition, Egerton and Powling[38] have shown that in mixtures in which non-combustible diluents such as nitrogen, argon, or carbon dioxide were present, the adiabatic flame temperature of lean limit mixtures was nearly the same as that observed in air, as shown in Table II. These investigators also reported that when the reactants were preheated to an elevated temperature, the adiabatic flame temperature of lean limit mixtures was nearly the same as that observed when the reactants were at room temperature.

c) The temperature T_T, here called the "threshold temperature", is frequently termed "ignition temperature" in technical literature. However, the numerical values of this temperature quoted above are much higher than the self-ignition temperature of a mass of heated mixture[52,58,59,61]. It should be pointed out that in attempts by

TABLE I

ADIABATIC FLAME TEMPERATURES AT THE LEAN LIMIT

Degrees Rankine

Fuel	Burgoyne and Williams-Leir[32]	Zabetakis et. al.[48]	Egerton and Thabet[39]
Methane	2928	2874	2869
Ethane	2993	2951	--
Propane	3158	2888	2829
n-Butane	3270	3081	2888
n-Pentane	--	2994	--

TABLE II

EFFECT OF DILUENTS ON THE LEAN LIMIT

Mixture	Lower Limit Percent Fuel	Adiabatic Flame Temp. °R
CH_4-Air	5.26	2916
CH_4-O_2-CO_2	9.0	3276
CH_4-O_2-A	4.01	2970
CH_4-Air-19% CO_2	6.0	2974
CH_4-Air-19% N_2	5.4	2974
CH_4-Air-19% A	4.85	2907
CH_4-Air-33% A	4.57	2907

various investigators to measure ignition temperature, the combustible gases were maintained at the ignition temperature for a relatively long time, of the order of seconds. The heating area was also large. It has been shown that the temperature necessary to cause ignition of a mixture is reduced considerably by extending the heating time and by exposing the reactants to a heating element of large area[68]. Nevertheless, some ignition experiments using heated spheres projected into a cool mass of mixture give results comparable to the temperatures under a) and b) above[65,74,77]. It is apparent that in the heated sphere experiments the high temperature is confined to the immediate vicinity of the flame zone and the time delay is very short.

2. Measured Lean Limits

It is indicated in Equation (1.9) that a graph showing F_L as a function of the initial temperature T_R should yield a straight line with a slope of $-\frac{hRP}{CP}$ and an intercept T_T. Such a graph has been plotted in Figure 1.3, using data obtained by White[47] for flames propagating downward in tubes. The experimental points fall quite close to a straight line with an intercept at about 3000° to 3200°R. Taking T_T to be 3000°R, data obtained by several investigators[30,42,47,48] were plotted in dimensionless form in Figure 1.4. A fairly close correlation of the data with the experimental equation is indicated.

It should be noted that several other investigators have published data on the lean limit of various fuels in air as a function of mixture temperature[27,28,29,30,33,42,45,48,56]. These studies show that progressively leaner mixtures can be burned as the mixture

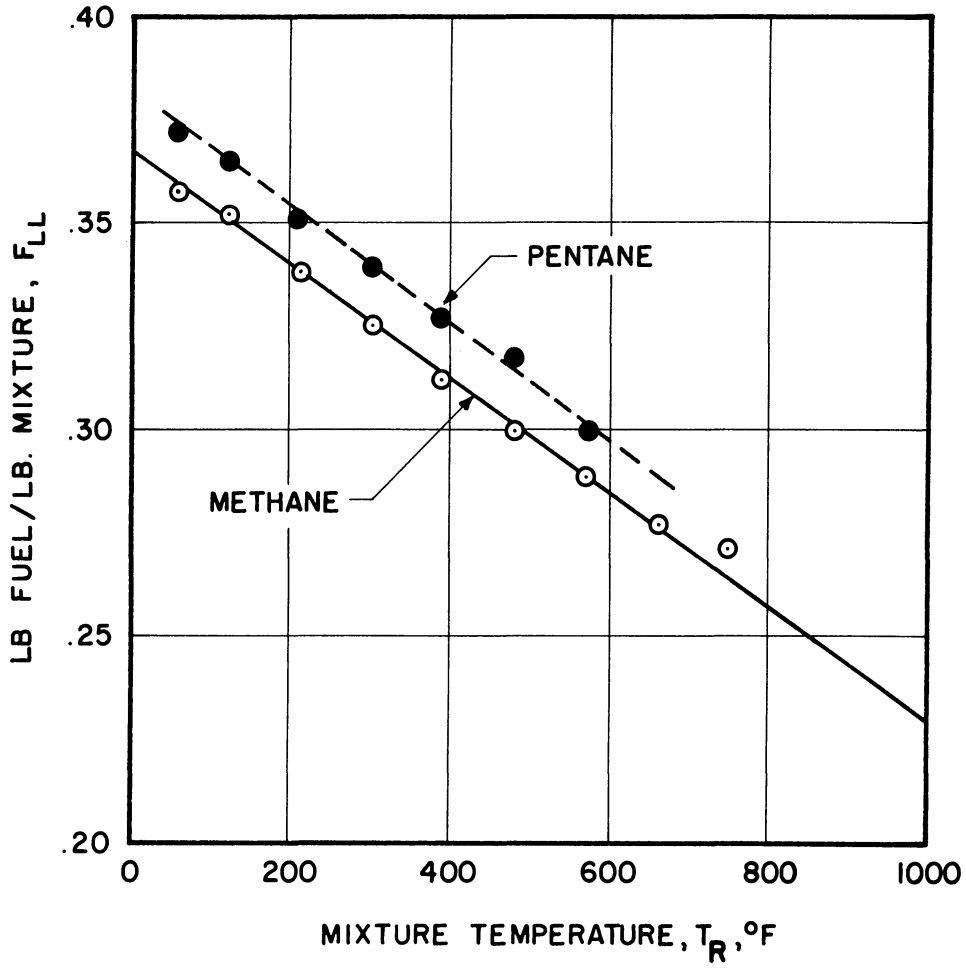

Figure 1.3 Effect of Temperature of Reactants on Lower Limit of Inflammability of Hydrocarbon-Air Mixtures. Data from White[47].

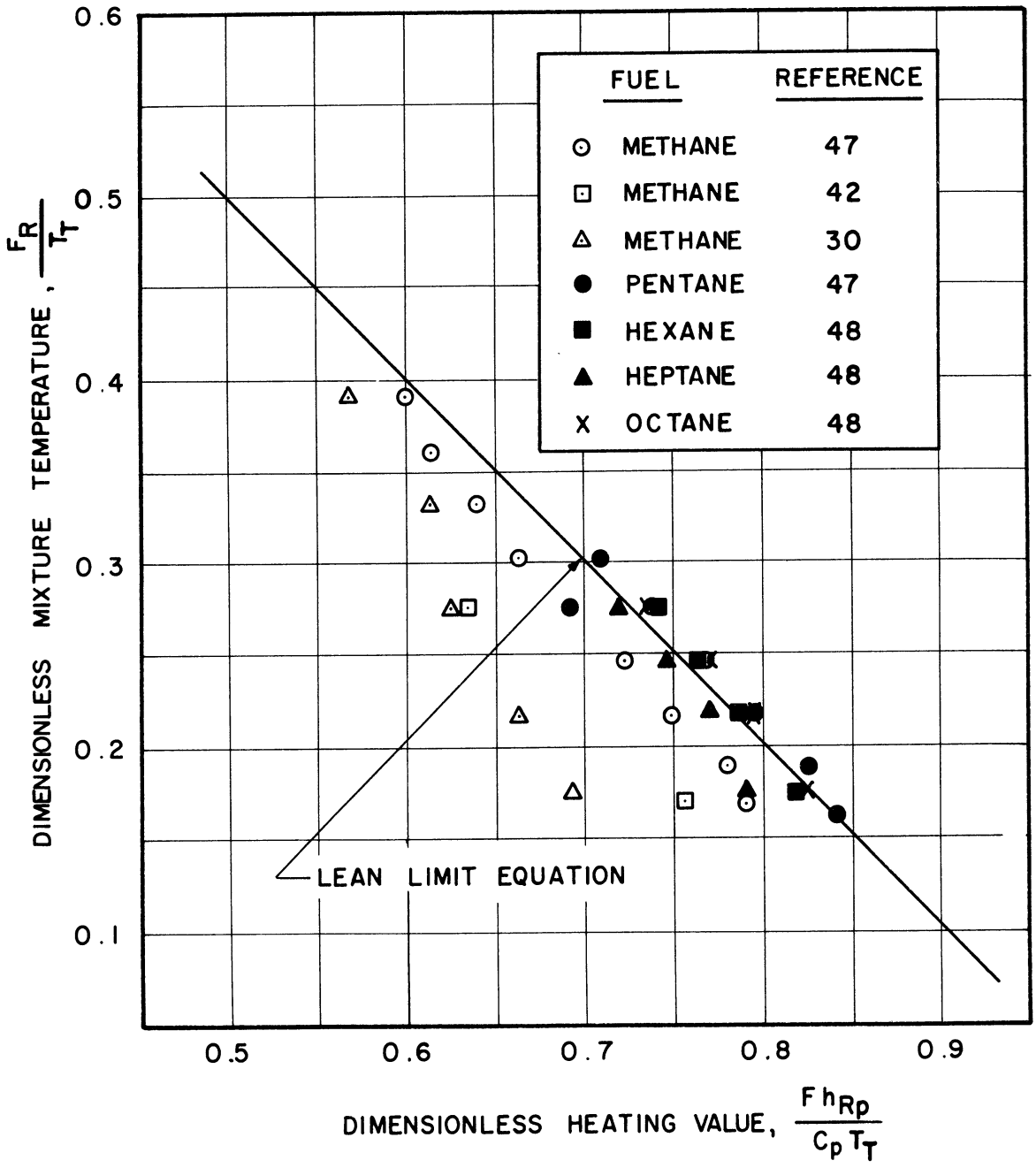

Figure 1.4 Lower Limit of Inflammability of some Paraffin Hydrocarbons

temperature is raised. The actual mixture strength of the leanest combustible mixture seems to vary, however, depending on the duration of the mixture heating period and on whether propagation is upward or downward[33,47]. It has also been shown [26] that the lean limit is a function of mixture turbulence.

CHAPTER II

EXPERIMENTAL APPARATUS

A. Description of Equipment

Experimental tests were performed to obtain data on engine operation with lean mixtures. Photographs of the engine and some of the instrumentation that was used are shown in Figures 2.1, 2.2, and 2.3. The apparatus can be divided into six major parts:

1) the engine and accessories,
2) the air supply and metering system,
3) the fuel supply and metering system,
4) the engine output power and speed measuring and controlling system,
5) the engine cylinder pressure recording system, and
6) the temperature measuring system.

These parts of the apparatus are described separately below.

1. Engine and Accessories

Engine tests were run with a single-cylinder 3-1/4 inch bore x 4-1/2 inch stroke Cooperative Fuel Research (CFR) Engine built by the Waukesha Motor Co., Waukesha, Wisconsin. A high-speed crankcase assembly (Part No. 500459) was used. The engine was fitted with a variable compression ratio, split-head cylinder assembly (Part No. 416-69), permitting the compression ratio to be adjusted from a minimum of about 5.0 to a maximum of about 15. A cross-section of this cylinder assembly is shown in Figure 2.4. The spark plug was installed in the 18 mm. tapped hole provided, and the pressure pickup was installed in the other (7/8 inch x 18) tapped hole in the cylinder head. This cylinder head assembly is equipped

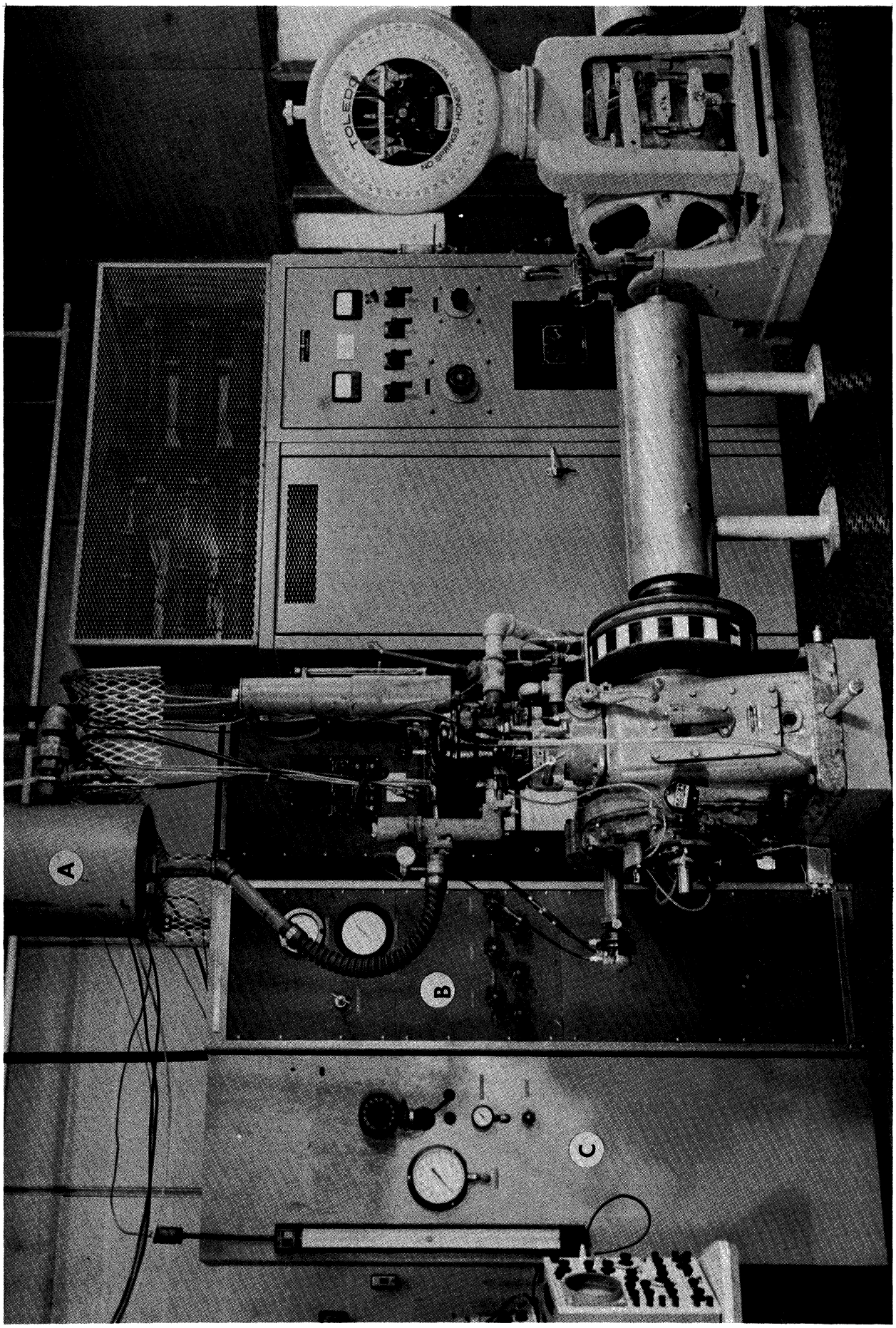

Figure 2.1 Photograph of Test Equipment

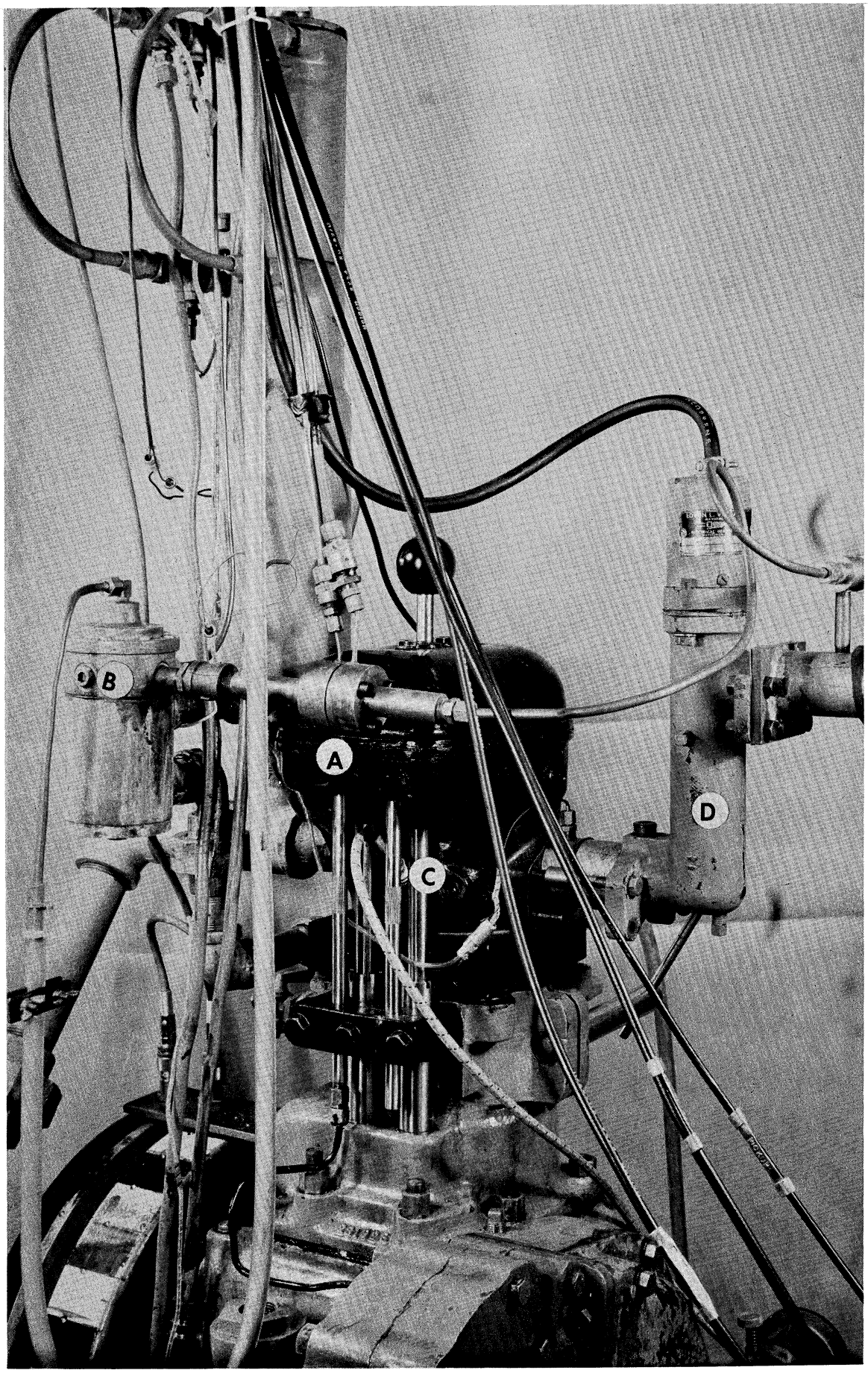

Figure 2.2 Photograph of Engine - Left Side

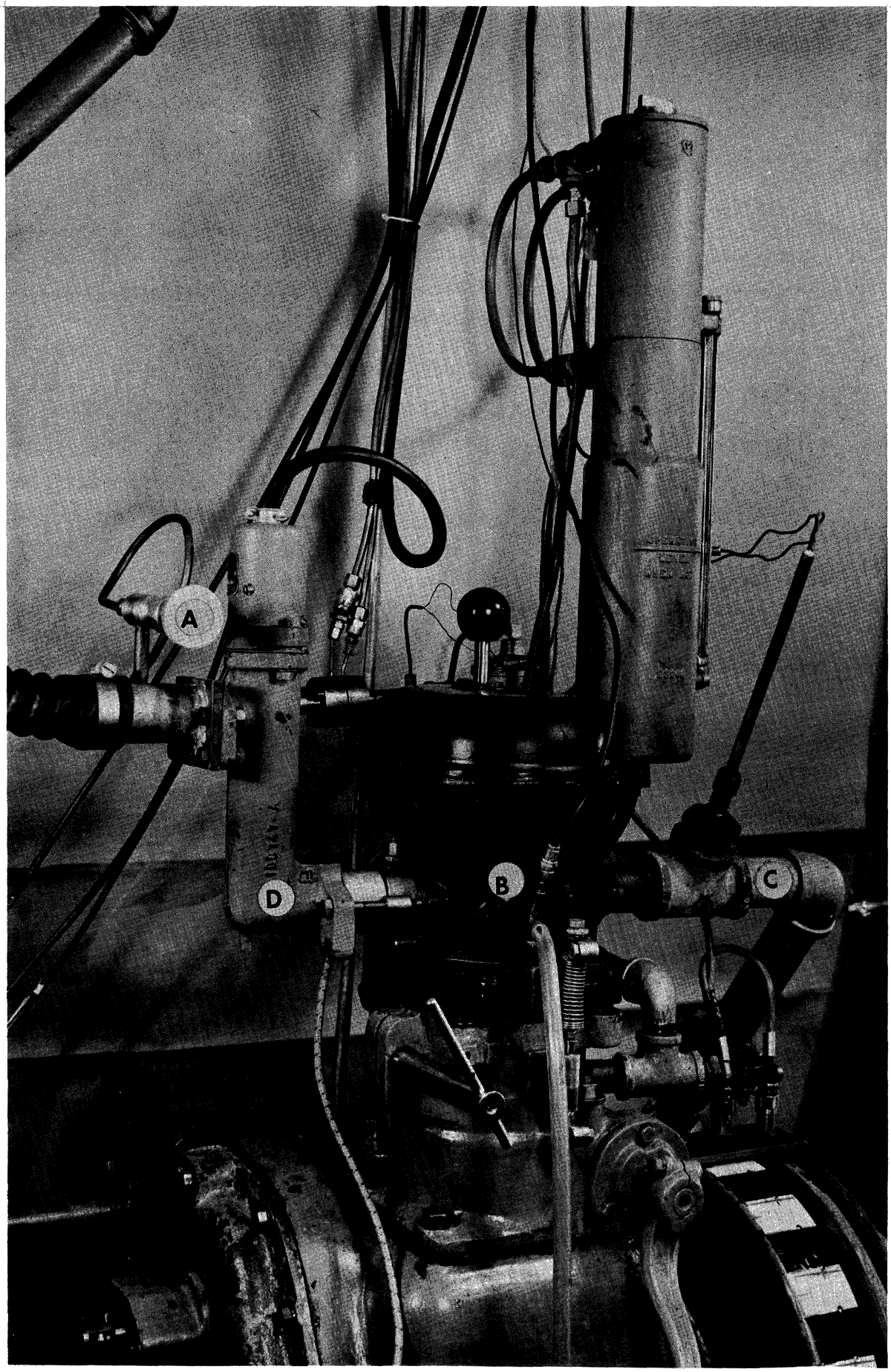

Figure 2.3 Photograph of Engine - Right Side

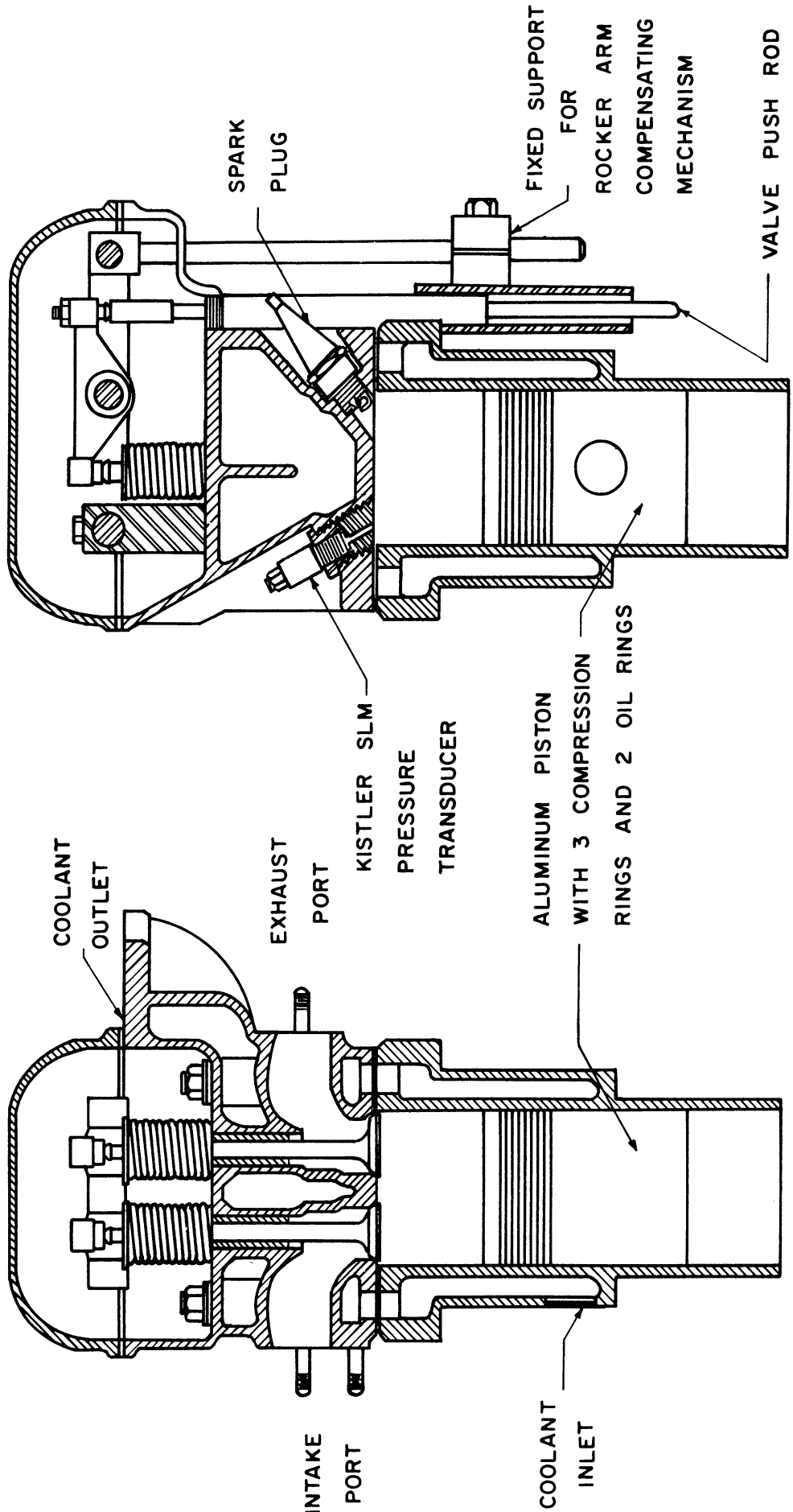

Figure 2.4 Cross Section of Engine Cylinder

with unshrouded overhead valves approximately 1-3/8 inches in diameter. An aluminum piston was used and was fitted with three plain compression rings and two oil rings. A standard camshaft, (Part No. 105620-A) was used. The valve timing provided by this camshaft is specified by the manufacturer as follows:

Intake valve, opens 10° after top center,
closes 34° after bottom center,
Exhaust valve, opens 40° before bottom center,
closes 15° after top center.

The engine was equipped with a bypass-type oil filter; the filtered oil was used to lubricate the valve rocker arm mechanism and then returned to the sump. The temperature of the oil in the engine sump was measured with an iron-constantan thermocouple. An electric heater on the bottom of the crankcase and an external oil cooler were provided, and these were used as necessary to maintain the oil temperature at 150 ± 3°F. The engine was pressure lubricated throughout; the oil pressure was maintained by a regulator at 40 to 45 psi.

The engine was water-cooled, using the standard CFR system. The water in the engine cooling jacket was allowed to boil and the vapor given off was condensed in a water-cooled condenser attached to the engine cylinder head. The condensate was used to preheat the fuel and was then returned to the bottom of the water jacket.

A CFR ignition system, shown schematically in Figure 3.1, was used. This system differs from the usual automotive system and will therefore be described briefly. The CFR ignition system is a 150 volt impulse-type system in which the coil serves as a high voltage

pulse transformer. A half-wave rectifier, operating from the 110 volt A.C. line, charges the 4 micro-farad condenser to approximately 150 volts during the time that the ignition contactor is open-circuited. When the ignition contacts close, the condenser discharges rapidly through the primary winding of the ignition coil, creating a high voltage pulse at the spark plug. The spark timing is readily adjusted by rotating the contactor assembly. A neon-bulb indicator attached to the engine crankshaft shows the crankshaft position at the beginning of the spark. AC type C85 spark plugs were used.

2. Air System

The measurement of the rate of air consumption of a single cylinder engine is complicated by the fact that the air flow is not steady but intermittent. It has been shown(105) that accurate measurement of the air consumption rate of a single cylinder engine cannot be obtained by measuring the average pressure drop across a sharp-edged orifice unless a very large surge tank is interposed between the engine and the orifice. An orifice is inherently inaccurate for measuring pulsating flows because of the non-linear relationship between the instantaneous flow rate and the instantaneous pressure drop. Because of this non-linear relationship, the average pressure drop is dependent on both the average flow rate and the manner in which the flow rate varies with time.

To avoid the error inherent in a sharp-edged orifice system, the air flow was metered by a critical flow nozzle system. This metering system subjects the selected flow nozzle to a pressure differential sufficient to insure that the gas velocity at the nozzle

throat is equal to the speed of sound at all times. The required upstream pressure is[105]

$$P = P_o\left(\frac{2}{k+1}\right)^{\frac{k}{k-1}} \quad \text{or approx. } 2\ P_o \qquad (2.1)$$

where P = the absolute pressure upstream
P_o = the absolute pressure downstream

When P exceeds the required pressure, the flow rate is entirely independent of the downstream pressure and is therefore insensitive to downstream pressure fluctuations. The mass rate of flow through the nozzle is then given by the following equation:

$$\dot{W}_a = \frac{K_N\ P}{\sqrt{T}} \qquad (2.2)$$

where $\dot{W}_a$ = the flow rate lb./hr.
K_N = a constant
P = the absolute stagnation pressure upstream of the nozzle
T = the absolute stagnation temperature upstream of the nozzle.

Because the air flows through the nozzle at a constant rate, whereas the engine consumes air intermittently, a surge tank must be placed between the nozzle and the engine. This surge tank must be of sufficient size to limit the peak pressure developed between intake strokes to a level that will not affect the nozzle flow.

A critical flow air system capable of measuring flow rates from 8 lb./hr. to 300 lb./hr. was constructed (see Figures 2.5 and 2.6). It was provided with five rounded-entrance nozzles ranging in throat diameter from .055 inch to .220 inch and constructed according to the A.S.M.E. Power Test Code[103]. A shut-off valve was provided for each nozzle making it possible to select any desired nozzle or combination of nozzles. The upstream nozzle pressure, and consequently the

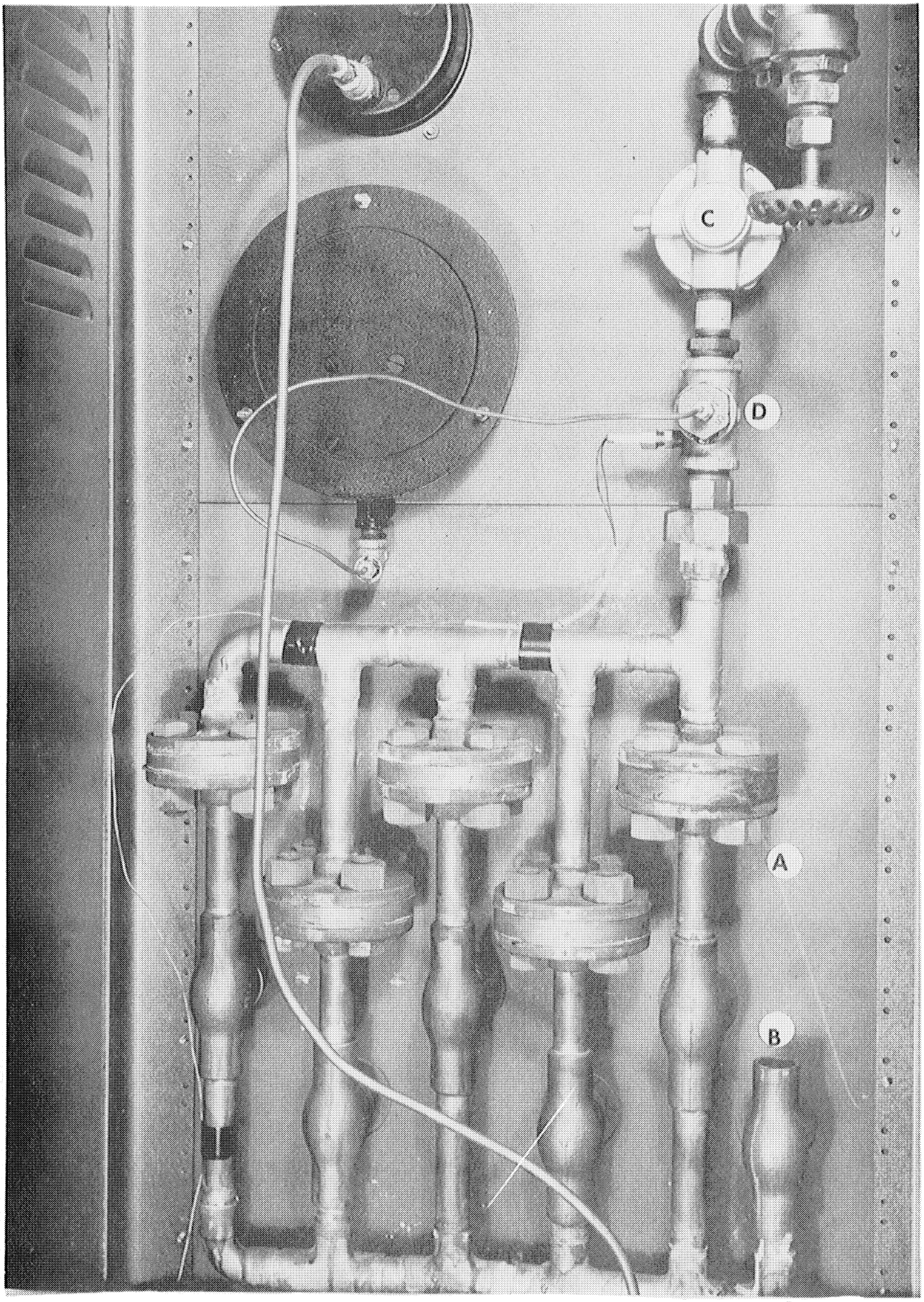

Figure 2.5 Photograph of Air Measuring System

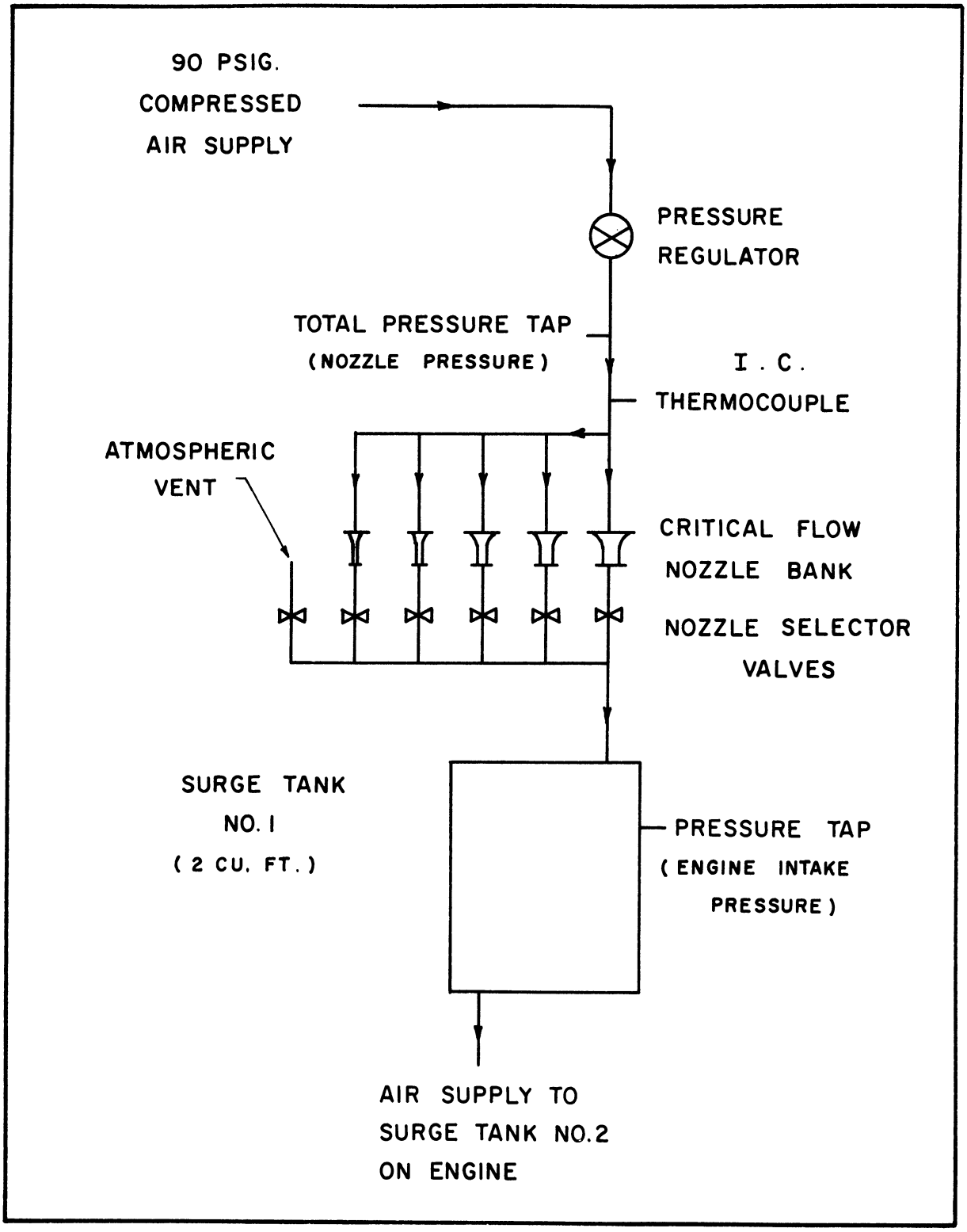

Figure 2.6 Schematic Diagram of Air Measuring System

air flow rate, was controlled by a pressure regulator. A two cubic foot surge tank was provided on the discharge side of the nozzles. Bourdon-type pressure gauges were used to measure the upstream stagnation pressure and the pressure in the surge tank, and an iron-constantan thermocouple was used to measure the upstream air temperature. The unit was supplied with air from a 90 psi. shop air line. The entire unit was housed in a Bud Relay Rack Cabinet.

An overhead line consisting of 1-1/2 inch pipe was used to bring air, at intake manifold pressure, from the surge tank to the engine. To eliminate possible resonance effects in this line, a second two-cubic-foot surge tank was installed at the engine.

3. The Fuel System

In order to eliminate problems which might arise in vaporizing and mixing a liquid fuel, the engine was operated on propane gas. The same difficulties in measuring the flow rate under unsteady flow conditions were encountered with fuel as with air. However, the fuel flow rate was so much smaller than the air-flow rate that critical flow nozzles of practical size could not be used. An alternate type of critical flow system, shown schematically in Figure 2.7 was used instead. In this system, critical flow takes place in the flow control needle valve; the rate of the flow through this valve is constant, dependent only on the upstream temperature and pressure and on the valve setting. The flow through the measuring orifice, upstream of the control valve, is therefore entirely steady and thus can be accurately computed from the pressure differential across the orifice.

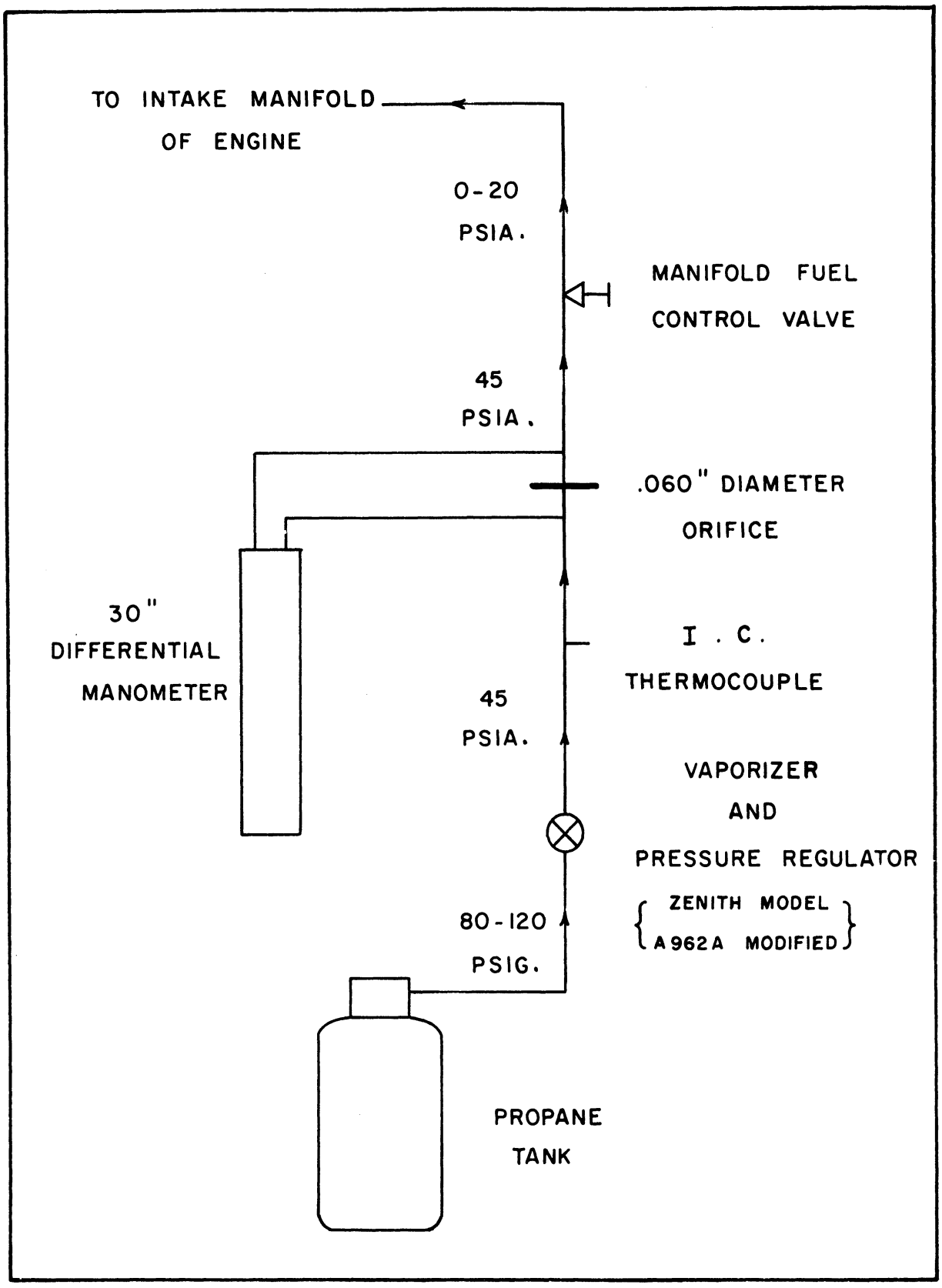

Figure 2.7 Schematic Diagram of Fuel System

The mass rate of flow of gas was measured with a .060 inch diameter sharp-edged orifice and a 30 inch differential manometer. The indicating liquid was a commercial oil mixture having a specific gravity of 1.00. Most of the tests were run at manometer readings varying from 3 inches to 15 inches. The fuel flow was calculated according to the equation:

$$\dot{W}_f = K_o \sqrt{\frac{P\,h}{T}} \qquad (2.3)$$

where $\dot{W}_f$ = the fuel flow rate lb/hr.
P = the absolute pressure upstream from the orifice, psia.
h = the differential manometer reading, inches H_2O.
T = the absolute temperature of the gas upstream from the orifice, °R.
K_o = the orifice constant, determined by calibration.

The pressure and temperature of the fuel at the orifice were controlled to approximately 30 psig. and 160°F by the fuel regulator and heat exchanger, a modified Model A962A vaporizer-regulator made by the Zenith Carburetor Division, Bendix Aviation Corporation. Although the original purpose of the unit was to vaporize liquid propane under pressure, it was found that less pressure fluctuation was encountered if the propane was allowed to vaporize in the supply tank. The heat exchanger incorporated in the vaporizer was retained to insure against any liquid carry-over and to heat the gas to a temperature well above saturation so that ideal gas laws could be applied.

4. Power and Speed Measurement

The engine was coupled to a 10/15 hp. D.C. cradle dynamometer. The dynamometer was used to start and motor the engine, and to

absorb engine power and control engine speed when the engine was running. The dynamometer was equipped with a 50 lb. Toledo scale with 1/10 lb. divisions for measuring torque. A 10.5 inch torque arm was used; the corresponding horsepower equation is:

$$\text{Horsepower} = \frac{\text{rpm x Scale Reading}}{6000} \qquad (2.4)$$

The dynamometer stator balance was checked, the scale linkage was adjusted, and the scale calibration was checked with test weights. The maximum scale error was less than 0.1 pounds.

The speed of the engine was measured with a Hewlett-Packard Model 521-A Electronic Counter. An Electro Products Model 3010-A magnetic pickup was used in conjunction with a 60 tooth gear attached to the dynamometer shaft to provide electrical pulses at the rate of sixty per revolution. These pulses were counted for a one second period by the counter; a reading in engine revolutions per minute was thus obtained directly.

5. Engine Pressure Pickup

In order to study the combustion process in the engine the instantaneous pressure existing in the engine cylinder throughout the operating cycle was displayed as a function of time on a Tectronix Model 512 Oscilloscope. Photographs of the oscilloscope face were made for permanent records.

A Kistler SLM Pressure Pickup, Model PZ-14, was used to sense the pressure. This pressure pickup is a piezoelectric device, containing a quartz sensing element, and is designed to be used in the pressure range of 0-3000 psia. Additional manufacturer's ratings

are: resolution .1 psi, linearity .1 percent of full scale. The pressure pickup was mounted in the 7/8 inch x 18 tapped hole in the engine head using an adapter, as shown in Figure 2.8. The pressure in the engine cylinder was transmitted to the pickup through a 3/64 inch[110] hole about 3/4 inch long. The pressure pickup was coupled to the oscilloscope through an electrostatic amplifier (Kistler Model PC14 Piezo-Calibrator). The Piezo-Calibrator includes a calibration circuit by means of which a pulse of known amplitude can be produced; the calibration circuit was actuated during part of the intake stroke by a contactor geared to the camshaft. It was found that the Piezo-Calibrator picked up a small stray electrical charge from the engine ignition system each time the spark occured. The accumulation of these charges caused the pressure trace to tend to drift off the oscilloscope screen. A second contactor was therefore added to ground the Piezo-Calibrator input circuit during part of the exhaust stroke, removing the charge and thus stabilizing the pressure trace on the oscilloscope screen. A circuit diagram of the pressure recording apparatus is shown in Figure 2.9.

An Electro Products Model 3010-A magnetic pickup was mounted to register with a small drilled hole in the rim of the flywheel at bottom dead center position; a pulse derived from this pickup was used to synchronize the oscilloscope sweep generator with the engine. A second magnetic pickup was mounted to register with a series of holes spaced at 10° intervals in the flywheel; the pulses derived from this second pickup were superimposed on the pressure trace and served to act as timing marks. The pulse corresponding to top dead center was witnessed by two additional pulses occurring about 2° before and 2° after, respectively.

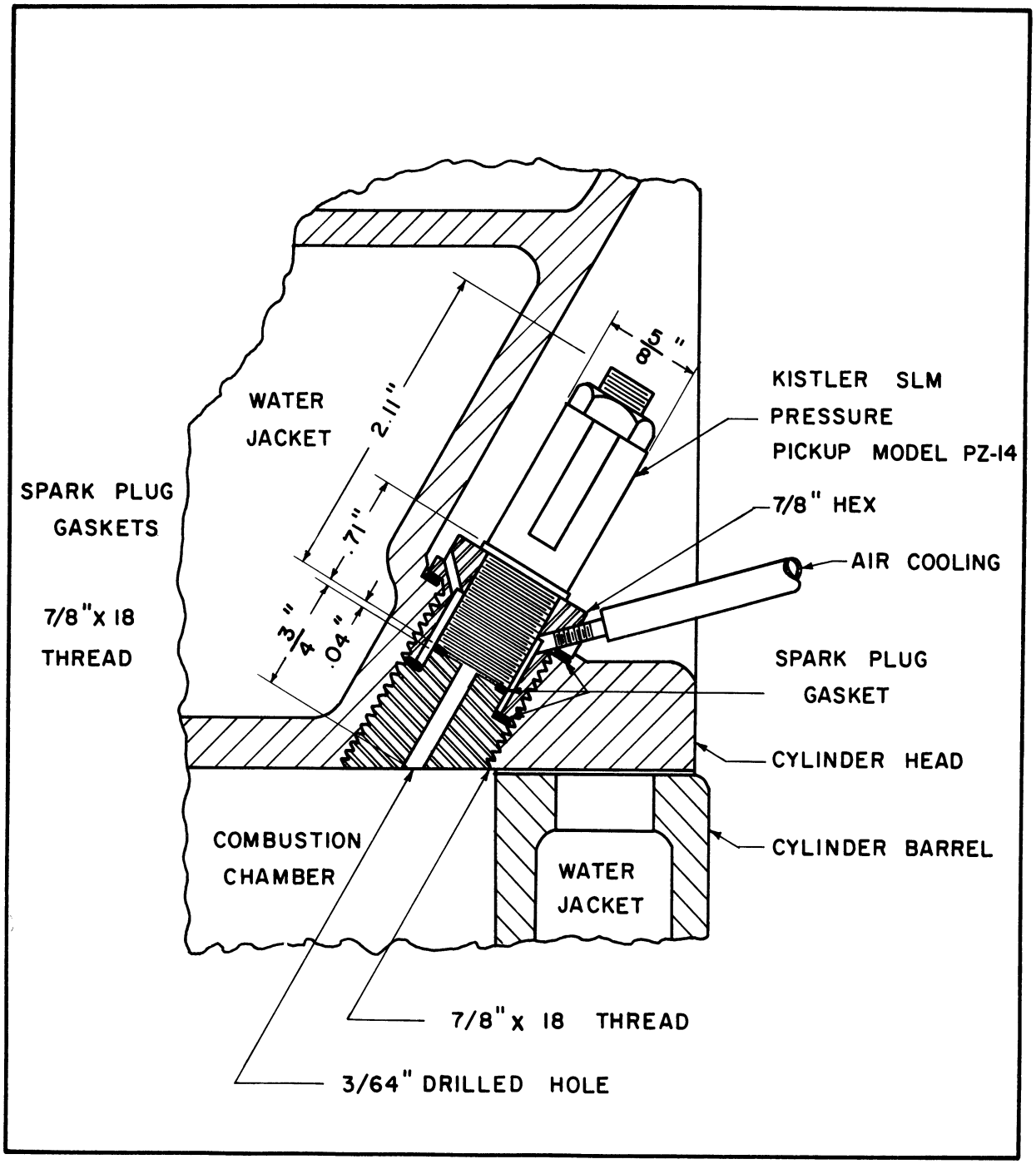

Figure 2.8 Mounting of Pressure Pickup

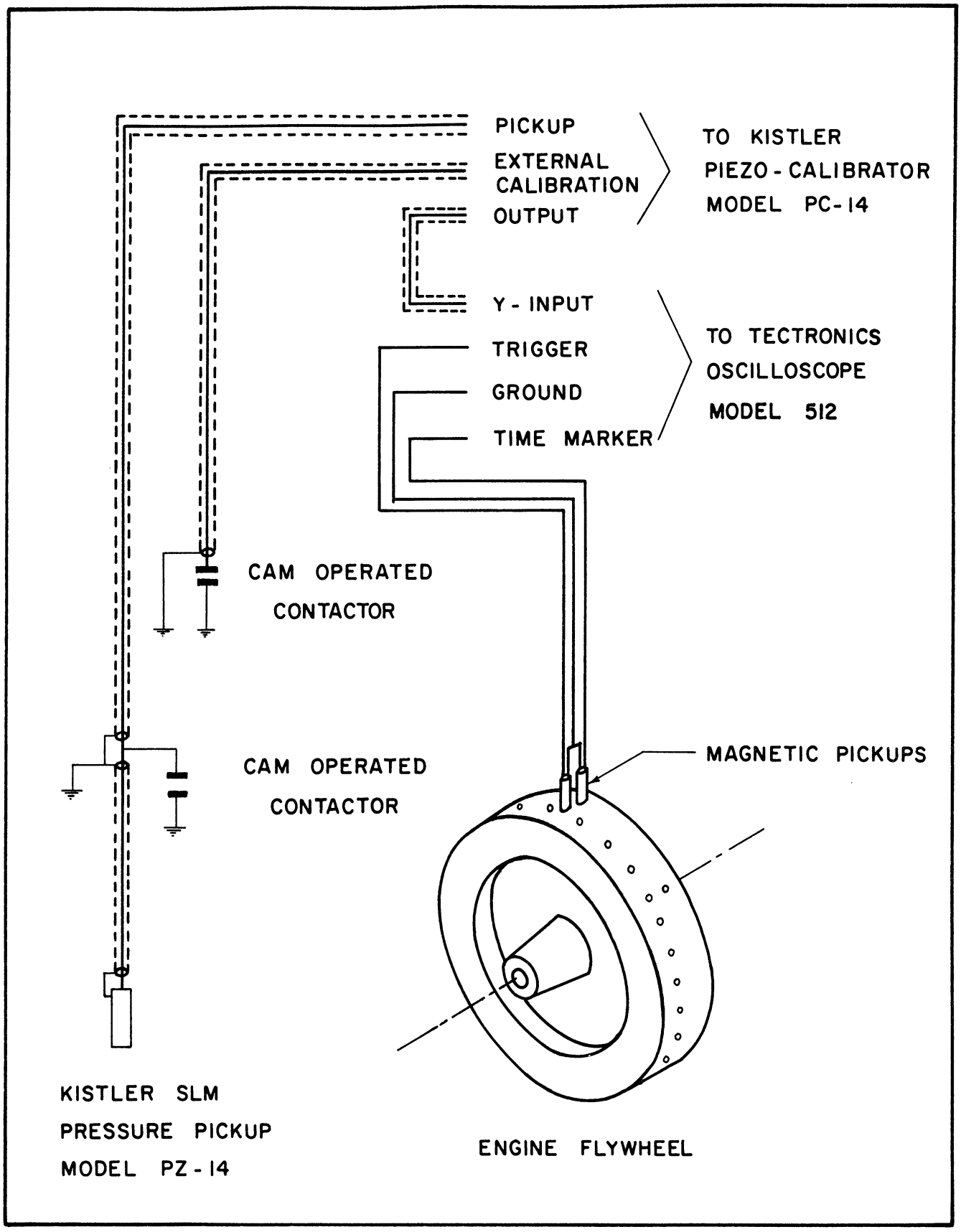

Figure 2.9 Circuit Diagram - Pressure Recording Apparatus

6. Temperature Measuring Equipment

The engine exhaust temperature was measured in the exhaust pipe about three inches from the exhaust port. A chromel-alumel thermocouple with five concentric radiation shields was used to measure the exhaust temperature. The thermocouple was read with a Leeds and Northrop Model 8667 millivolt potentiometer; the cold junction temperature was measured with a thermometer lying on the potentiometer case.

All other temperatures were measured with iron-constantan thermocouples and were recorded on a Brown Type Y153X62(PSD12)-(W7)-(60)(G)(V) recording potentiometer which had been calibrated against steam and ice points.

B. Calibration of Instruments

1. Engine Compression Ratio Gauge

A micrometer gauge was attached to the engine to measure the position of the cylinder assembly relative to the crankcase so that the engine compression ratio could be computed. A calibration procedure for setting the zero point of the micrometer scale was carried out as follows. The engine was allowed to stand for a sufficient time to attain room temperature throughout. The flywheel was rotated to a position at which the piston was brought to top center position with the valves closed. A measured amount of water from a burette was put in the cylinder through the spark plug hole. The cylinder head was lowered, raising the compression ratio, until the water began to rise in the spark plug hole. The valves were then opened manually to eliminate air trapped around the valve seats. After the air had been

relieved, the head was adjusted to bring the water level in the cylinder to the bottom edge of the spark plug hole and the micrometer reading was noted.

The volume contained in the spark plug recess with the spark plug in place was measured with the cylinder head removed and was found to be .262 cubic inches. The pressure pickup adaptor was found to enclose an additional .012 cubic inches. The clearance volume was computed by adding the volume contained in the spark plug recess and the pressure pickup adaptor to the volume of water used. The micrometer was reset so that a reading of -.300 inches corresponded to zero clearance volume. The micrometer setting for any desired compression ratio was then calculated by the formula:

$$MR = \frac{D}{r_V - 1} - .300 \qquad (2.5)$$

where MR = the micrometer reading in inches
D = the engine stroke, 4.500 inches
r_V = the engine compression ratio.

After performing this calibration, the water was removed from the cylinder and the engine was operated for about 15 minutes to dry it out.

2. The Air Measuring System

Each nozzle of the critical flow air measuring system was calibrated at at least two flow rates against a ten cubic foot air displacement tank. The results of the calibration are shown in Table XII.

3. The Fuel Measuring System

The calibration of the fuel measuring system was checked periodically. The fuel tank was placed on a platform scale and a measurement

was made of the time required to use a specified amount of fuel at a flow rate corresponding to an orifice pressure differential of about ten inches of water. The scale was read to ± .01 pound. The results of several calibrations are shown in Table XIII.

4. Pressure Pickup Calibration

The pressure pickup was calibrated on a dead weight tester. Because of a slow drift in the output of the Piezo-Calibrator when the pickup was subjected to a static pressure, a three-way valve was used to switch the pickup rapidly from atmospheric pressure to the test pressure. The pressure pickup system was found to be linear, within the limits of accuracy with which the oscilloscope could be read. The calibration circuit of the Piezo-Calibrator was adjusted to correspond to the measured pressure.

5. The Pressure Gauges

The two Bourdon-type pressure gauges, which were used to measure the air pressure at the metering nozzles and the fuel pressure at the metering orifice respectively, were calibrated on a dead weight tester at 5 psi. intervals. The air pressure gauge was found to be correct within ± .2 psi. The fuel pressure gauge was found to read about .5 to .6 psi. too high. Appropriate corrections to the gauge readings were made in computing data.

CHAPTER III

THE EFFECT OF ENGINE VARIABLES ON THE LEAN LIMIT

A. Measurement of the Lean Limit in an Engine

The minimum fuel-air ratio for steady firing in the engine was measured at compression ratios of 7, 10, 13, and 16 and at intake temperatures of 100°, 150°, 180°, and 300°F. It was found that the ignition timing had some effect on the lean limit, as discussed on page 59. Consequently, the ignition timing was maintained at 19° B.T.C. for all tests. The speed of the engine was controlled to 1200± 10 rpm. by adjusting the dynamometer load. In most cases, combustion was so poor with these very lean mixtures that the power output of the engine was not sufficient to overcome engine friction and the dynamometer was used to supply the additional power necessary. In one series of tests the intake pressure was varied from 7 psia. to 19.4 psia. In all other tests, however, the mass rate of flow of air was held constant for reasons given on page 66. The intake pressure therefore varied from about 11 psia. at 100°F to 13.3 psia. at 300°F.

Prior to making a series of tests, the engine was operated at a moderate load for about one hour, until the desired temperatures had been reached. The fuel flow rate was then reduced to the point when misfiring began, while simultaneously adjusting the dynamometer to maintain constant engine speed. Misfiring was detected by observing the pressure-time trace on the oscilloscope. Misfires were indicated by a pressure-time trace that was symmetrical about top dead center position up to 40° after top center.

B. Effect of Ignition System Characteristics

In the preceding discussion of the lean limit, it was implied that the term "lean limit" refers to the ability of a fuel-air mixture to sustain a flame, presupposing that any such mixture can be ignited by a suitable source. Since the criterion by which the lean limit is judged is combustibility rather than ignitability, it follows that the ignition system can have no effect on the measured lean limit. That is, in order to measure the lean limit, an ignition system capable of igniting any combustible mixture must be employed. Insofar as the ignition system has any influence on the lean limit, the ignition system is inadequate for the purpose of measuring the lean limit. A spark-type ignition system, as used in this study, may be inadequate in two ways: (1) it may fail to provide energy in an adequate quantity and at a suitable rate for ignition, or (2) the spark plug electrodes may quench the flame. An investigation of these two possible effects of the ignition system was made.

1. Ignition Energy

It has been shown that a spark must have at least a certain minimum amount of energy to insure ignition of a combustible mixture under a given set of conditions. The minimum amount of ignition energy necessary depends on the pressure, the temperature, and the fuel-air ratio of the mixture and on the duration of the spark[68,69,72,86]. It has been reported that the initial portion of the spark is most effective in causing ignition, and the amount of energy required for ignition increases as the duration of the spark is increased, at least for sparks in excess of 100 microseconds duration[68,86]. The required

energy also is approximately inversely proportional to the absolute pressure of the mixture at sub-atmospheric pressures; the energy required for ignition of a slightly rich propane-air mixture decreases from approximately 3.5 millijoules at 7.5 inches of mercury absolute to about 0.5 millijoules at atmospheric pressure[68]. Extrapolation of these data is recognized as being a questionable procedure and is undertaken here only because of the lack of data on ignition energy requirements under engine conditions. On the basis of the relationship observed at sub-atmospheric pressures, a quenching distance of .025 inches was estimated to correspond to the compression pressure of the engine operating at an intake pressure of 10 psia. and a compression ratio of 7. In addition, raising the temperature of the charge reduces the amount of spark energy required[68,86]; at the compression temperature of the engine the minimum spark energy is probably reduced by an additional factor of ten over that which obtains at room temperature. The resulting figure of .0025 millijoules for the minimum ignition requirement should be taken only as indicating the order of magnitude because of the approximations involved in arriving at this figure. This figure also applies to an approximately chemically correct propane-air mixture; lean mixtures require considerably more energy. It has been shown that the required ignition energy increases rapidly as the fuel-air ratio approaches the lean limit. Available data[68,69,86] are limited to energies of approximately ten times the amount required for a chemically correct mixture. However, it appears that very large increases in energy are required to permit appreciably leaner mixtures to be ignited.

All engine tests reported in this study were made using a standard CFR ignition system. A circuit diagram of the ignition system is shown in Figure 3.1. The high voltage necessary to form a spark at the spark plug electrodes was furnished by an ignition coil, essentially a high voltage transformer. A high voltage pulse was produced by discharging a capacitor through the primary winding of the coil at a selected point in each engine cycle by means of an engine-driven contactor. An attempt was made to measure the energy of the spark and to evaluate various methods for controlling the energy of the spark in order to determine the effect that variations in spark energy would have on the lean limit. The energy of the spark can be determined by measuring the instantaneous voltage and current of the spark with an oscillograph and integrating the product of current and voltage. However, because of the high voltages involved, such measurements require specialized equipment which was not available. Some measurements were therefore made of sparking voltage using a Heyer Dynatester; the accuracy of this instrument is unknown, however. Typical results of this kind of test show an initial voltage pulse of approximately ten kilovolts followed by several periods of arcing at a voltage of about one kilovolt. After the last period of arcing the system oscillates until the remaining energy has been dissipated. Some measurements of the current of sparks in air at room temperature and pressure were also made using a Tectronix Model 512 Oscilloscope. The current pattern of a spark was found to consist of several surges ocrresponding to several arcing periods. The first surge had a peak current of about 100 milliamperes and lasted about 100 microseconds. The amount of energy dissipated in this first surge of current is estimated on the basis of the above measurements of current

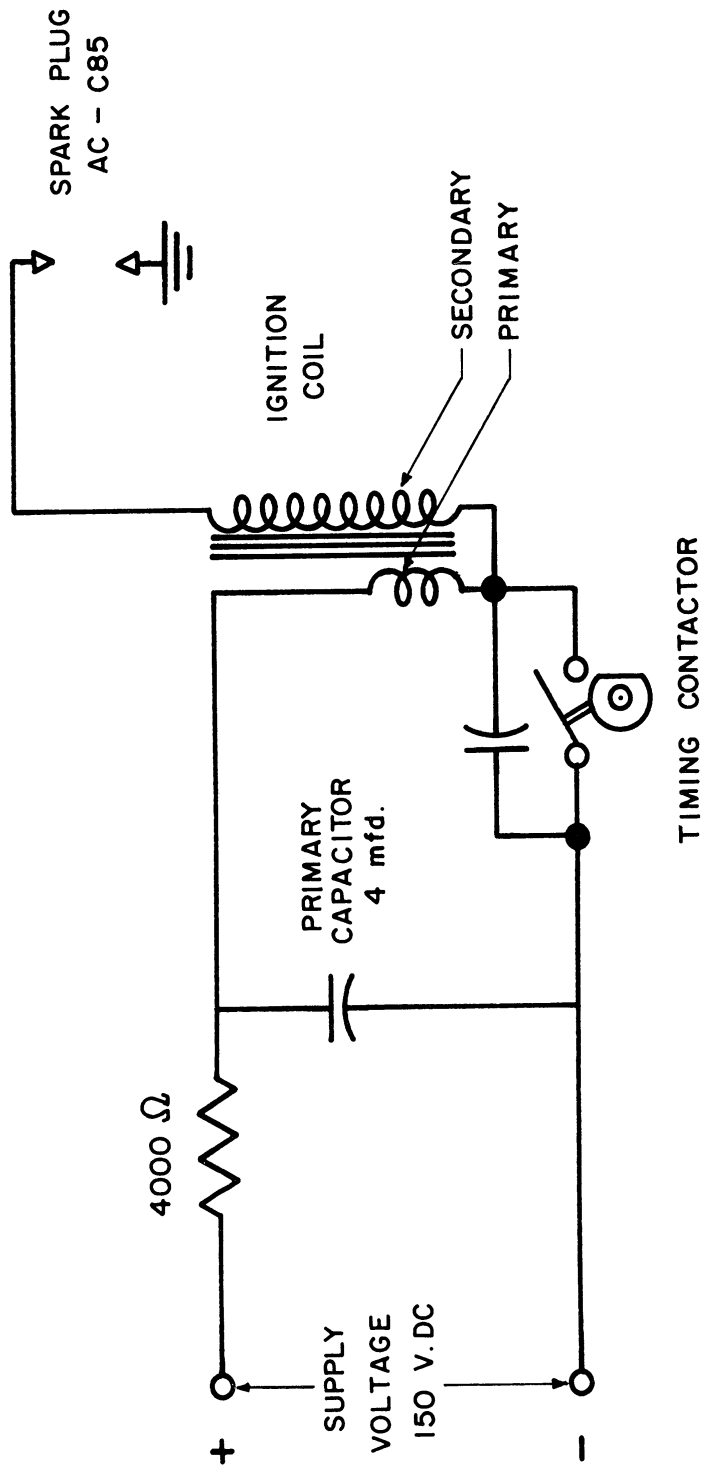

Figure 3.1 Diagram of Ignition Circuit

and voltage to be between ten and twenty millijoules, about half the total amount of energy supplied to the primary circuit.

The energy available at the spark gap was therefore several orders of magnitude larger than the minimum energy required for a chemically correct mixture, and it was concluded that the CFR ignition system provides an adequate amount of energy for measuring the lean limit. Direct experimental evidence to support this conclusion is presented below.

Several methods of varying the spark energy in air were attempted. The results are summarized in Table IV. Series resistors of various sizes were also placed in the secondary circuit. They were not effective in reducing the energy of the first surge of current, although the overall duration of the spark was reduced by the presence of the resistor. Calculation of the IR drop across the resistors at the measured current shows that the voltage rating of the resistors was far exceeded and apparently internal breakdown of the resistance occurred during the arc. Some tests were also made with a primary capacitor of 1.5 microfarads instead of the regular primary capacitor of 4.0 microfarads; the effect of reducing the primary capacitance seemed to be similar to the effect of reducing the primary voltage, namely, both the peak voltage and the number of arcs formed were reduced. Finally, some tests were run in which the primary voltage was changed.

The range of primary voltages that could be used for engine operation was determined. First, the effect of primary voltage on the peak secondary voltage available was measured; the results are shown in Figure 3.2. Second, the actual firing voltage in an operating engine was measured. It was found that the firing voltage required under the conditions of the test was eight to ten kilovolts at the

TABLE III

EFFECT OF IGNITION SYSTEM CONDITIONS
ON LEAN LIMIT IN CFR ENGINE

Speed.....1200 rpm.
Ignition Timing.. 19°B.T.C.
Compression Ratio.....7.
Intake Temperature...100°F.
Intake Pressure....10° psia.
Fuel....Commercial Propane.

Minimum Fuel-Air Ratio	Electrode Diameter	Electrode Gap	Supply Voltage
	Inches	Inches	Volts
.0415	.024	.020	135
.0415	.024	.020	150
.0411	.024	.020	200
.0415	.024	.030	150
.0413	.024	.030	250
.0413	.024	.035	250
.0416	.024	.025	150
.0412	.024	.020	150
.0422	.024	.015	150
.0437	.024	.012	150
.0416	.024	.025	150
.0416	.040	.025	150
.0428	.064	.025	150
.0454	.120	.025	150
.0481	.120	.020	150
.0454	.120	.025	150
.0438	.120	.030	150
.0421	.120	.035	175
.0411	.120	.060	200

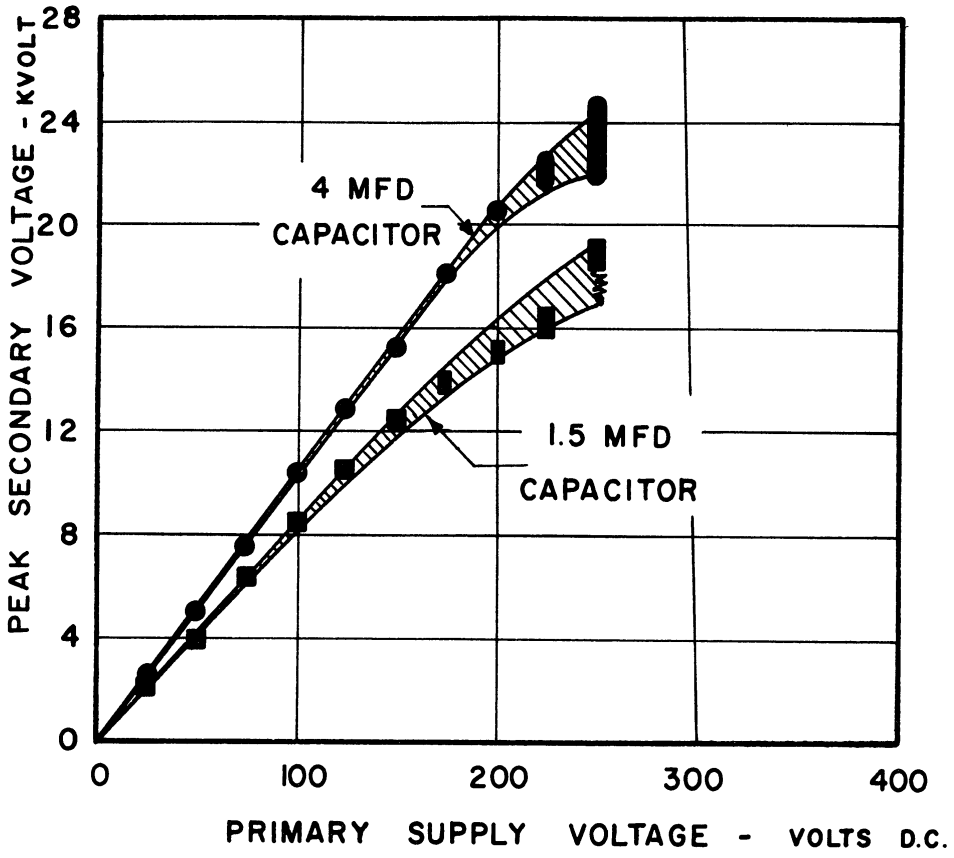

Figure 3.2 Available Secondary Voltage as a Function of Primary Voltage. CFR Ignition System. Motoring Engine at 1200 rpm. Secondary Voltage Measured with Heyer Dynatester.

leanest mixtures used (see Figure 3.3). A minimum primary voltage of approximately 135 volts was thus established. It was also found that the peak current and amount of charge passing through the arc could be increased by raising the primary voltage, as shown in Figure 3.4. Thus, by varying the primary voltage, the energy of the spark could be varied somewhat, provided that the primary voltage available was sufficient to initiate the spark. Accordingly, some measurements of the lean limit were made with various primary voltages between 135 and 250 volts DC. The results of these measurements are shown in Figure 3.5. No clear evidence of a substantial variation in the lean limit produced by varying the primary voltage was found. It was therefore concluded from both extrapolations of data of other investigations and actual tests that the ignition system presently used provides adequate energy for igniting the mixtures used in this study.

2. Quenching Effects

It has been observed that when the spark plug gap is made very small, the amount of energy necessary for ignition increases[68,69]. This effect has been ascribed to the quenching properties of the electrodes. The spark plug electrodes absorb a certain amount of heat from the mixture in the gap and may also destroy important active radicals or ions generated in the flame zone, thus tending to have a quenching action. In general, the distance over which a body is effective in quenching a flame depends on the geometry of the body and the properties of the fuel-air mixture burned. The susceptibility of a combustible mixture to quenching by a cool body is usually defined in terms of the parallel-plate quenching distance, the minimum separation of two parallel plates that will not

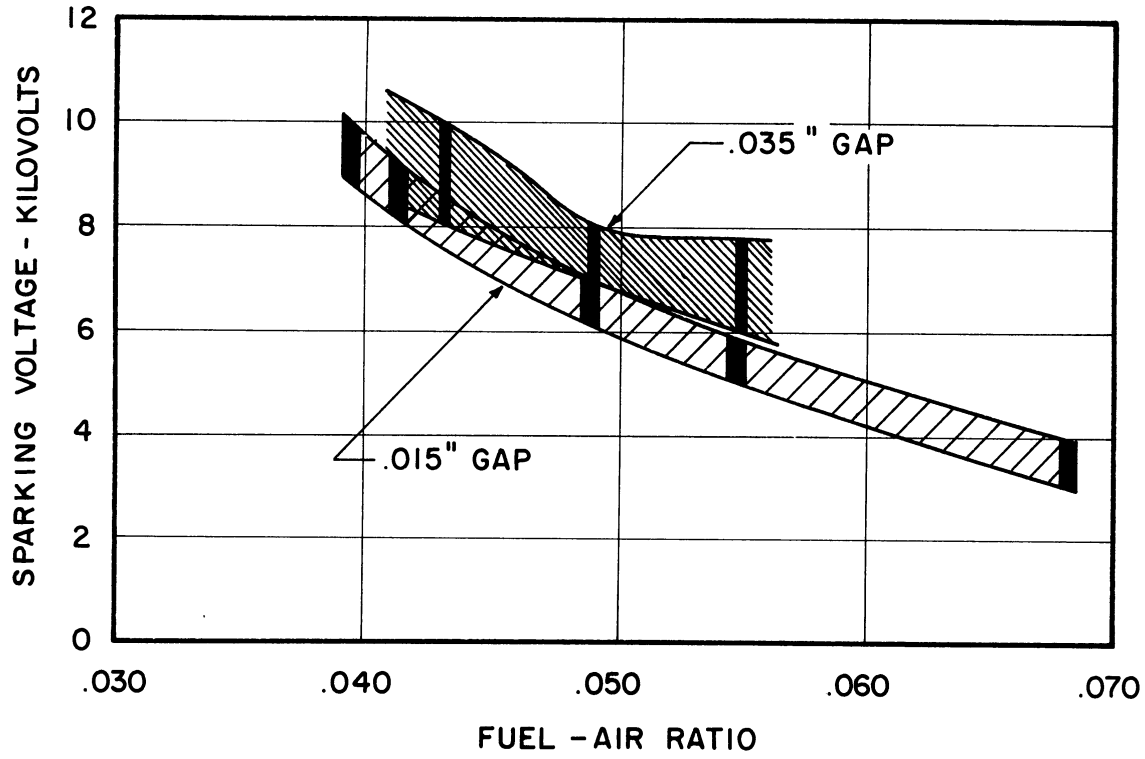

Figure 3.3 Required Secondary Voltage in Firing Engine. CFR Engine, Standard CFR Ignition System. AC Type C85 Spark Plug with .025 inch diam. electrodes. Conditions: 1200 rpm., 10 inch vacuum, 90°F intake temperature.

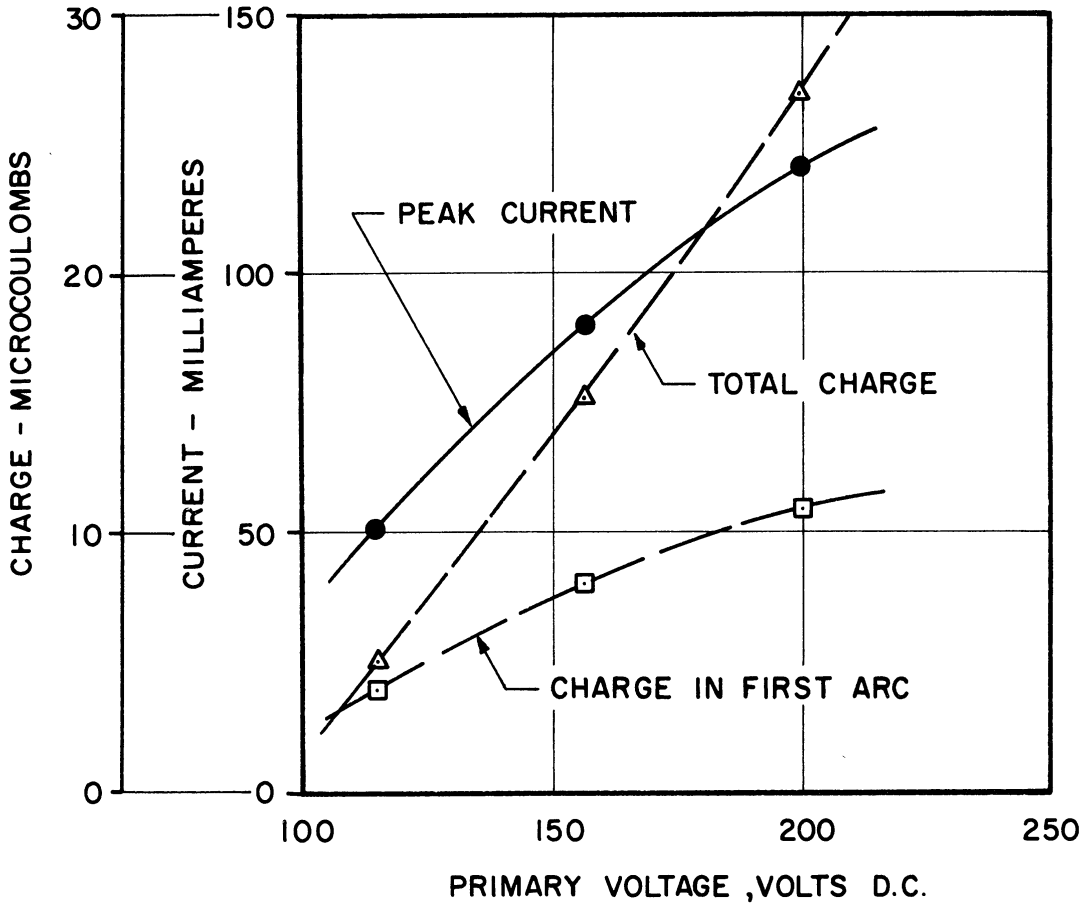

Figure 3.4 Secondary Current and Charge. CFR Ignition System Arcing 1/4 inch Gap in Air at 1 atm. and 75°F. Electrodes - .03 inch diam. wire.

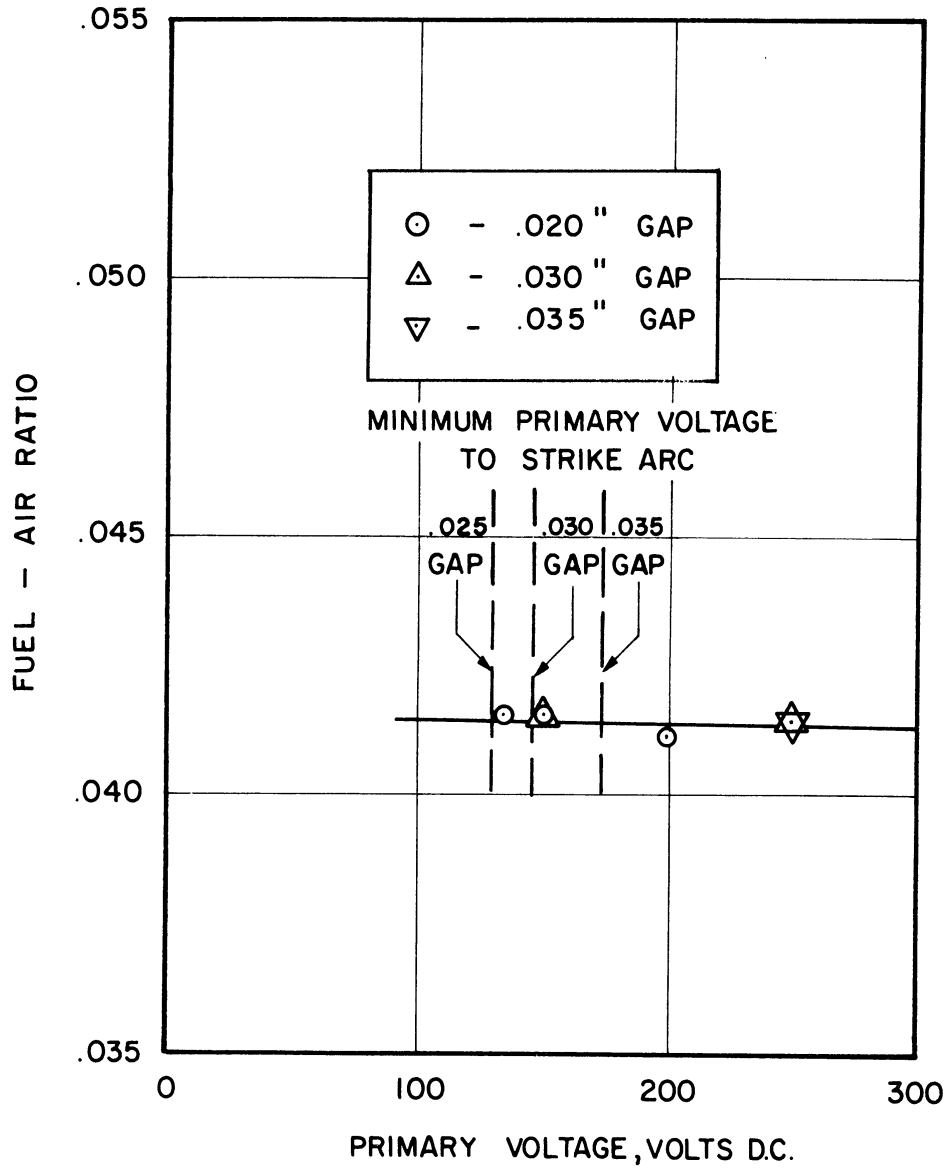

Figure 3.5 Effect of Primary Voltage on Minimum Fuel-Air Ratio for Steady Firing. Split-Head CFR Engine. Speed 1200 rpm. Intake Temperature = 100°F, Intake Pressure = 10 psia., Ignition = 19° B.T.C., Fuel - Commercial Propane, Spark Plug - AC Type C85 with .025 inch diam. Electrodes.

inhibit flame propagation in the gas enclosed between them, and in the ensuing discussion the term "quenching distance" means this parallel-plate quenching distance. If the spacing of the spark plug electrodes is less than the quenching distance of the mixture being used, quenching may take place in the spark plug gap and ignition of the mixture may thus fail to occur.

The quenching distance of a fuel-air mixture depends on the pressure and temperature of the mixture[68,69,79] and probably on the temperature of the quenching body. The temperature of the electrode surfaces under near lean-limit operation is not known but is probably relatively low. In general, the quenching distance seems to be approximately inversely proportional to the pressure; the quenching distance also decreases with increases in initial mixture temperature. Most of the data on the quenching distance have been taken at pressures below atmospheric pressure and at room temperature. In order to estimate the quenching distance in an engine, it was assumed that the relationships between pressure, temperature, and quenching distance observed at low temperatures and pressures obtain under the conditions existing in the engine. The validity of this assumption should be considered questionable and the estimated quenching distance uncertain in view of the data available. The quenching distance of a stoichiometric mixture in the engine is estimated to be .010 inches at a compression ratio of seven, and less at higher compression ratios. The quenching distance increases as the mixture is made leaner; as the lean limit is approached, the rate of increase of the quenching distance becomes large[68]. Although the quenching distance of a lean limit mixture has not been measured, the

data available show that increasing the electrode spacing to five to ten times the quenching distance of a chemically correct mixture is adequate to avoid quenching mixtures having substantially the same fuel-air ratio as the lean limit mixture.

In cases where the spacing of the electrodes is less than the quenching distance of the mixture, it may still be possible to ignite the mixture by supplying sufficient spark energy[69,84]. The amount of additional energy which must be supplied to make ignition possible depends on the relative diameter of the electrodes. If the diameter of the electrodes is equal to or smaller than the quenching distance, ignition may be secured with electrode gaps appreciably smaller than the quenching distance with very little increase in energy.

A series of tests was made in the engine at a compression ratio 7, with an intake pressure of 10 psia. and temperature of 100°F, to determine under what conditions the measured lean limit was independent of the electrode configuration. The results of these tests are shown in Figure 3.6. Following from the preceding discussion the quenching distance under the operating conditions of these tests and with approximately a lean limit mixture is estimated to be .050 inches to .100 inches. It will be seen that with .120 inch diameter electrodes, which were standard spark plug electrodes, the leanest combustible mixtures could not be ignited with spark plug gaps of less than .040 inches. On the other hand, when the diameter of the spark plug electrodes was reduced to .025 inches the spark plug gap could be reduced to .020 inches without affecting the measured lean limit. If follows therefore that these data define the range of spark plug gaps that may be used for

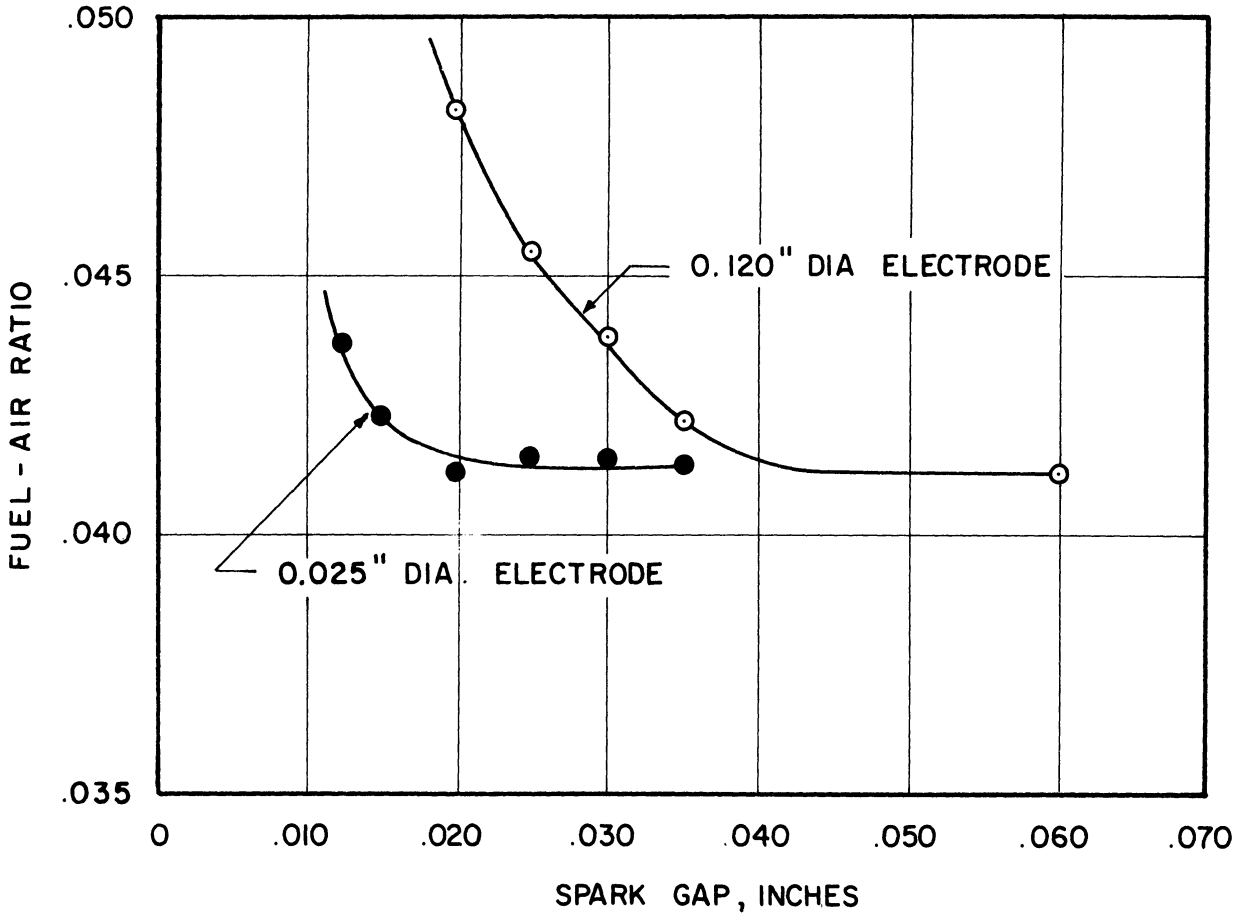

Figure 3.6 Effect of Spark Plug Size and Spacing on Minimum Fuel-Air Ratio for Steady Firing. Split-Head CFR Engine. Speed = 1200 rpm., Intake Temperature = 100°F, Intake Pressure - 10 psia., Ignition - 19° B.T.C., Fuel - Commercial Propane, Compression Ratio = 7, Spark Plug - AC Type C85.

measuring the lean limit in the engine. It also follows from the preceding discussion that the gap sizes which may be used at this compression ratio and intake temperature will also be adequate to avoid quenching at higher compression ratios and higher intake temperatures.

3. Effect of Ignition Timing

It was found that the ignition timing had some effect on the lean limit, as shown in Figure 3.7. With the spark occurring at 40° before top center, the minimun fuel-air ratio for steady firing was about five percent richer than that for 10° to 20° of advance. On the basis of the data shown in Figure 3.7, lean limit measurements were made with the ignition timing set at 19° before top center throughout.

The effect of ignition advance can be explained on the basis of the compression temperature. At 40° B.T.C. the piston has completed about 85 percent of its stroke, whereas at 20°, 95 percent of the stroke has been completed. At a compression ratio of 7, 61 percent of the computed total temperature rise has taken place at 40° B.T.C. and 87 percent of the temperature rise has taken place at 20° B.T.C. When the compression ratio is raised to 13, the temperature rise at 40° B.T.C. is only 51 percent of the total temperature rise for a full stroke, while at 20° B.T.C., 80 percent of the total temperature rise has taken place. When ignition takes place at 40° B.T.C., therefore, the temperature of the mixture is appreciably lower than the full compression temperature, and consequently the measured lean limit is somewhat richer than it would be if ignition took place at 20° B.T.C.

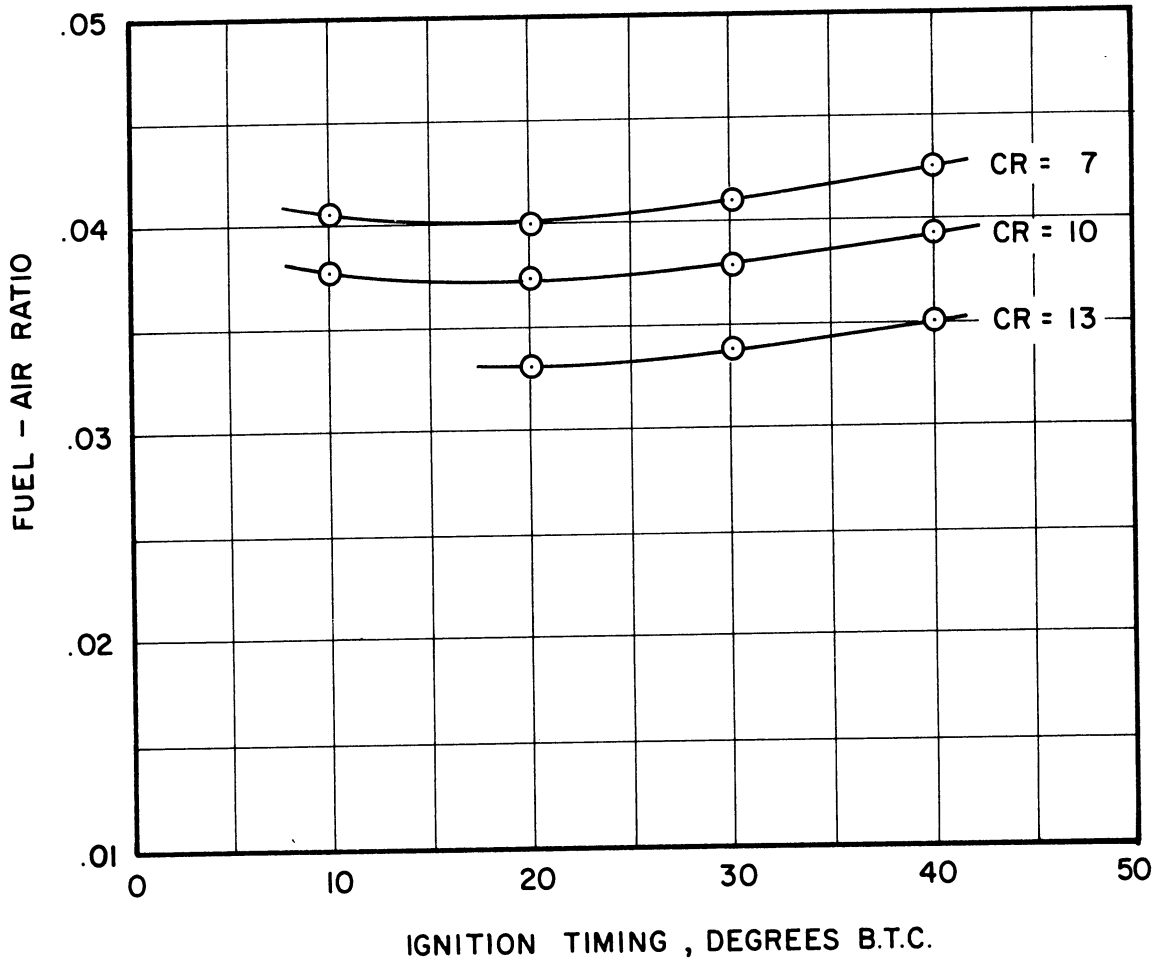

Figure 3.7 Effect of Ignition Timing on the Minimum Fuel-Air Ratio for Steady Firing. Split-Head CFR Engine. Speed = 1200 rpm., Intake Temperature = 190°F, Intake Pressure = 10 psia., Fuel - Commercial Propane.

C. Effect of Residual Exhaust Gas

In an operating engine, a part of the exhaust gas from the previous cycle is present in the cylinder when the intake valve opens and this residue mixes with the incoming fuel-air mixture. The precentage of residual gas present in the total charge is decreased when the compression ratio is increased and also when the density of the mixture in the intake manifold is increased relative to the density of the exhaust gases. In addition, the amount of residual gas varies as a function of engine speed, valve timing, valve flow characteristics, and inertia effects in the intake and exhaust manifolds.

For purposes of estimating the amount of residual gas present in the charge, the intake process is idealized as follows:

1). The exhaust valve closes at T.D.C., ending the exhaust process. The residual gas trapped in the clearance volume has the measured exhaust gas temperature and a pressure of 16.5 psia. Actually, the exhaust valve is partially open at this time and does not close completely until 15° after T.D.C. The actual temperature of the gas present in the cylinder is also probably different from the average temperature of the gas discharged into the exhaust manifold because of expansion during blowdown and heat transfer to the engine.

2). During the first part of the intake stroke the intake valve remains closed, while the residual exhaust gas expands isentropically to the intake pressure.

3). When the pressure in the cylinder reaches the average intake pressure, the intake valve opens. Fresh mixture is drawn into the cylinder and mixed adiabatically and at constant pressure with residual gas for the remainder of the intake stroke.

4). It is assumed that all processes are adiabatic and that the molecular weights and specific heats of the gases involved are constant and equal.

It can be shown (see Appendix A) that under these conditions, the fraction of residual gas is

$$f = \frac{1}{1 + r_T \left[\frac{r_V}{r_P} - \left(\frac{1}{r_P} \right)^{(k-1)/k} \right]} \tag{3.1}$$

The temperature of the mixed charge is

$$T_c = f \frac{r_V}{r_P} T_e \tag{3.2}$$

Equations similar to Equations (3.1) and (3.2) above are cited in References 9 and 17. The quantity $\frac{k-1}{k}$ was taken as .24 by these authors, corresponding to a mean specific heat at the temperatures involved, and this value has also been used in the computations in connection with this study. The computed amounts of residual exhaust gas ranged from about 8.5 percent to about three percent with most tests run in the range of three to five percent. The presence of the residual gas raised the charge temperature by varying amounts ranging from 20° to 80°F.

Other methods of determining the fraction of residual exhaust gas in the charge have been used[22,23]. The expansion of the residual gas from exhaust pressure to intake pressure has been considered as a throttling process and the flow work done during the expansion may be taken as lost to the surroundings or as added to the enthalpy of fresh

mixture. No great difference in the computed amount of residual gas results from the use of either of these assumptions instead of the method that was used.

There is some evidence that the percentages of residual gas calculated by this method are too low. In one study[23], measured values were two or three times as large as the values calculated. There is very little information available about this discrepancy and no satisfactory explanation has been given.

No tests were made in which the effect of residual exhaust gases could be directly evaluated. However, in succeeding sections of this paper, the effect of charge dilution and increase of charge temperature by the residual exhaust gases have been included in the calculations. In considering the effect of dilution, the residual gas has been treated as having the same effect as an equal mass of air. This procedure is based on data of Reference 38, where the effect of a diluent is shown to depend mainly on its specific heat. In view of the fact that the residual gas is about 80 percent nitrogen and at least six percent oxygen with the remaining 14 percent being combustion products, the effect of residual gas as a diluent should not differ appreciably from that of an equal amount of air.

D. Effect of Pressure, Temperature, and Compression Ratio

Since an increase in the engine compression ratio results in an increase in compression temperature and pressure and a decrease in the amount of residual exhaust gas, the lean limit is a function of the compression ratio, as well as the engine inlet conditions. The geometry of the combustion chamber is also changed when the compression

ratio is varied. Such a change in geometry may affect the lean limit if the heat transfer or flame quenching properties of the combustion chamber are altered significantly. In the following paragraphs, the separate effects of pressure and temperature and the overall effect of compression ratio are evaluated.

1. Effect of Intake Pressure

The effect of changing the intake manifold pressure, and thereby changing the compression pressure, is shown in Figure 3.8. The lean limit fuel-air ratio decreased from about .0410 pounds of fuel per pound of air at a pressure of 7 psia. to about .0375 at 19.4 psia.

An analysis of the data shows that the change in the lean limit was primarily due to a decrease in the amount of dilution by residual exhaust gases, however. The lower curve in Figure 3.8 is plotted in terms of the fraction of fuel in the charge where the charge includes the residual exhaust gases. The fraction of fuel in the charge decreased from about .0372 at 7 psia. to about .0364 at 19.4 psia. In view of the uncertainties in determining the point of misfiring, this change is not necessarily significant. It may therefore be concluded that changing the compression pressure produces little, if any, change in the minimum percentage of fuel required in the charge.

The fact that changing the pressure does not change the lean limit significantly except at pressures of the order of 0.1 atmospheres or less has been reported in several other investigations[29,33,42,58]. It is to be noted that the lean limit equation which has been proposed predicts that the lean limit will be independent of pressure. The experimental data are therefore consistent with this prediction.

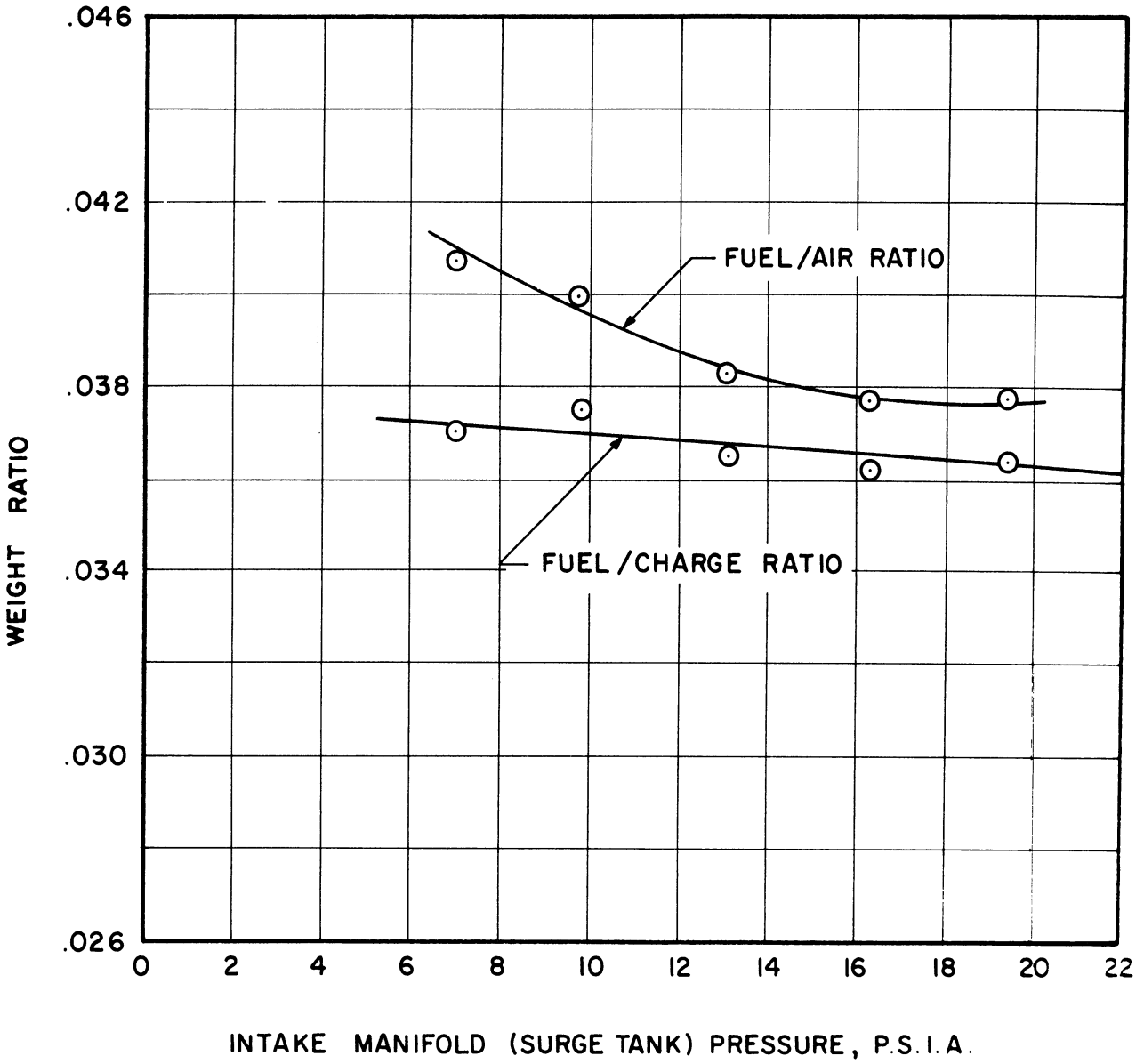

Figure 3.8 Effect of Intake Pressure on Minimum Fuel-Air Ratio for Steady Firing. Split-Head CFR Engine. Speed = 1200 rpm., Intake Temperature = 100°F, Ignition = 19° B.T.C., Exhaust Pressure = 1 atm., Compression Ratio = 9, Fuel - Commercial Propane.

2. Effect of Temperature and Compression Ratio

The effects of intake manifold temperature and engine compression ratio on the minimum fuel-air ratio for steady firing are shown in Figure 3.9. It will be seen that the minimum fuel-air ratio decreases about five percent for an increase of 100°F in the intake temperature. The minimum fuel-air ratio also decreases about 20 percent when the compression ratio is raised from 7 to 16.

These data were taken with the ignition timing fixed at 19° B.T.C. If the ignition were to occur too early in the cycle, the charge would be only partly compressed and the temperature and pressure of the charge would be appreciably lower than at top dead center. The ignition timing was therefore chosen in accordance with the data presented in Figure 3.7, where the effect of ignition timing is shown and where it can be seen that the lean limit is not affected by ignition timing when the ignition occurs within 20° before top dead center.

Because the engine speed and mass rate of flow of air were held constant during these tests, the intake manifold pressure increased from 11 psia. to 13.3 psia when the intake temperature was changed from 100°F to 300°F. The intake manifold pressure was measured in the surge tank from which air was supplied to the engine and represents the average pressure in the intake manifold. Due to the pulsating type of flow present in the intake manifold, the pressure at the intake port of the engine varies during the engine cycle, and the average surge tank pressure does not therefore necessarily represent an accurate measurement of the effective intake pressure. In contrast, the air consumption of the engine was readily controlled and measured with the

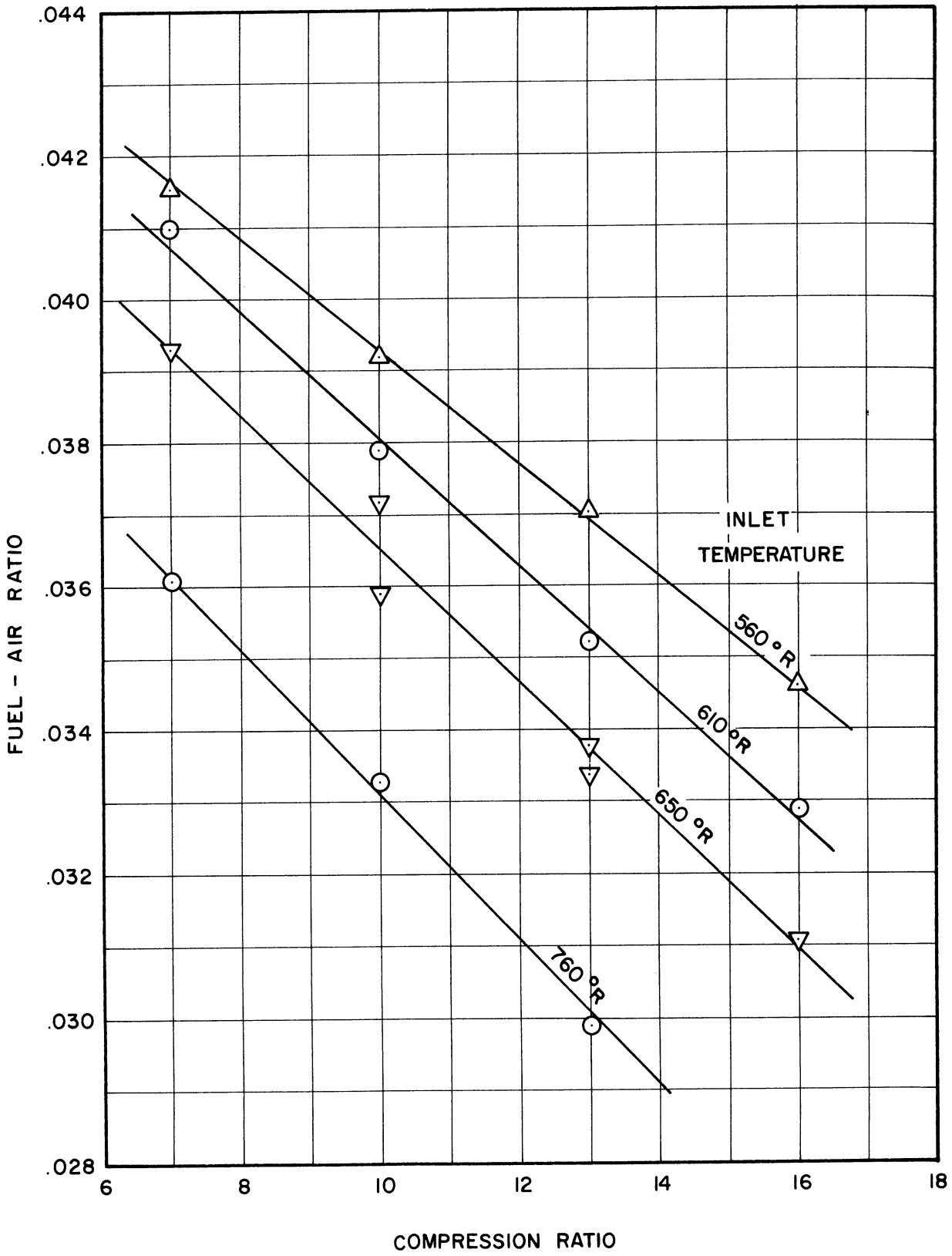

Figure 3.9 Effect of Temperature and Compression Ratio on Minimum Fuel-Air Ratio for Steady Firing. Split-Head CFR Engine. Speed = 1200 rpm., Ignition = 19° B.T.C., Air Flow = 29.5 lb/hr., Fuel - Commercial Propane.

instrumentation used in this study. Consequently, it was felt that in this series of tests the air flow should be regulated and no attempt should be made to maintain a given intake pressure.

In summary, it can be said that variations in intake pressure result in little change in the minimum fraction of fuel in the charge necessary for steady firing. When the intake temperature is raised or the compression ratio increased, however, somewhat leaner mixtures can be burned.

E. Correlation of Effects of Engine Variables

In Chapter I, the propagation of flame was considered as a thermal phenomenon. It was shown that the minimum fraction of fuel necessary to render a mixture combustible was a function of the temperature of the mixture and some of the properties of the components of the mixture. With a given set of components, for example propane and air, this lean limit was shown to be a function of temperature only, according to the equation:

$$-\frac{F_L h_{RP}}{C_P} = T_T - T_R \qquad (1.9)$$

The results of the experimental study may be interpreted in the light of this equation.

First, the effect of pressure on the lean limit is similar to that predicted by this equation. It was shown in Figure 3.8 and also predicted by Equation (1.9) that the minimum fraction of fuel necessary to sustain combustion in the charge is independent of the pressure. A number of other investigations have shown that the lean limit is

essentially independent of pressure over a wide pressure range[27,28,32,33,42,44,58,59,61]. An exception to this general principle occurs at low pressures of the order of 0.1 atmospheres, where a minimum pressure for flame propagation apparently occurs. This exception is not accounted for by the equation that has been proposed and is evidence that the equation is somewhat oversimplified. In this study, however, pressures during combustion were at least several atmospheres in all cases.

Secondly, the effect of intake temperature and compression ratio on the lean limit may be shown in relation to the temperature of the charge after compression. To use the terms of the lean limit Equation (1.9) the compression temperature and heating value of the mixtures corresponding to the data presented in Figure 3.9 were expressed in the dimensionless terms, T_R/T_T and $-\frac{F_L\ hRP}{C_P\ T_T}$, respectively. The relationship between the dimensionless heating value and the dimensionless temperature of the reactants is shown in Figure 3.10. The data included here apply to a range of compression ratios from 7 to 16 and intake temperatures from 100°F to 300°F. The minimum dimensionless heating value necessary for combustion, i.e., the lean limit, was found to range from .884 to .608 corresponding to dimensionless temperatures ranging from .426 to .700. The onset of misfiring is shown to occur with mixtures about 35 percent richer than the predicted lean limit mixture. As shown in Figure 3.10, the effect of increasing the compression ratio on the lean limit is very similar to the effect of raising the inlet temperature. The lean limit apparently depends on the compression temperature rather than the compression ratio itself, as shown by the fact that, at a given compression temperature, the lean limit for various compression ratios is approximately the same.

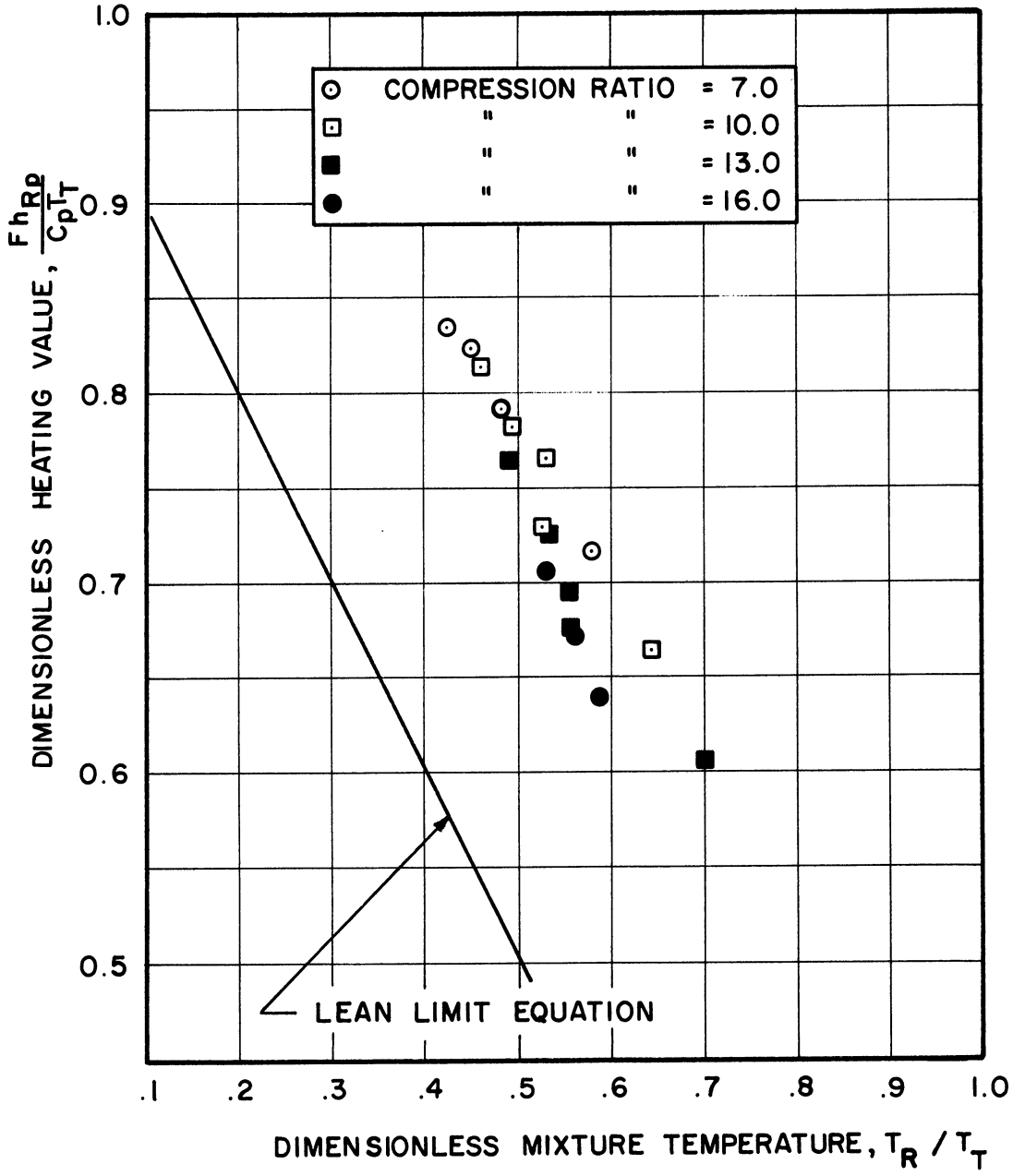

Figure 3.10 Mixture Heating Value as a Function of Compression Temperature. Split-Head CFR Engine. Speed = 1200 rpm., Ignition = 19° B.T.C., Intake Pressure = 11-13 psia., Exhaust Pressure = 1 atm., Fuel - Commercial Propane.

It should be pointed out that the results shown in Figure 3.10 were computed on the basis of an assumed isentropic compression of the charge from an initial state attained after mixing with the residual gas. It has been shown that the compression process is approximately isentropic[13,14,23]. However, the initial state of the charge is somewhat uncertain due to lack of accurate knowledge of the amount and temperature of the residual exhaust gas. It is probable that the actual temperature of the residual gas is lower than was assumed due to heat loss to the body of the engine. There is some evidence that the amount of residual gas is appreciably larger than that calculated[14,23], possibly due in part to the lower temperature. The errors resulting from the inexactness of the residual gas computation are such that the actual compression temperature may be up to 100° lower than the calculated temperature, and the dimensionless heating value also as much as .03 less than the calculated value. These possible errors are largest at the lowest compression ratio, and become small at a compression ratio of 16.

An important reason that the lean limit was found to occur at appreciably richer mixtures than was expected probably lies in the way the lean limit was defined. The lean limit was measured at the onset of misfiring, that is, the leanest mixture that would ignite on every cycle. It was noted that the engine could be run on appreciably leaner mixtures before misfiring became as frequent as one cycle out of four or five. Other investigators have reported the existence of a range of lean fuel-air ratios where laminar flame propagation occurs irregularly[28,33,42,58]. The direction of flame propagation is important in establishing the lean limit[28,33], probably as a result of flame-induced convection currents. In an engine, where turbulence, temperature gradients, and mixing with residual gases all occur, flame

propagation irregularities are likely to be greater than those encountered in laminar flame experiments. Therefore, the onset of misfiring in an engine will probably occur at a richer mixture than the lean limit measured in a combustion bomb or tube.

An additional factor tending to make the onset of misfiring occur at a richer mixture is the possible nonuniformity of the mixture due to inadequate mixing of the fuel and air. The fuel-air mixture passes through two elbows and an air heater before entering the cylinder, and the turbulence induced by these elements aids in mixing the fuel and air. No change in engine operation was observed when a copper mesh flame arrestor was inserted in the intake passage of the engine; the additional turbulence generated by the flame arrestor apparently did not improve the mixing of fuel and air significantly. The uniformity of the charge was not measured, and it is impossible to state positively whether the mixing of fuel and air was adequate.

The compression stroke of the engine occupies a period of .025 seconds at the speed used in these tests, 1200 rpm. It was pointed out at the end of Chapter I that the duration of preheating of the fuel-air mixture has an effect on the lean limit[47]. This effect is probably due to preflame chemical reactions in the mixture. Although the rate of such reactions undoubtedly increases with the preheating temperature, there is insufficient information available to predict the effect of preflame reactions during the high temperature portion of the compression stroke. No attempt was made in the present study to determine the effect of variations in the rate of compression, i.e., engine speed, on the lean limit.

In summary, it may be said that the minimum percentage of fuel in the charge required for steady firing in an engine is independent of the pressure in the cylinder and decreases linearly as the compression temperature increases. The only effect that a change in the intake manifold pressure could clearly be shown to have on the minimum fuel-air ratio is a secondary effect due to changes in the amount of residual exhaust gas. The minimum fuel-air ratio decreased with an increase in either compression ratio or intake manifold temperature in a manner such that the fraction of fuel in the total charge was a linear function of the compression temperature. The only effects of changes in compression ratio on the lean limit that could be clearly demonstrated were the effect of compression temperature and the secondary effect of changes in the amount of residual exhaust gas.

CHAPTER IV

ENGINE PERFORMANCE WITH LEAN MIXTURES

A. Performance Tests

In addition to information about the range of mixtures which can be successfully ignited in an engine, it is of considerable practical interest to know the performance characteristics of an engine with a lean mixture. Performance tests were therefore made to determine the power and efficiency of the engine operating with a range of lean fuel-air ratios. Data were taken at compression ratios of 5.5, 7, 10, 13, and 14.9. The engine was operated at 1200± 5 rpm. and at part throttle; the intake pressure was approximately 10 psia. Part throttle operation was used because the anti-knock requirement could not be met satisfactorily at full throttle. The intake temperature was held fixed at 100° ± 2°F. M.b.t. ignition timing was used in all tests. That is, the ignition timing was adjusted for maximum power and when a range of ignition advance settings gave the same maximum power, the minimum advance in this range was used. The spark plug gap used in these tests varied from .020 inches to .060 inches; in general, the largest gap that would arc reliably under engine operating conditions was used.

B. Observed Performance Characteristics

1. Power Output

The power output of the engine operating over a range of fuel-air ratios from about .040 to .060 lb. fuel/lb. air is shown in Figure 4.1. The horsepower figures given refer to indicated horsepower, obtained by adding the friction horsepower absorbed in motoring the engine

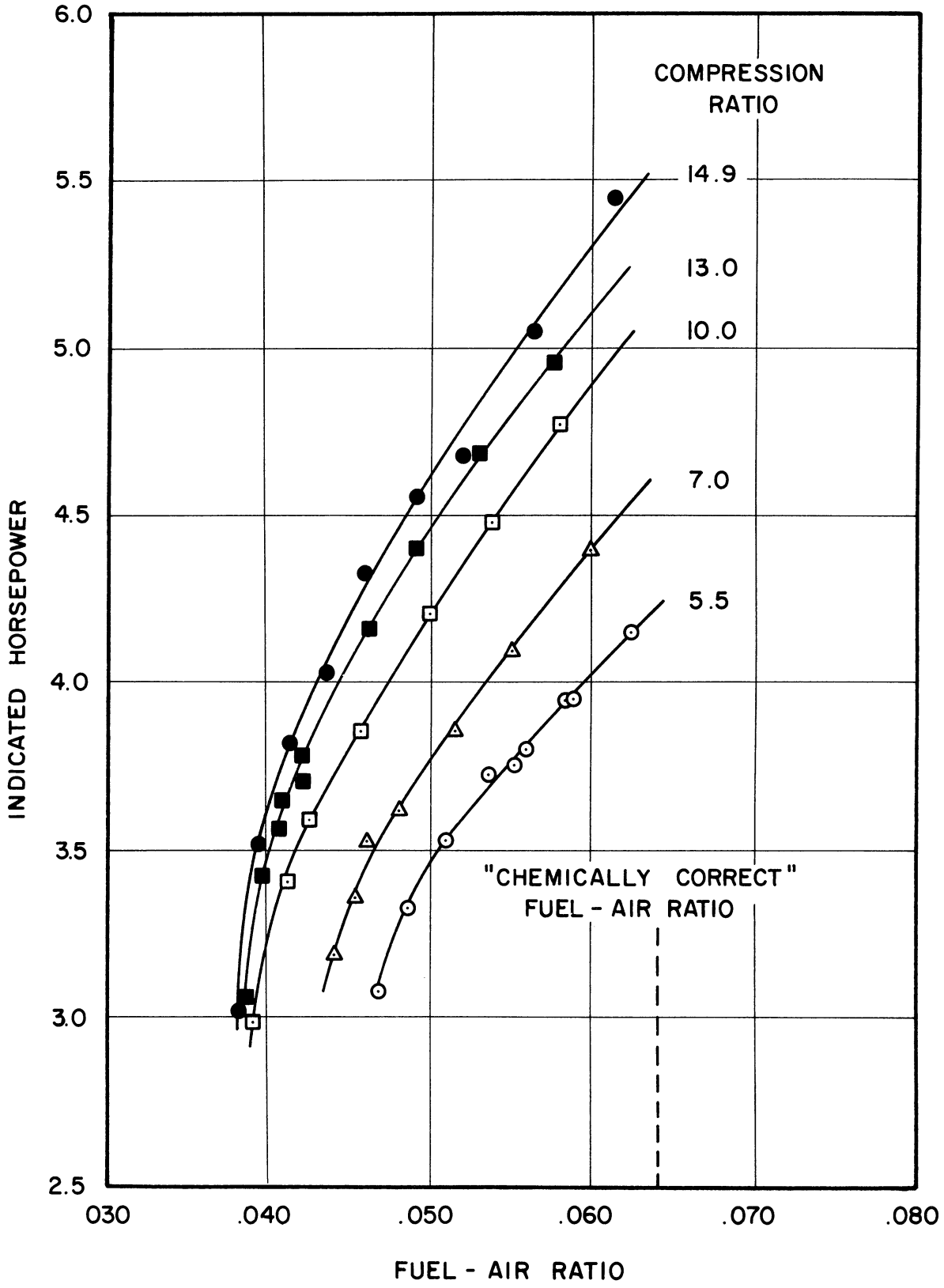

Figure 4.1 Effect of Fuel-Air Ratio on Indicated Horsepower. Split-Head CFR Engine. Speed = 1200 rpm., Intake Pressure = 10 psia., Intake Temperature = 100°F, Exhaust Pressure = 1 atm., Ignition Timing - m.b.t., Fuel - Commercial Propane.

to the brake horsepower of the engine. In all cases, horsepower decreased appreciably as the mixture was made leaner, and over most of the mixture range horsepower was roughly proportional to the fuel-air ratio. Within this proportional range, the decrease in power with lean mixture was simply due to supplying less energy in the form of fuel. For the leanest mixtures, however, the horsepower decreased more rapidly than the fuel-air ratio, indicating that the engine did not utilize the very lean mixtures as efficiently as the somewhat richer mixtures. Leaner mixtures could be burned when the compression ratio was increased, and for a given fuel-air ratio the engine produced more power at high compression ratios.

2. Optimum Ignition Timing

It was found that when either the compression ratio or the fuel-air ratio was altered, the combustion characteristics were changed to the extent that it was necessary to adjust the ignition timing for maximum efficiency at each operating point. The experimentally determined optimum ignition timing is shown in Figure 4.2. The effect of fuel-air ratio is such that the point of ignition had to be advanced about 30 crankshaft degrees in spanning the range from a stoichiometric fuel-air ratio of .064 to the leanest mixture used at each compression ratio. At the lowest compression ratio, 5.5, the engine required 20° to 40° more spark advance at a given fuel-air ratio than at a compression ratio of 14.9. The amount of ignition advance required under given conditions is related to the duration of combustion. The fact that ignition timing must be advanced when the mixture is made leaner signifies the combustion takes a longer time when the mixture is lean than when it is rich. A more detailed discussion of the effect of fuel-air ratio and compression ratio on combustion time will be found in Chapter V.

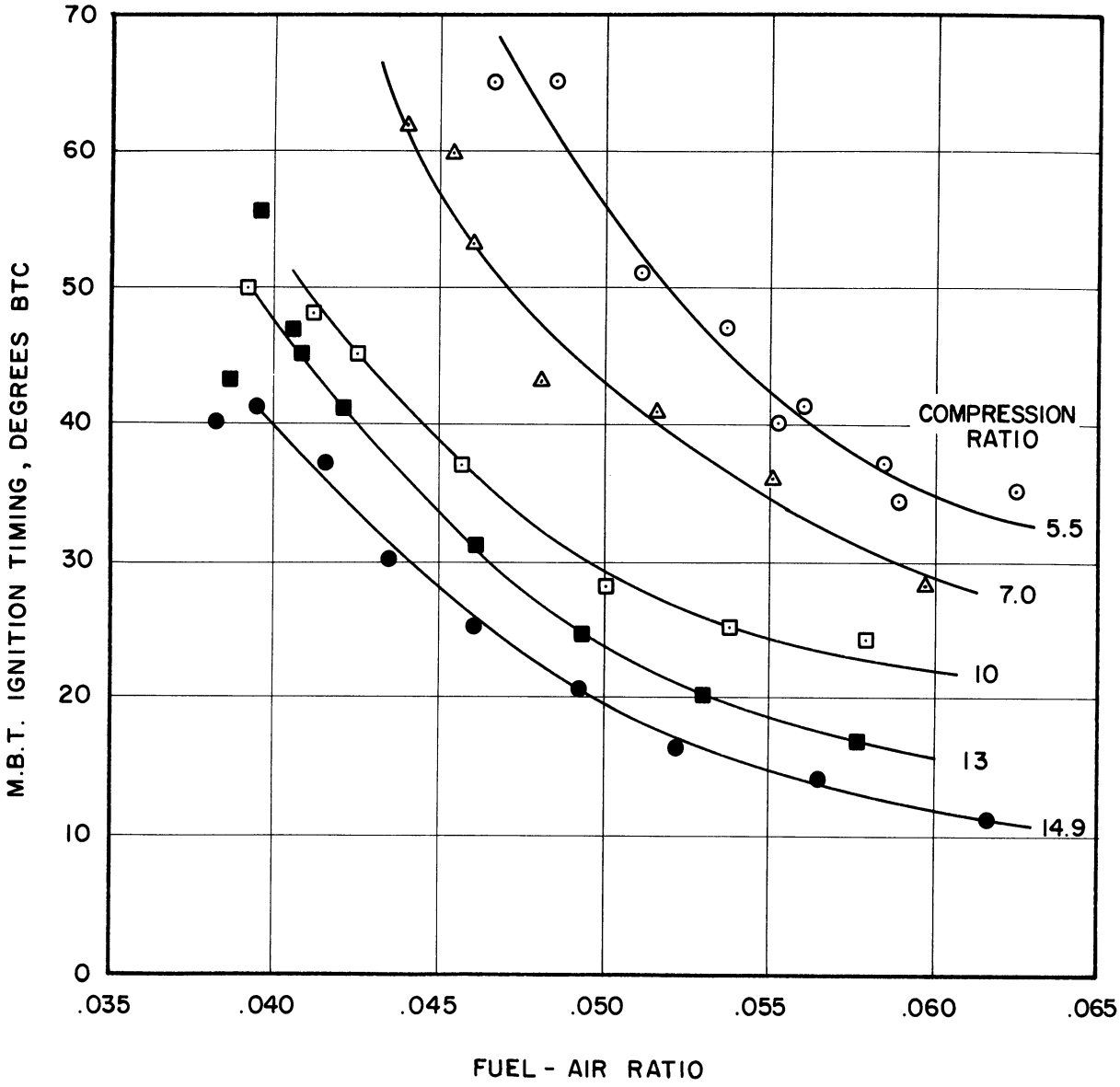

Figure 4.2 Effect of Fuel-Air Ratio on Optimum (m.b.t.) Ignition Timing. Split-Head CFR Engine. Speed = 1200 rpm., Intake Pressure = 10 psia., Intake Temperature = 100°F, Exhaust Pressure = 1 atm., Ignition Timing - m.b.t., Fuel - Commercial Propane.

3. Exhaust Temperature

The exhaust temperature, measured in the exhaust pipe about five inches from the exhaust port, is shown in Figure 4.3 as a function of the fuel-air ratio and compression ratio. It was found that the exhaust temperatures decreased 150° to 250°F as the mixture was made leaner in nearly linear fashion except at the very lean mixtures. The exhaust temperature also was less at high compression ratio than at low compression ratio, varying about 250°F over the range of compression ratios used, namely, 5.5 to 14.9.

The exhaust process represents the heat rejection phase of the fundamental Otto cycle. When the mass flow is constant, as in the series of tests in this study, the quantity of heat rejected is indicated by the elevation of exhaust temperature above the intake temperature. Unfortunately the exhaust temperature does not represent all of the heat rejected in a practical working engine because of an appreciable amount of heat transferred to the walls of the combustion chamber and ultimately to the engine cooling water or the atmosphere. The exhaust temperature can therefore be taken only as a relative measure of the amount of heat rejected.

The data on exhaust temperatures shown in Figure 4.3 can be interpreted as showing that the amount of heat rejected by the engine decreases as the mixture is made leaner and as the compression ratio is raised. The effect of compression ratio on the amount of heat rejected results from the fact that at high compression ratios, a larger portion of the energy supplied is converted to useful work than at a low compression ratio. The remaining energy, to be rejected as heat, is consequently reduced as the compression ratio is raised. When the

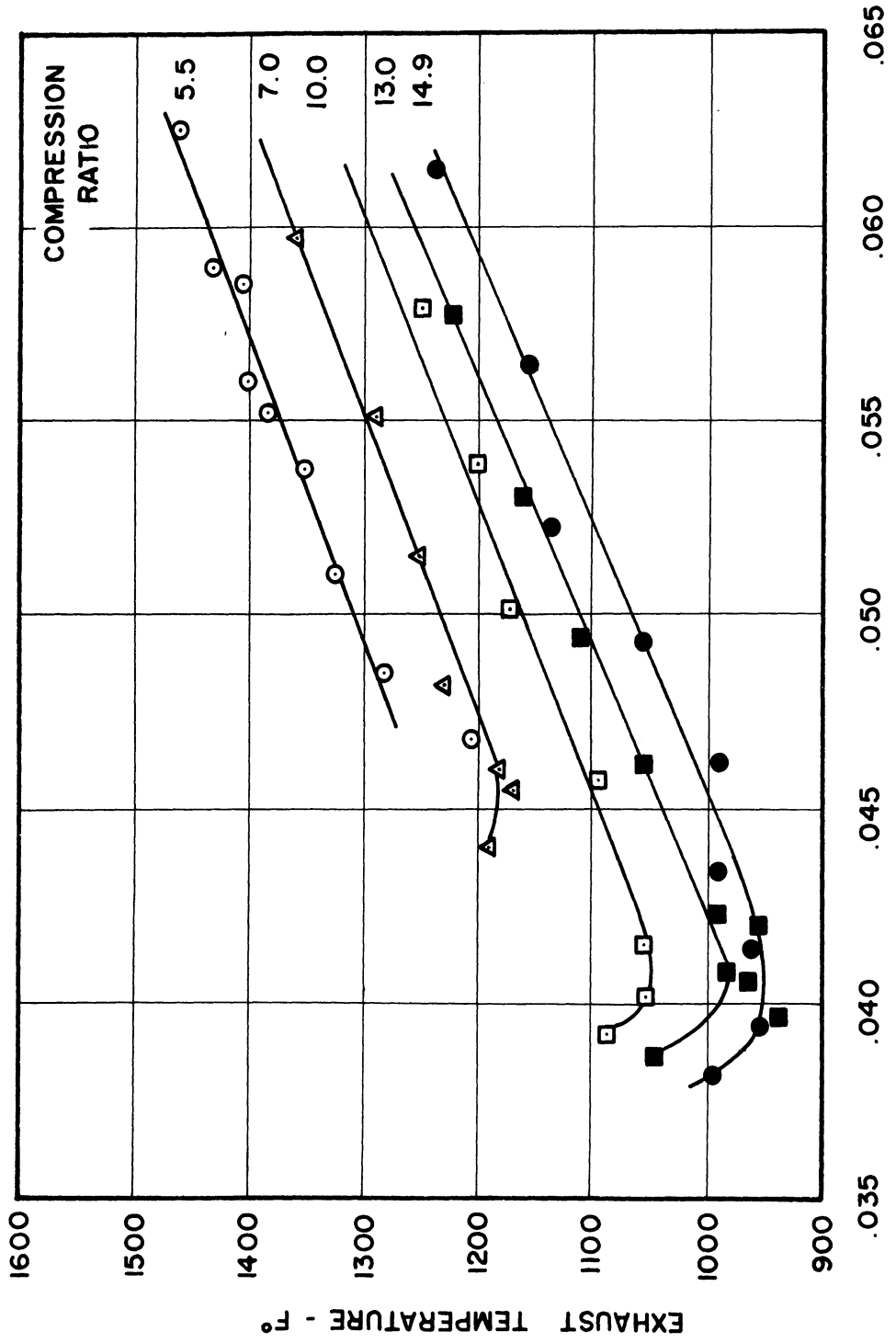

Figure 4.3 Effect of Fuel-Air Ratio on Exhaust Gas Temperature. Split-Head CFR Engine. Speed = 1200 rpm., Intake Pressure = 10 psia., Intake Temperature = 100°F, Exhaust Pressure = 1 atm., Ignition Timing - m.b.t., Fuel - Commercial Propane.

fuel-air ratio is changed, however, the efficiency of the engine is nearly constant over most of the mixture range, as will be shown in a subsequent section. The reduction in exhaust temperature obtained with lean mixtures within the range of nearly constant efficiency is due entirely, therefore, to a reduction in the amount of energy supplied as fuel.

It will be observed that in the region of the very leanest mixtures the exhaust temperature rises. As will be shown subsequently, this region of rising exhaust temperature corresponds to a range of fuel-air ratios where the efficiency is no longer constant but decreases rapidly with a reduction in the fuel-air ratio. In this range of fuel-air ratios, engine operation is marginal, and it is difficult to obtain consistent data. At some points in this region, a reduction in exhaust temperature instead of an increase was found. This reduction in temperature probably represents the effect of incomplete combustion in an appreciable number of cycles.

4. Friction Horsepower

In Figure 4.4, the variation in motoring friction horsepower with changes in compression ratio is shown. The friction horsepower increased about 15 percent as the compression ratio was raised from 5.5 to 14.9. This increase in friction is probably the result of the increased bearing loads caused by the high gas pressures accompanying an increase in compression ratio. The friction horsepower was independent of the power level at which the engine was operated immediately prior to the motoring test, provided the oil temperature was closely regulated.

The friction horsepower was measured by motoring the engine with the ignition system shut off, other conditions being the same as

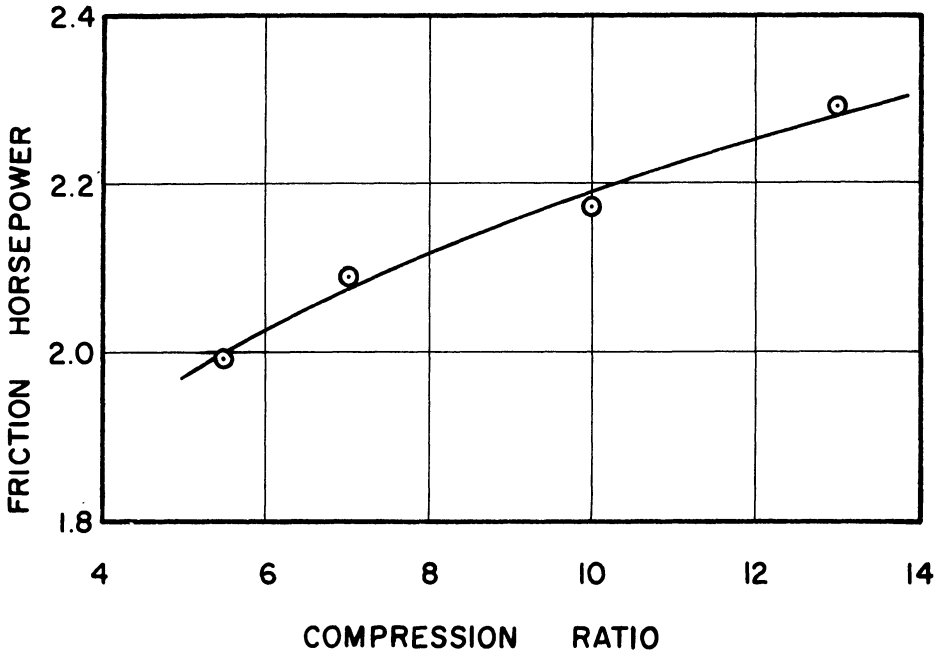

Figure 4.4 Motoring Friction Horsepower as a Function of Compression Ratio. Split-Head CFR Engine. Speed = 1200 rpm., Intake Pressure = 10 psia., Intake Temperature = 100°F, Exhaust Pressure = 1 atm., Oil Temperature = 150 ± 2°F.

when the engine was firing. This method may be criticized as being inaccurate. In particular, if the conclusion drawn above, namely, that high gas pressures increase the friction horsepower, is valid, it is clear that the friction horsepower will be greater when the engine is firing than when it is not firing. Moreover, the friction will tend to increase as the mixture is made richer and progressively higher gas pressures are developed. On the basis of a comparison of the compression pressures to the firing pressures, it is estimated that the actual friction horsepower when firing a nearly stoichiometric mixture is about seven percent or .15 horsepower greater than that measured. With the leanest mixtures used, the friction horsepower when firing is estimated to be about 3.5 percent or .07 horsepower greater than the motoring friction. The figures given for indicated horsepower correspond to the measured friction and are therefore probably too low by the amounts given above.

It should also be pointed out that the "pumping work" involved in inducting the air to the engine is considered as friction work when measuring engine friction by motoring. This pumping work originates from the difference in pressure between intake and exhaust and from other pressure differences due to flow losses in valves and manifolding. The pumping work is probably somewhat greater when the engine is firing than when it is not firing because the gas exhausted is considerably hotter, and therefore greater in volume, when the engine is firing. The pressure during the initial part of the exhaust stroke is also somewhat different when the engine is firing from that present when it is not firing.

C. Efficiency of the Engine

The efficiency of the engine as a device for energy conversion is shown in Figures 4.5, 4.6, and 4.7. In general, the thermal efficiency is a measure of the extent to which the chemical energy supplied as fuel is converted to the desired form, namely mechanical work. Several bases for calculating efficiency have been used to aid in understanding various aspects of engine operation.

Most of the data is given here in terms of the indicated thermal efficiency, which is based on the power developed by the working medium in the cylinder, that is, the indicated horsepower, and the enthalpy of combustion of the fuel supplied. The indicated thermal efficiency is useful for analyzing the efficiency of energy conversion processes within the engine cylinder. The effect of fuel-air ratio and compression ratio on the indicated thermal efficiency is shown in Figure 4.5 and a second time in Figure 4.6. It will be noted that over most of the range of fuel-air ratios used, the efficiency rises when the mixture is made leaner. The maximum thermal efficiency was about five percent greater than that obtainable with a stoichometric mixture. It was shown in Figure 4.1 that the horsepower decreases as the mixture is made leaner. However, as shown in Figure 4.5, this decrease in horsepower does not result from a failure to use fuel efficiently but simply from the fact that less fuel is supplied. As the mixture is made very lean, however, a point of maximum efficiency is reached. It was found that the efficiency falls very rapidly if the mixture is made still leaner. This point of transition can then be taken as the lean limit of useful mixture ratios.

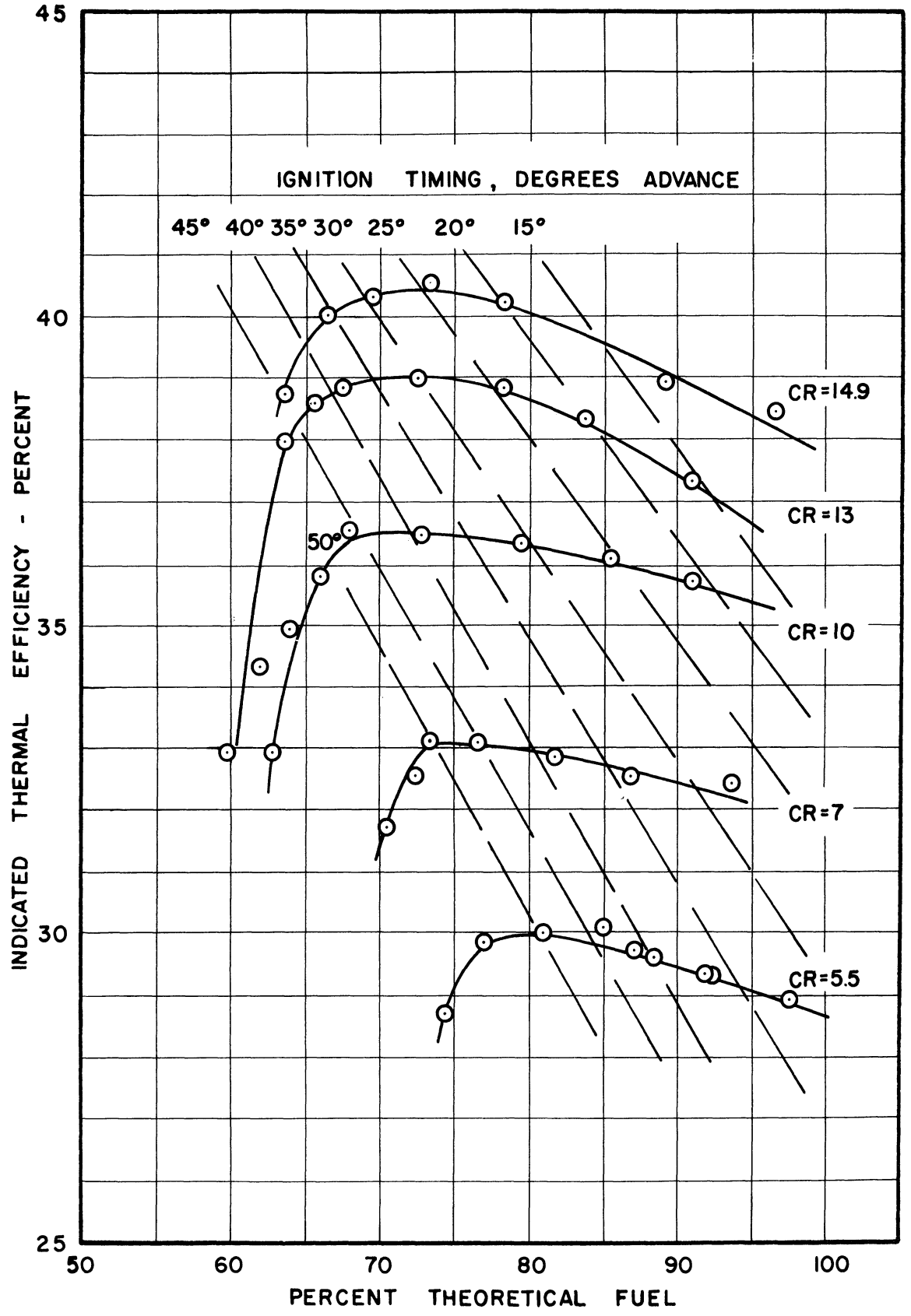

Figure 4.5 Effect of Fuel-Air Ratio on Thermal Efficiency and Optimum Ignition Timing. Split-Head CFR Engine. Speed = 1200 rpm., Intake Pressure = 10 psia., Intake Temperature = 100°F., Exhaust Pressure = 1 atm., Oil Temperature = 150 ± 2°F.

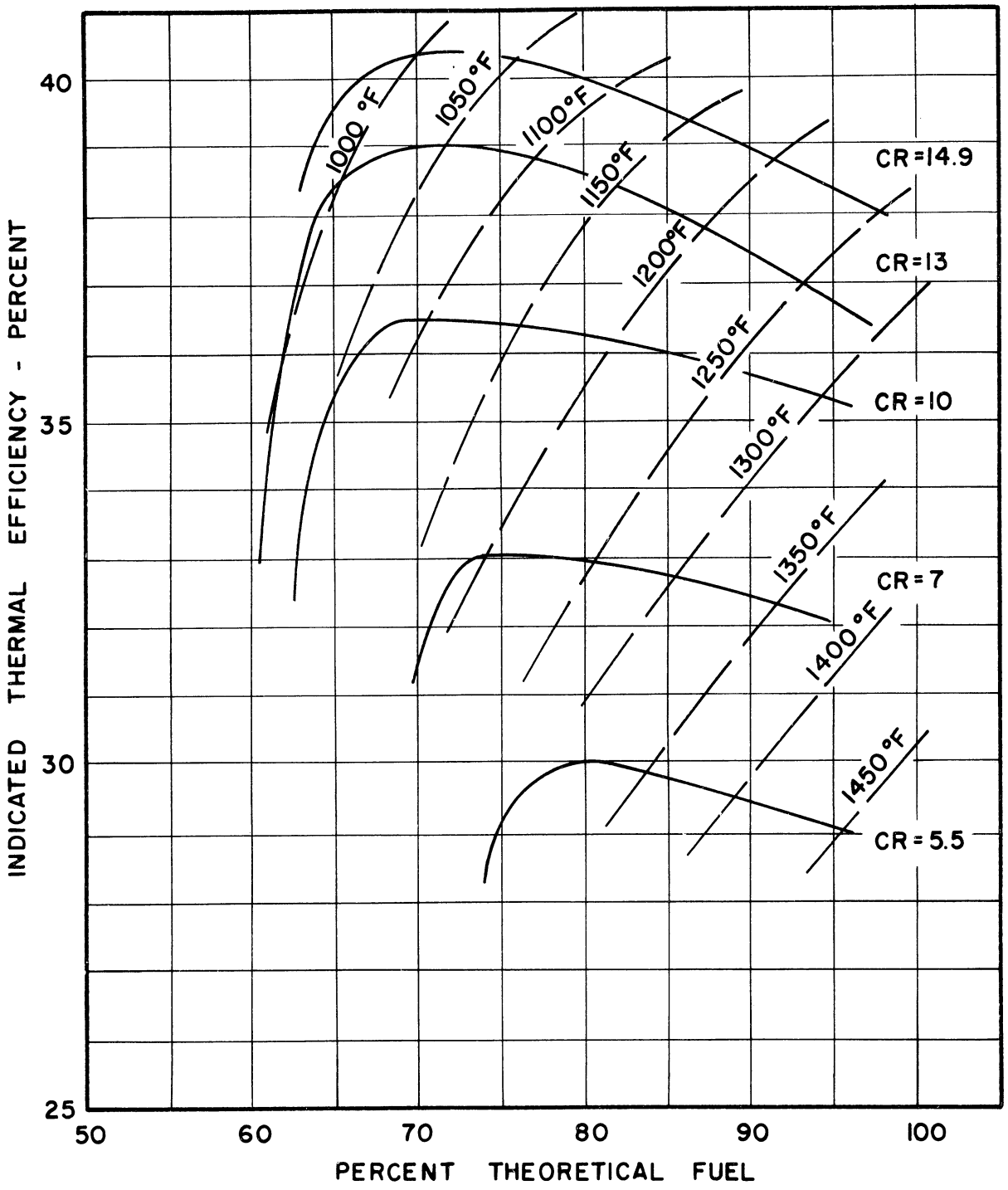

Figure 4.6 Effect of Fuel-Air Ratio on Thermal Efficiency and Exhaust Gas Temperature. Split-Head CFR Engine. Speed = 1200 rpm., Intake Pressure = 10 psia., Intake Temperature = 100°F., Exhaust Pressure = 1 atm., Oil Temperature = 150 ± 2°F.

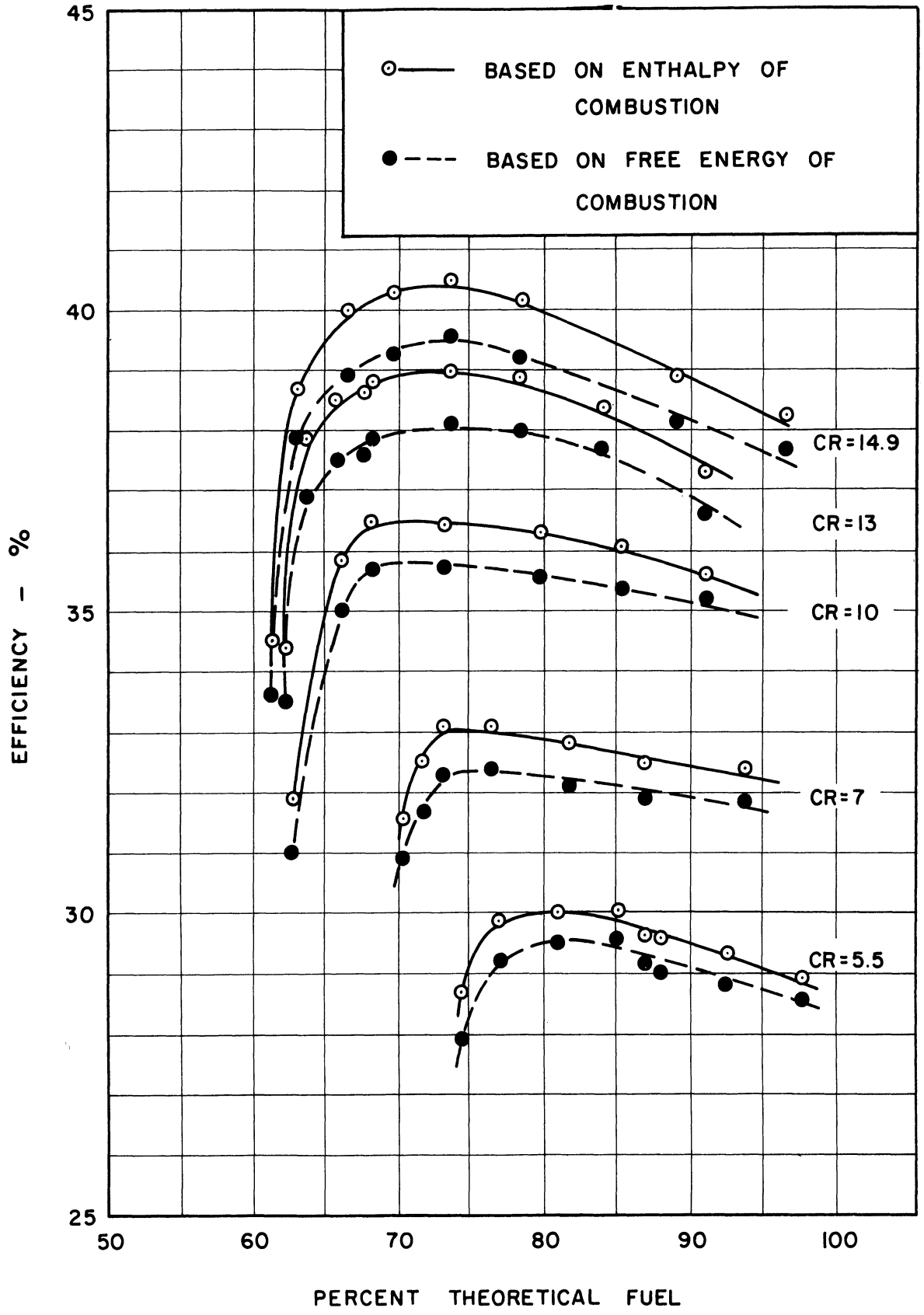

Figure 4.7 Thermal Efficiency Computed on Free Energy Basis. Split-Head CFR Engine. Speed = 1200 rpm., Intake Pressure = 10 psia., Intake Temperature = 100°F., Exhaust Pressure = 1 atm., Oil Temperature = 150 ± 2°F.

Referring again to Figure 4.5, it will be seen that lines of optimum ignition timing have been superimposed on the efficiency curves. In general, the ignition timing must be advanced as the mixture is made leaner, and retarded as the compression ratio is raised. At any given compression ratio the ignition timing must be varied by at least 20° in order to span the range of fuel-air ratios from stoichiometric to the leanest useful mixture.

Exhaust temperature lines have been superimposed on Figure 4.6, which is otherwise the same as Figure 4.5. Throughout the range of efficient operation, the exhaust temperature decreased as the mixture was made leaner. Exhaust temperatures also decreased when the compression ratio increased. It was found that the exhaust temperature was dependent on the ignition timing and these data therefore apply only when the optimum timing is used at each operating point.

D. The Available Energy

The efficiency data given above are intended to show what fraction of the energy supplied by the fuel is converted to useful work. In accordance with the usual practice, the amount of energy supplied has been taken to be equivalent to the enthalpy of combustion of the fuel. It can be shown, however, that the maximum amount of energy available as work from a thermodynamically reversible oxidation of propane is equal to the change in free energy (Gibbs' function, h - Ts), computed on the basis of the initial and final states of the working medium being at ambient pressure and temperature[107,109]. The change in free energy may therefore be used as a basis for computing efficiency.

The available work, as given by the change in free energy, may be greater or less than the enthalpy of combustion, depending on whether heat is transferred from or to the surroundings. In the case of the combustion of propane-air mixtures the free energy of combustion is slightly greater in magnitude than the enthalpy of combustion and is also somewhat dependent on the fuel-air ratio. The enthalpy of combustion of propane is -20,060 B.T.U. per pound of fuel. The free energy of combustion varies from -20,360 B.T.U. per pound of fuel with a stoichiometric mixture to -20,515 B.T.U. per pound of fuel with a mixture containing 60 percent theoretical fuel. Therefore, the efficiency of the engine is a little lower when computed on the basis of the free energy of combustion than when computed on the basis of the enthalpy of combustion. Both sets of curves are shown in Figure 4.7.

E. Useful Mixture Range

On the basis of the indicated engine efficiency shown in Figures 4.5, 4.6, and 4.7 it is possible to define a lean limit of useful mixture ratios. This useful mixture limit can be taken as the point where the efficiency begins to decrease rapidly as the mixture is made leaner. The leanest useful mixture varies from about 77 percent theoretical fuel at a compression ratio of 5.5 to about 65 percent theoretical fuel at a compression ratio of 14.9. The engine can be operated efficiently at any mixture ratio between stoichiometric and the useful lean limit. However, it has been shown that the ignition timing must be adjusted to correspond with the mixture ratio being used. It has also been shown that the exhaust temperatures decrease as the mixture is made leaner in this range of fuel-air ratios. The use of lean mixtures should not, therefore, lead to problems in exhaust valve cooling if proper ignition timing is used.

CHAPTER V

IGNITION AND COMBUSTION CHARACTERISTICS

In view of the importance of the combustion process as part of the internal combustion engine cycle, an attempt was made to obtain some information concerning the effect of lean mixtures on combustion in an engine. It will be recognized that observed trends in engine operating characteristics, such as ignition timing requirements, are due to changes in combustion rate or other combustion characteristics brought about by changes in the fuel-air ratio. A knowledge of the changes in the fundamental process of combustion will therefore help to explain the changes in engine performance that are observed when the fuel-air ratio is changed. In the paragraphs which follow, the combustion process is analyzed with the aid of pressure indicator diagrams, and two stages of combustion have been distinguished. In addition, the duration of the terminal part of the combustion process at high compression ratios was found to be materially different when detonation occurred. Finally, there is a description of the change in combustion characteristics occurring when the lean limit of useful fuel-air ratios is reached.

A. Indicator Diagrams

To obtain information on combustion characteristics, charge pressures in the engine cylinder were measured with a quartz element pressure pickup[110] and were plotted as a function of charge volumes on logarithmic coordinates. The resulting curves are shown in Figures 5.1 to 5.19 inclusive. Each diagram represents two, three, or four immediately successive cycles superimposed, and shows only the compression and expansion strokes of the engine; the intake and exhaust strokes have been omitted. These figures have been placed at the end of this chapter.

These pressure data have been plotted in logarithmic coordinates of pressure and volume in order to distinguish the effects of combustion from the pressure changes brought about by compression and expansion of the charge due to motion of the engine piston. It has been shown that the compression process is approximately isentropic during the period prior to combustion[14,23]. The relationship between pressure and volume of a perfect gas undergoing such a compression process is:

$$PV^k = C, \text{ a constant,}$$

or:

$$\log P = -k \log V + \log C.$$

This relationship is also applicable to the mixture of real gases present in the charge, with reasonable accuracy. Therefore a graph of "log P" as a function of "log V" will show the compression process as a straight line with a slope of -k. It has been found that the expansion process subsequent to the completion of combustion follows a similar straight line of approximately the same slope. The effect of combustion on the cylinder pressure begins, therefore, at the point where the observed "log P - log V" relationship departs from the straight compression line. Similarly, the end of combustion is indicated by the point where the linear expansion curve, parallel to the compression line, begins. It should be mentioned that it is possible for heat release and heat transfer to occur simultaneously at such a rate that a straight expansion line can result. No attempt has been made here to eliminate such a possibility.

B. Observed Characteristics of the Combustion Process

It will be noted upon examining Figures 5.1 to 5.19 that there is a time delay between the ignition of the charge and the point where the curve deviates appreciably from the isentropic compression line. The presence of this time delay suggests that the combustion process in an engine consists of at least two parts: 1) a delay or "pre-pressure" period, and 2) a period of rapid flame travel and pressure rise. For purposes of measurement, the transition between these two intervals was considered to take place at the point where the pressure was four percent above the isentropic compression pressure at the same volume. The end of the pressure rise period was taken as the point where the pressure was 96 percent of the projected expansion pressure at the same volume.

The length of the delay period was found to be a function of the compression ratio and the fuel-air ratio, as shown in Figure 5.20. At compression ratios below 10:1, the delay period decreased quite rapidly when the compression ratio was raised, while at compression ratios in excess of 10:1 the decrease in the delay period was relatively small. The delay period also increased substantially as the mixture was made leaner, particularly at the lower compression ratios. In some cases there was a scattering of 10° or more in the measured length of the delay period in a series of cycles under a given set of operating conditions. The values given in Figure 5.20 represent the mean of one to four measurements and hence are subject to some uncertainty because of the relatively small sample size.

The duration of the remaining part of the combustion process, described as the pressure rise period, is shown in Figures 5.21 to 5.24

inclusive. In general, the time occupied by the pressure rise period increases as the mixture is made leaner, as shown in Figures 5.22 to 5.24. It is interesting to compare the mean rise time, shown in Figure 5.21, with the mean delay time, shown in Figure 5.20. The pressure rise time does not appear to be changed appreciably when the compression ratio is varied, whereas the delay period increases two to three times over the range of compression ratios from 14.9 to 5.5. When light knock was present at a compression ratio of 14.9, the flame travel period was appreciably shortened. However, the delay period during these knocking cycles was not significantly different from the delay period in non-knocking cycles.

C. Pre-Pressure Period of Combustion

The "pre-pressure" or delay period in the combustion process in spark-ignition engines has not been generally recognized as a separate phenomenon in technical literature on internal combustion engines. Several investigators, however, have published data indicating the existence of such a delay period[89,90,91,92,93,94,95,96,97,98,99,100,101,102], although not all of these considered this period to be a distinct phase of the combustion process. From the data available, at least four characteristics of the pre-pressure rise period may be identified.

First, it has been reported that the pre-pressure period is relatively long when lean mixtures are used[91,96,97,100], and a similar result has been shown in the present study (cf. Figure 5.20). It was also found in the present study that the duration of the pressure rise period, which follows the delay period, increased when the mixture was

made leaner. However, the change in the pressure rise time was about 50 percent over the range of mixtures used, whereas the change in delay time was about 300 percent.

A second characteristic of the pre-pressure phase of combustion was shown by Ricardo[99], who found that the duration of the pre-pressure period was independent of engine speed. In contrast, the subsequent rate of pressure rise was approximately proportional to the engine speed. In a series of experiments in a closed vessel containing a fan, David[92] later confirmed the conclusion that the duration of the pre-pressure period is independent of the degree of turbulence of the mixture, but the rate of pressure rise following the pre-pressure period increases rapidly as the mixture is made more turbulent.

Third, it has been shown in photographic studies of flame propagation that the flame, initiated at the spark plug, may travel as far as one quarter of the distance across the combustion chamber before a noticeable pressure rise occurs[93,101,102]. As discussed below, at least part of the delay period is due to the necessity for the flame to travel such a distance before a sufficient volume of mixture has been burned to cause a noticeable pressure rise. The area already inflamed shows a sudden increase in luminousity about the time that the pressure begins to rise, but it is not clear whether this luminousity indicates a cause or result of the pressure rise or is merely an unrelated phenomenon. In many of the flame photographs the occurrence of the spark is followed by an initial period during which no flame is visible. This period of no visible flame was quite short under the conditions existing when flame photographs were made. In general,

however, no clearly visible phenomenon has been shown to correspond to the relatively long delay period observed with lean mixtures.

Fourth, Withrow and Boyd[101] found that, in the case of gasolene-benzene fuel blends, the length of the delay period was independent of the knocking tendency of the fuel blend.

A number of attempts have been made to explain the existence of the delay period and the processes occurring during this time. It has been pointed out that because of the geometry of the flame, the pressure rise may be expected to be undetectable at first[93,95,98]. The initial volume and area of the flame formed at the spark plug are both very small. Since the rate of pressure rise is proportional to the mass rate of burning[19], the rate of pressure rise will depend on the area of the flame front, the density of the unburned mixture, and the flame speed relative to the unburned mixture. The pressure rise may be expected to be quite small until the flame has attained appreciable size and surface area, even though the initial flame speed be high. David[93] has calculated that less than five percent of the total pressure rise will have occurred when the volume of the burned gases has reached 20 percent of the total combustion chamber volume. It is therefore clear that the process of flame growth from a small source is one factor in accounting for the pre-pressure period.

There are some reasons for supposing that other factors besides the flame geometry are important in consideration of the delay period. The effects of changes in fuel-air ratio or compression ratio on the length of the delay period are much larger than the accompanying effects on the rate of pressure rise. Furthermore, turbulence has been

shown to have a marked effect on flame speed, but no effect on the length of the delay period. A number of authors have speculated as to other combustion mechanisms, with little heat release, which may occur during the delay period[93,94]. The details of these other mechanisms, if they exist, are obscure at present, and no satisfactory explanation of the "pre-pressure" phenomenon seems to be available at the present time.

D. Useful Mixture Limit

In Chapter IV, reference was made to the leanest useful fuel-air ratio. It was found that the efficiency decreased substantially if the mixture was made leaner than the leanest useful ratio, which varied from approximately 77 percent theoretical fuel at a compression ratio of 5.5 to 65 percent theoretical fuel at a compression ratio of 14.9. It might be expected that the attainment of the leanest useful mixture ratio would be accompanied by some significant change in combustion characteristics.

Engine operation was found to be very irregular in the very lean mixture range, and the variations from cycle to cycle were large. The irregularity of the combustion process made if difficult to observe any general trends in the characteristics of combustion. In many cases, the duration of the pressure rise period was increased significantly when the fuel-air ratio was made less than the leanest useful ratio mentioned above. The length of the pre-pressure period also increased in some cases, but does not show a clearly defined change corresponding to the decreasing efficiency. It was observed that the optimum ignition timing was not clearly defined when using very lean mixtures. However, the engine did not misfire at any mixture ratio used in the performance tests.

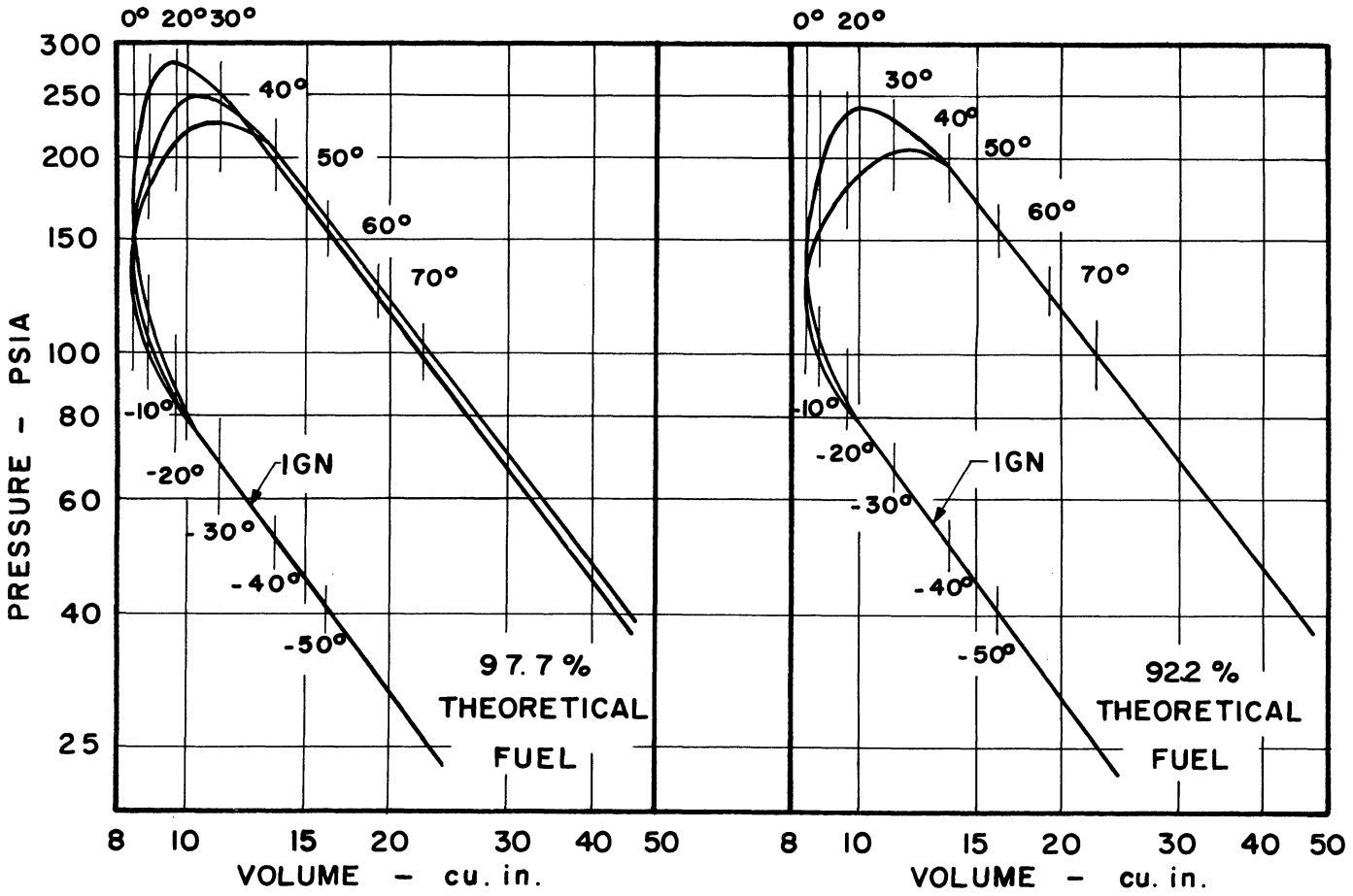

Figure 5.1 Pressure-Volume Diagrams. Compression Ratio = 5.5. Split-Head CFR Enging. Speed = 1200 rpm., Intake Pressure = 10 psia., Intake Temperature = 100°F., Exhaust Pressure = 1 atm., Oil Temperature = 150 ± 2°F.

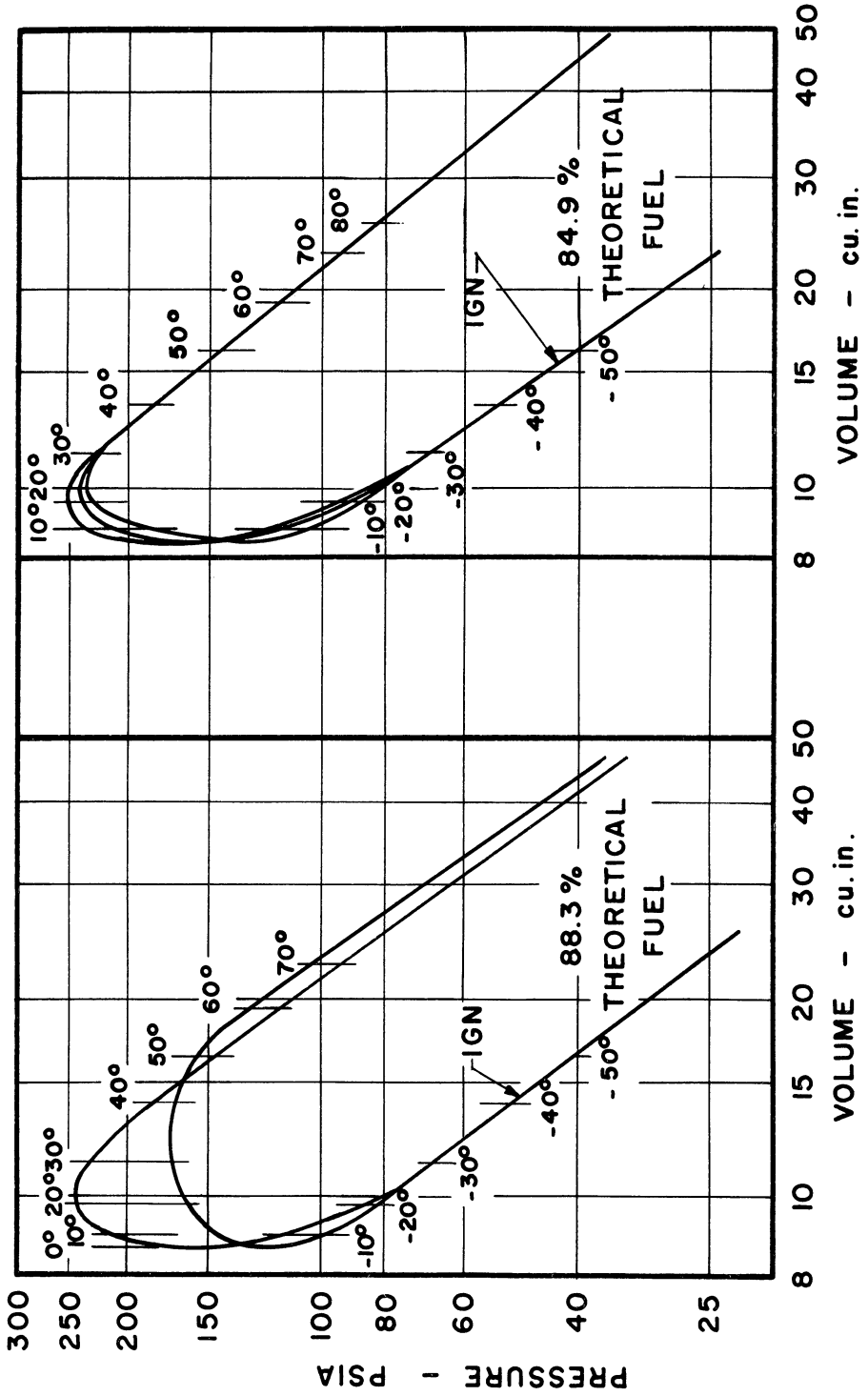

Figure 5.2 Pressure-Volume Diagrams. Compression Ratio = 5.5
Operating conditions same as in Figure 5.1.

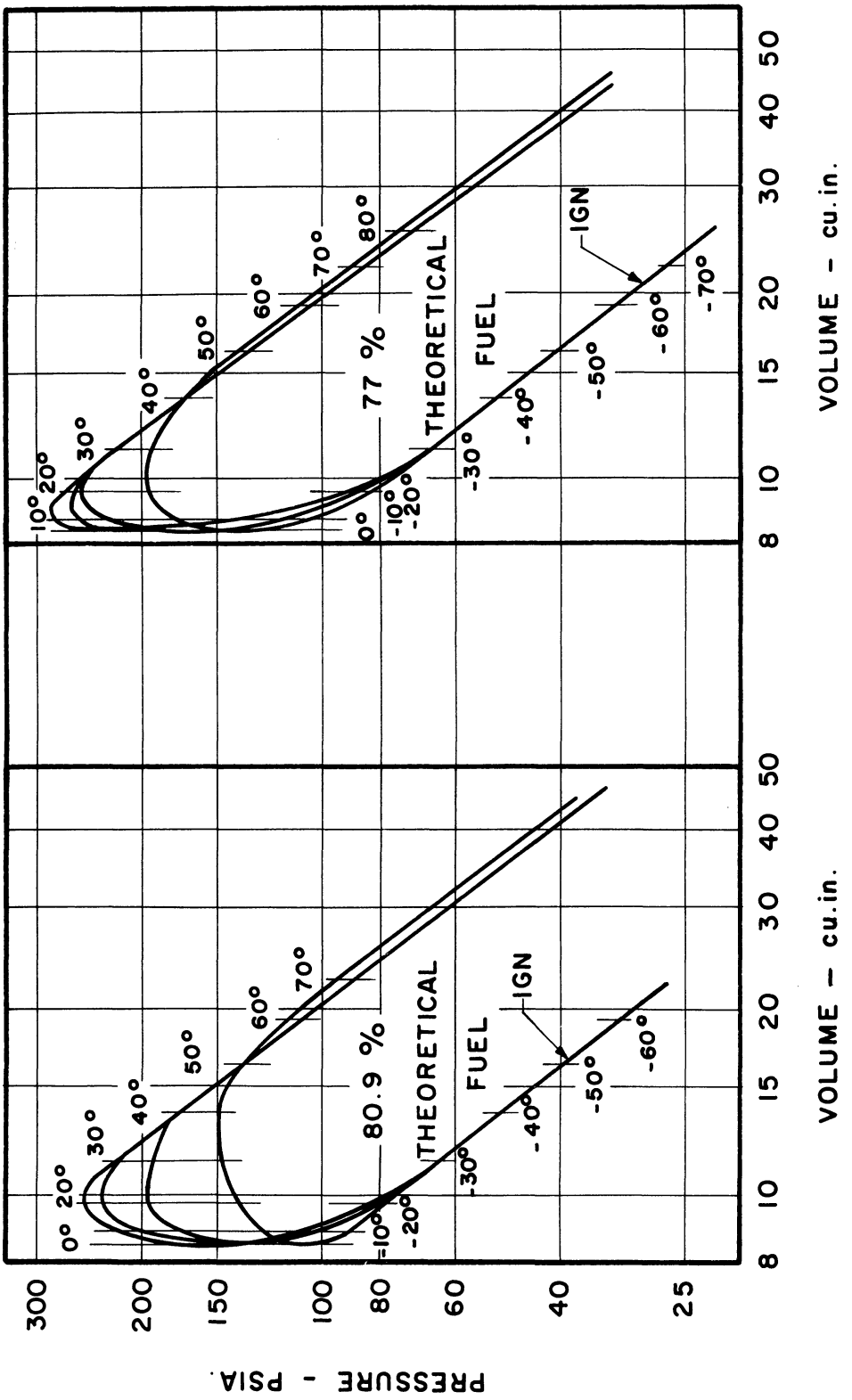

Figure 5.3 Pressure-Volume Diagrams. Compression Ratio = 5.5
Operating conditions same as in Figure 5.1.

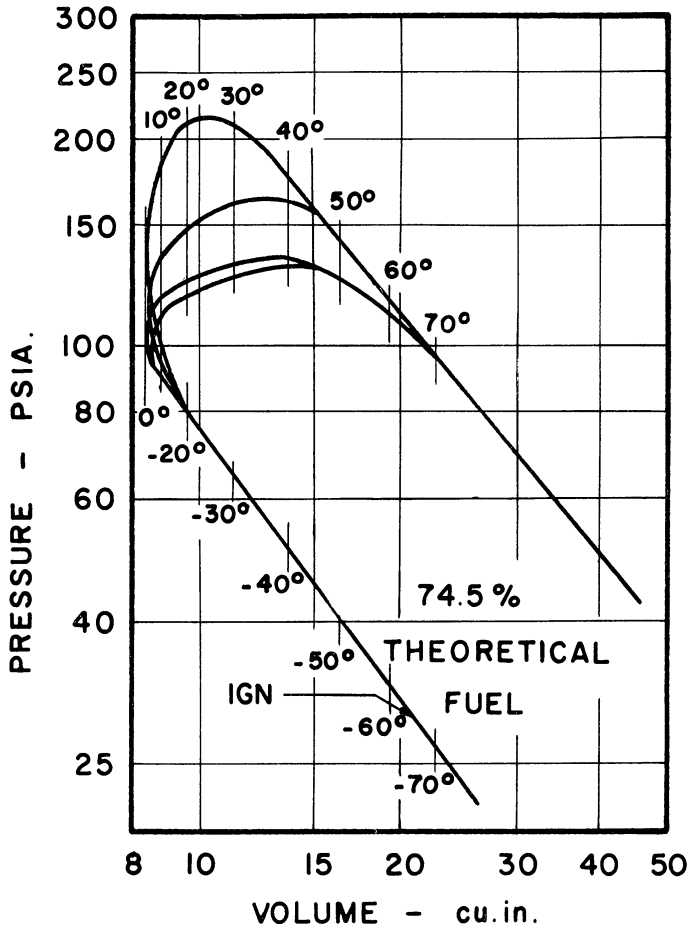

Figure 5.4 Pressure-Volume Diagrams. Compression Ratio = 5.5
Operating conditions same as in Figure 5.1.

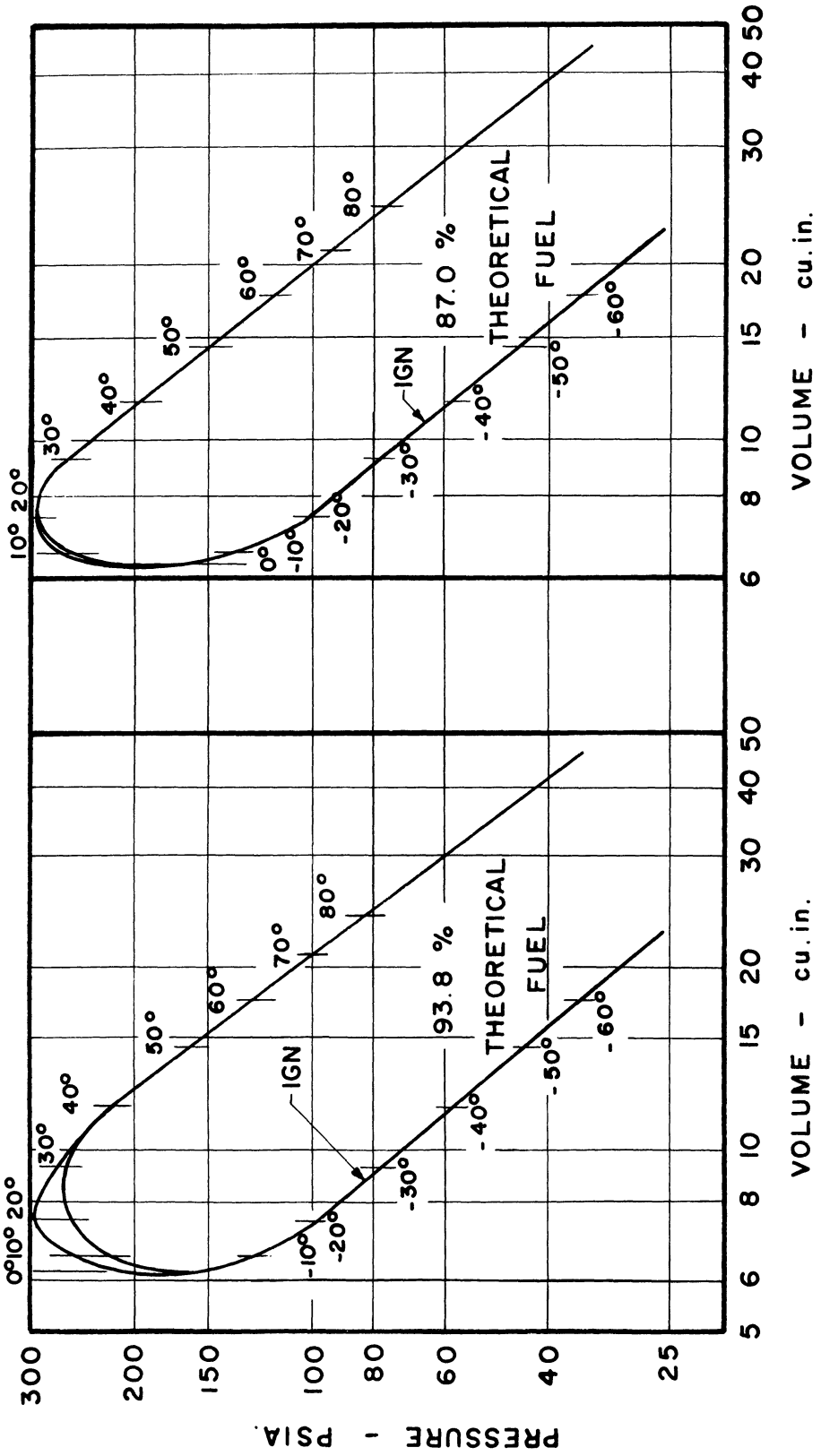

Figure 5.5 Pressure-Volume Diagrams. Compression Ratio = 7
Operating conditions same as in Figure 5.1.

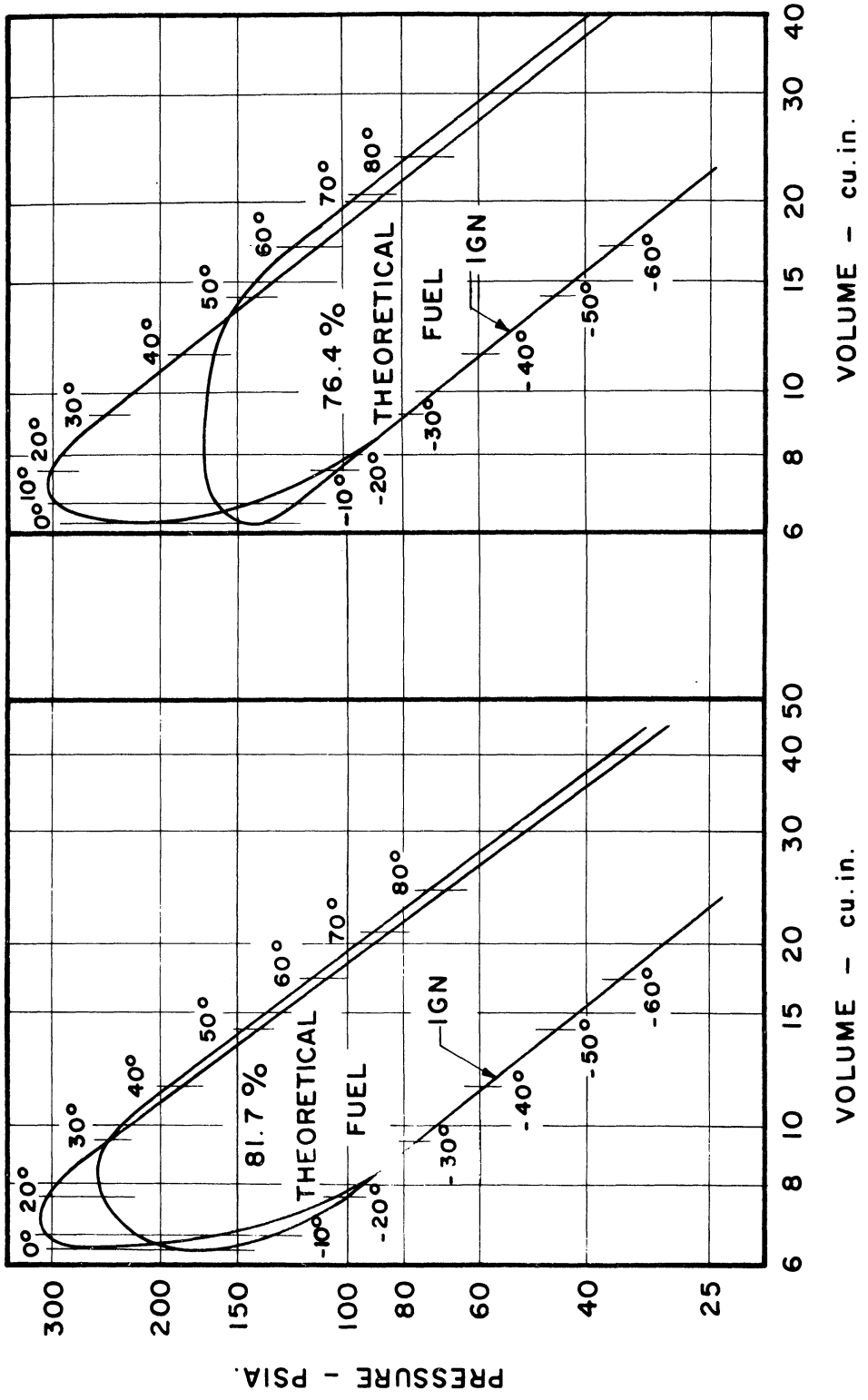

Figure 5.6 Pressure-Volume Diagrams. Compression Ratio = 7
Operating conditions same as in Figure 5.1.

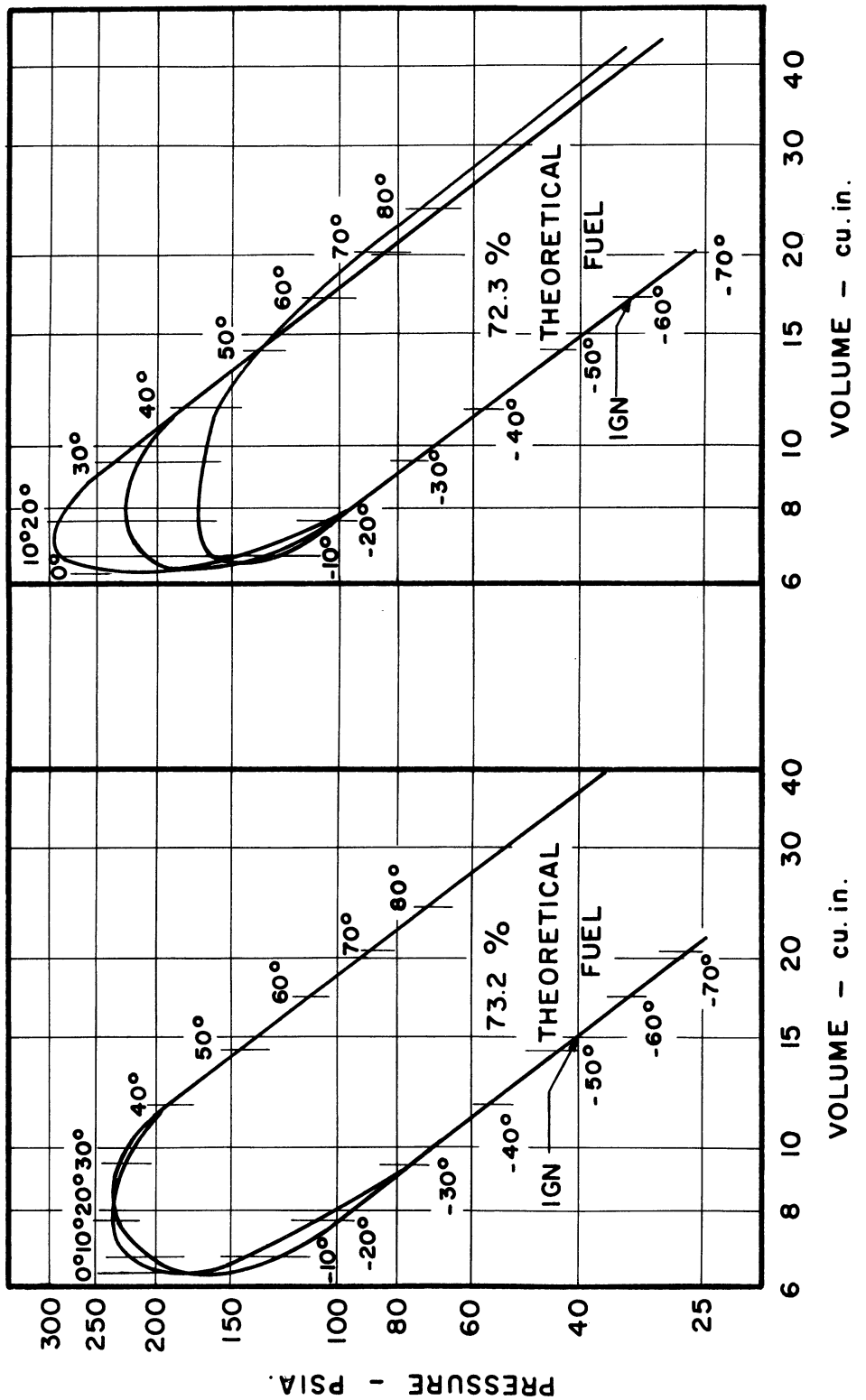

Figure 5.7 Pressure-Volume Diagrams. Compression Ratio = 7
Operating conditions same as in Figure 5.1.

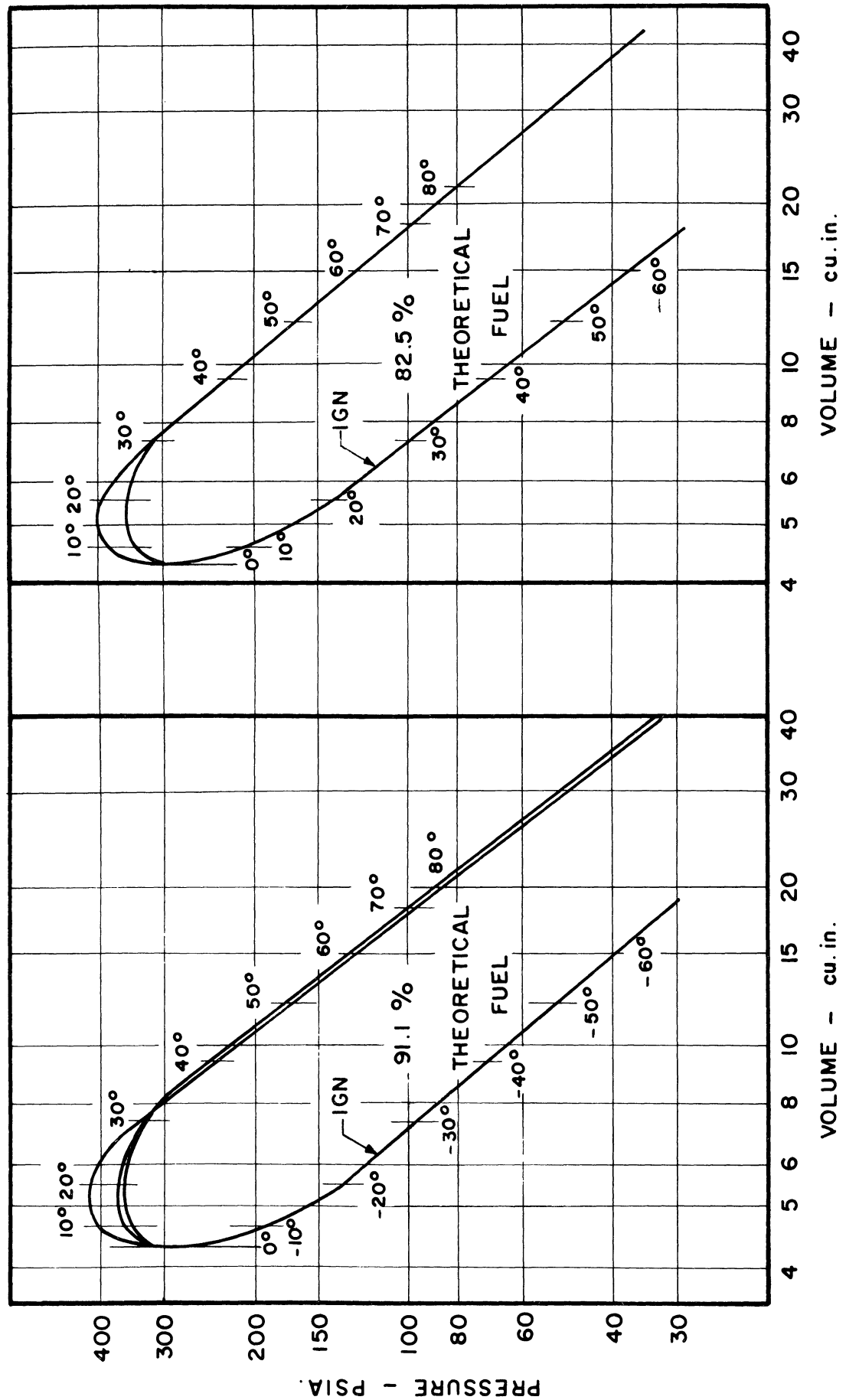

Figure 5.8 Pressure-Volume Diagrams. Compression Ratio = 10
Operating conditions same as in Figure 5.1.

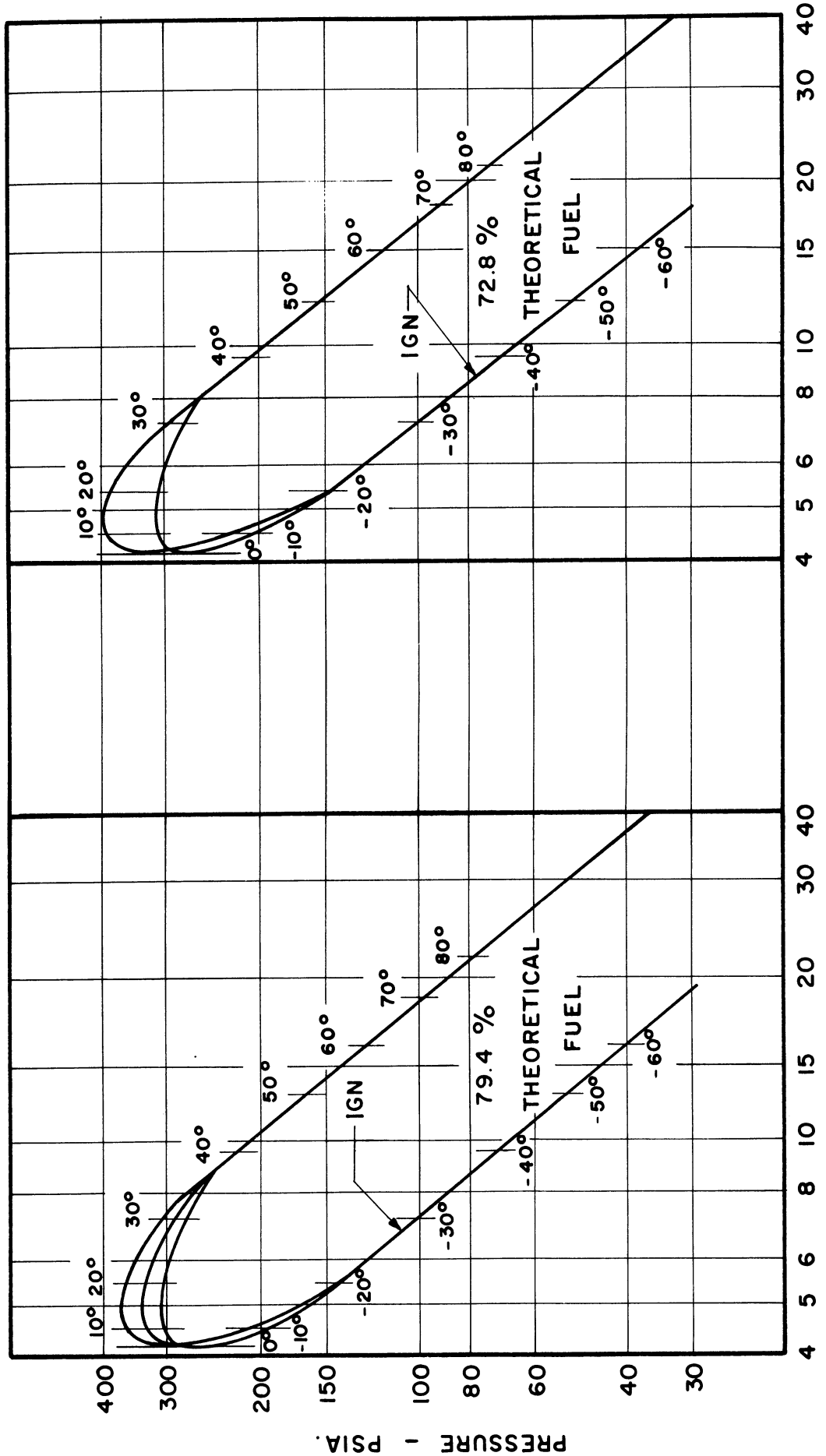

Figure 5.9 Pressure-Volume Diagrams. Compression Ratio = 10
Operating conditions same as in Figure 5.1.

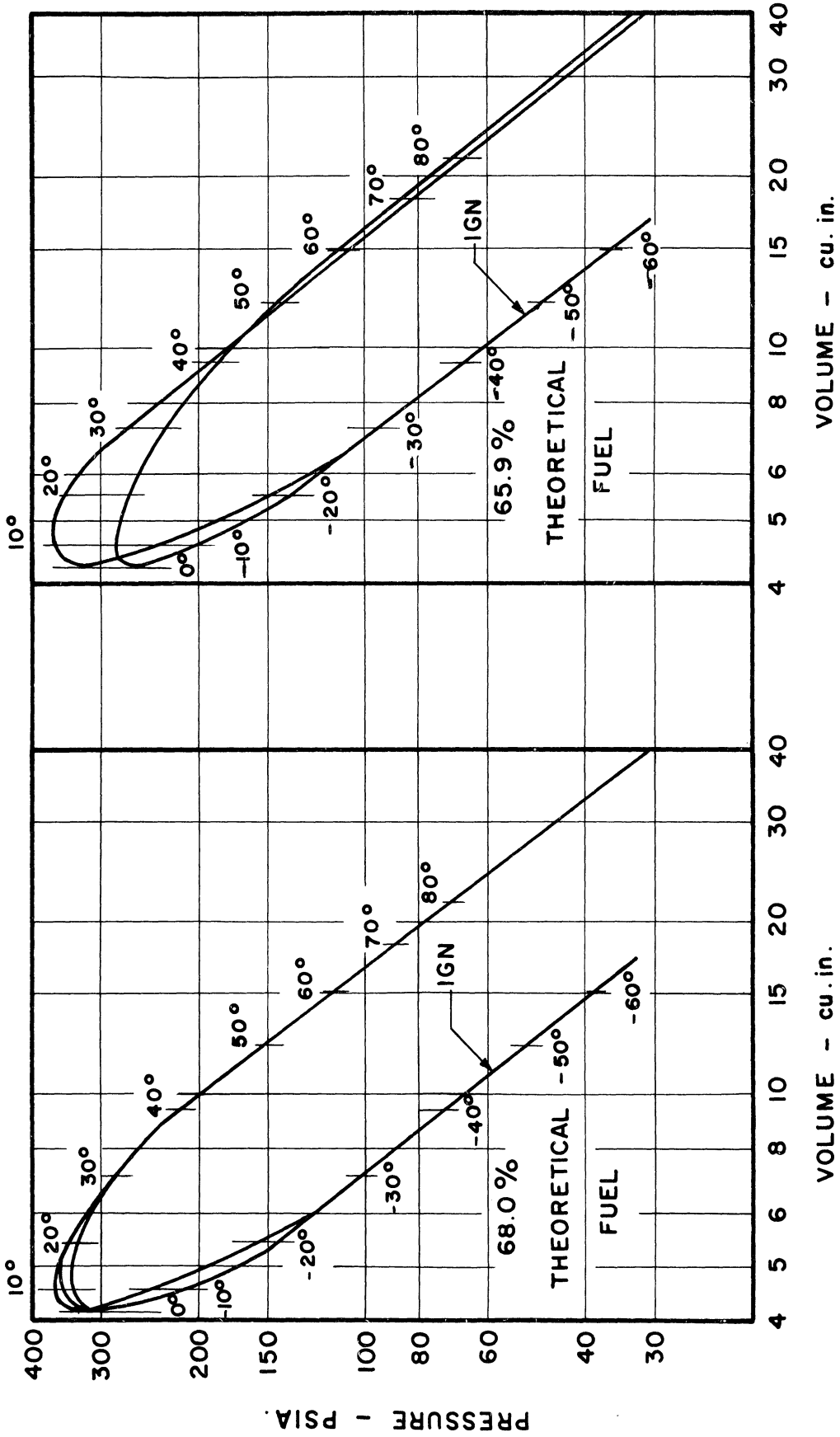

Figure 5.10 Pressure-Volume Diagrams. Compression Ratio = 10.
Operating conditions same as in Figure 5.1.

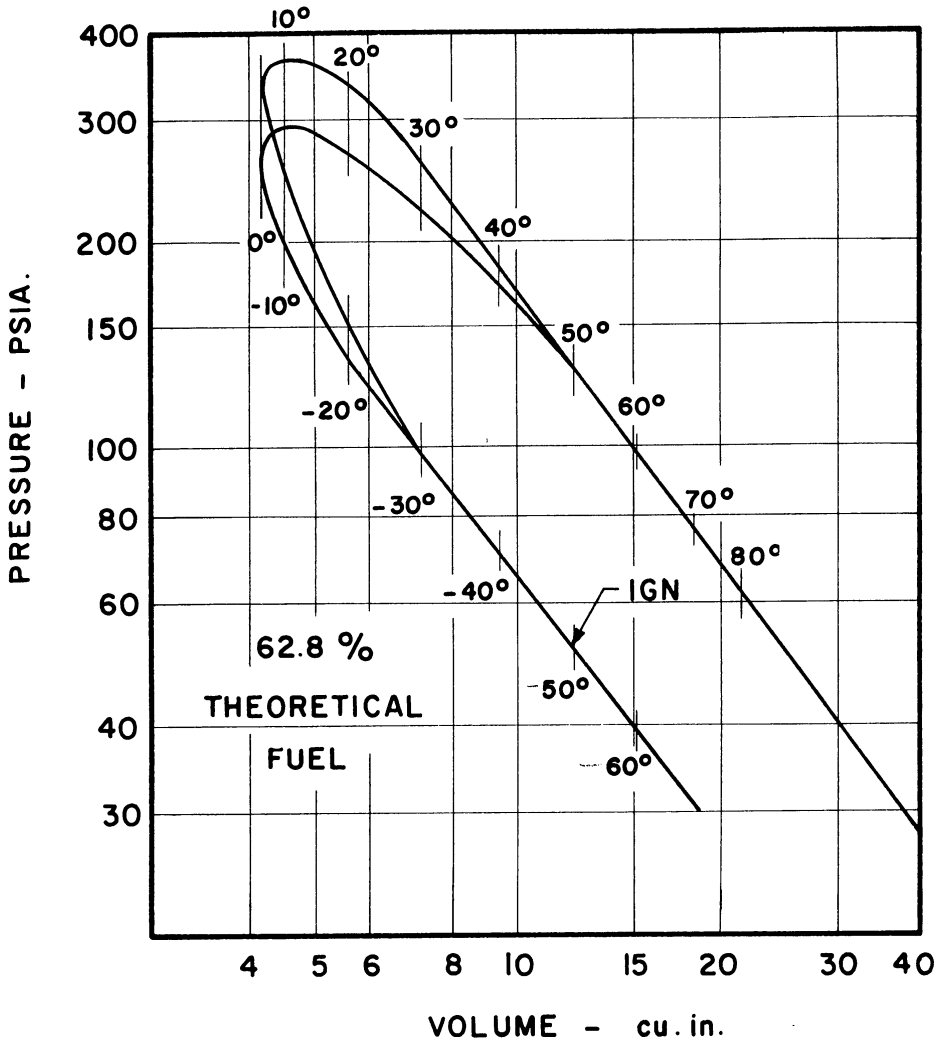

Figure 5.11 Pressure-Volume Diagrams. Compression Ratio = 10. Operating conditions same as in Figure 5.1.

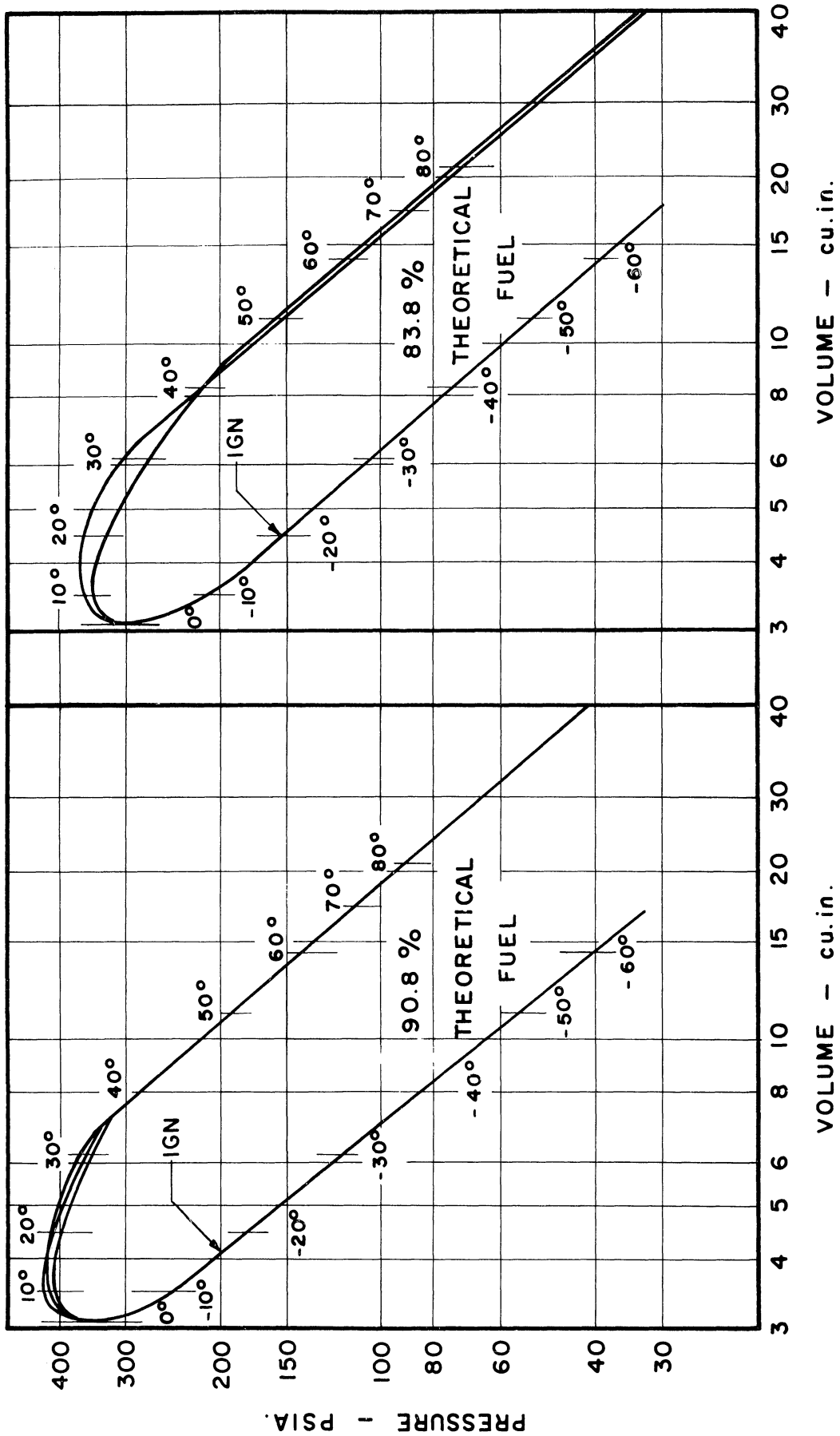

Figure 5.12 Pressure-Volume Diagrams. Compression Ratio = 13
Operating conditions same as in Figure 5.1.

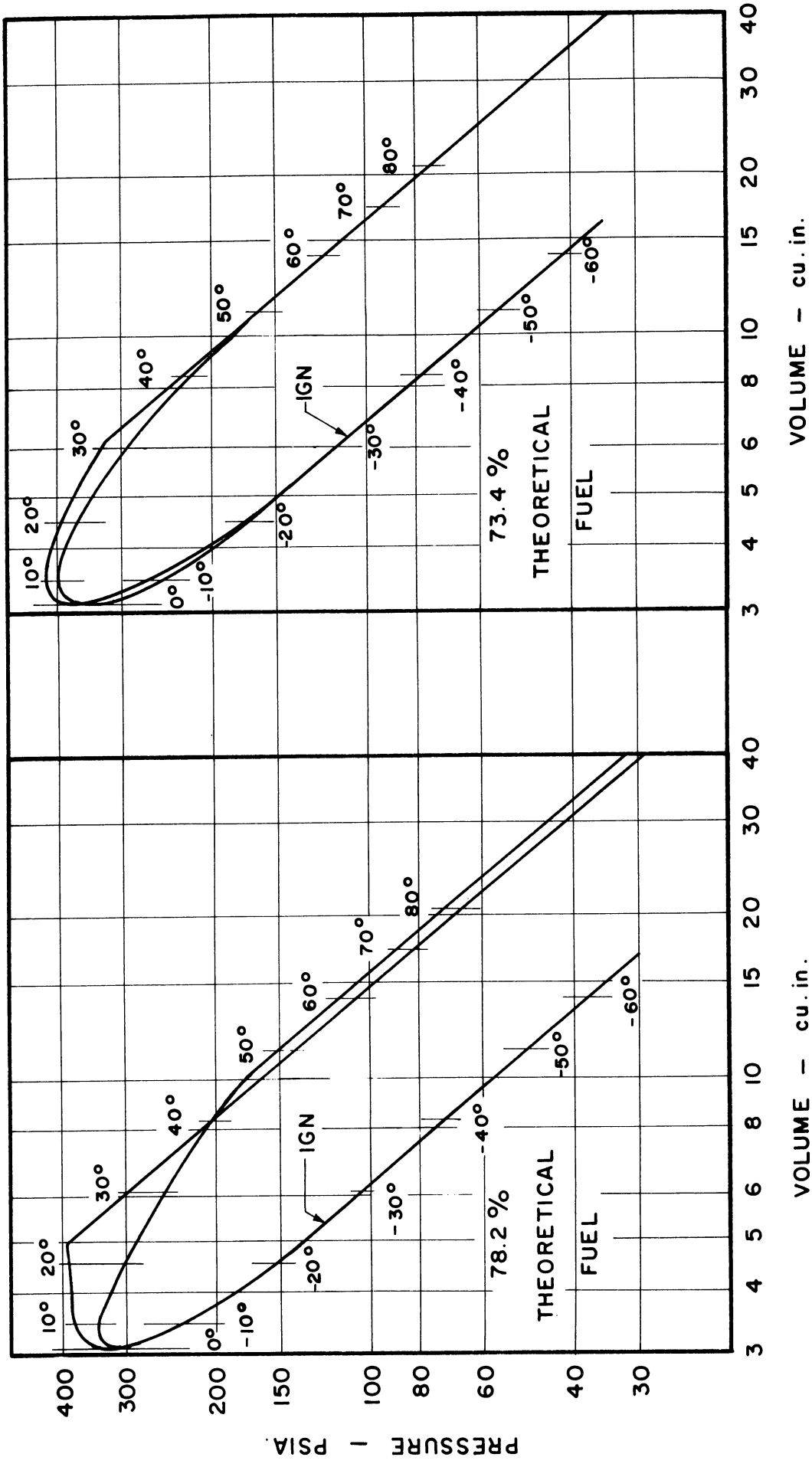

Figure 5.13 Pressure-Volume Diagrams. Compression Ratio = 13
Operating conditions same as in Figure 5.1.

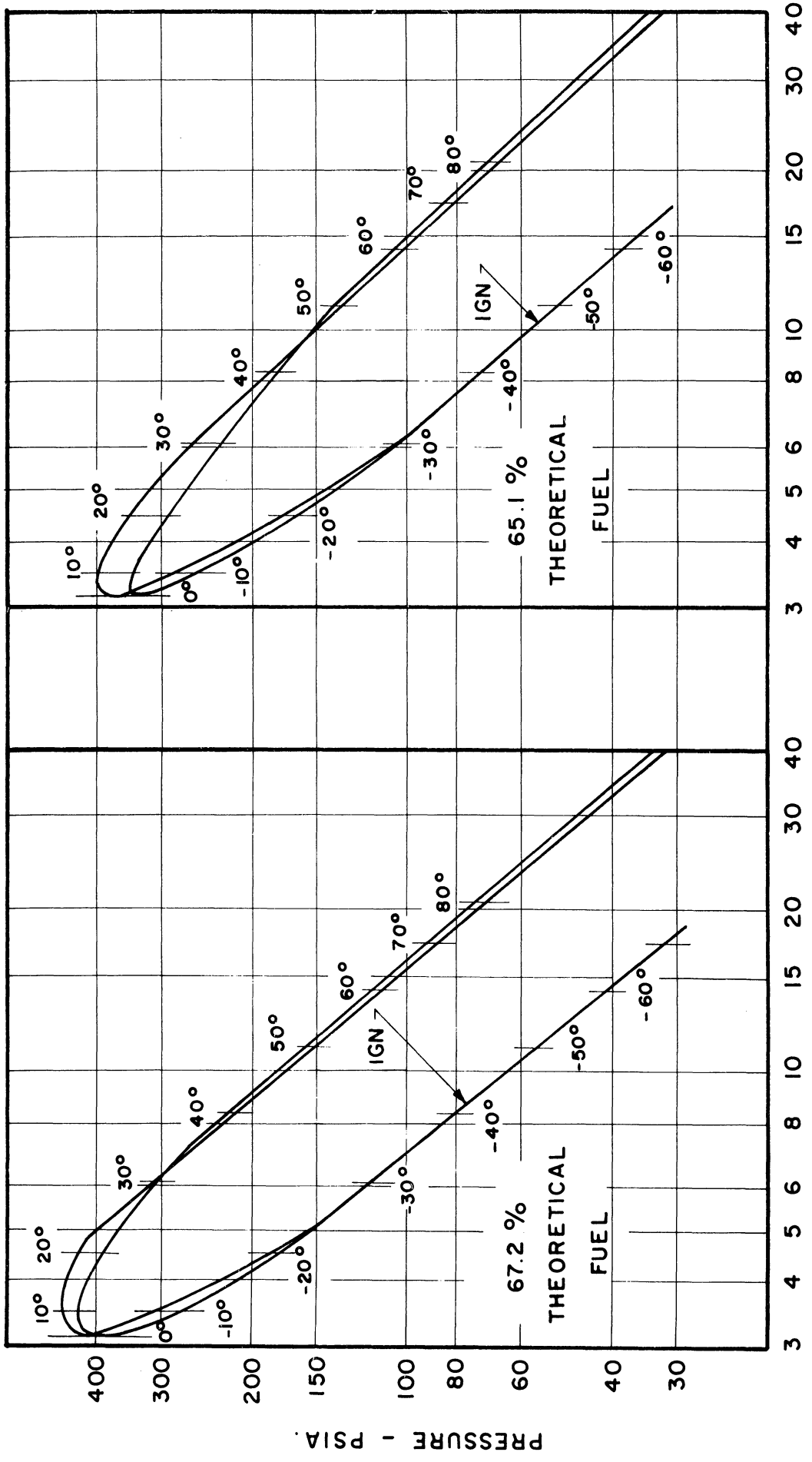

Figure 5.14 Pressure-Volume Diagrams. Compression Ratio = 13
Operating conditions same as in Figure 5.1.

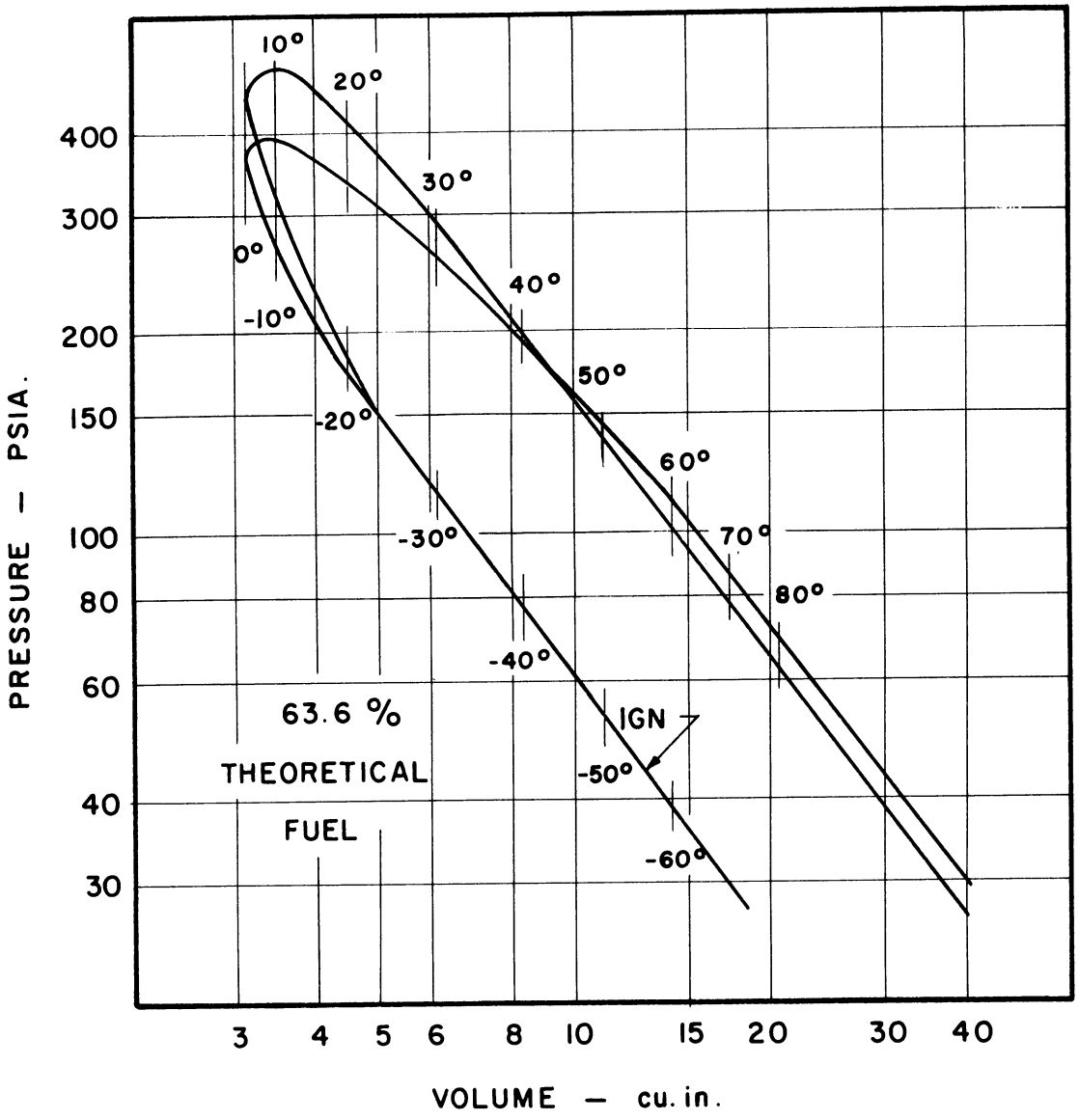

Figure 5.15 Pressure-Volume Diagrams. Compression Ratio = 13
Operating conditions same as in Figure 5.1.

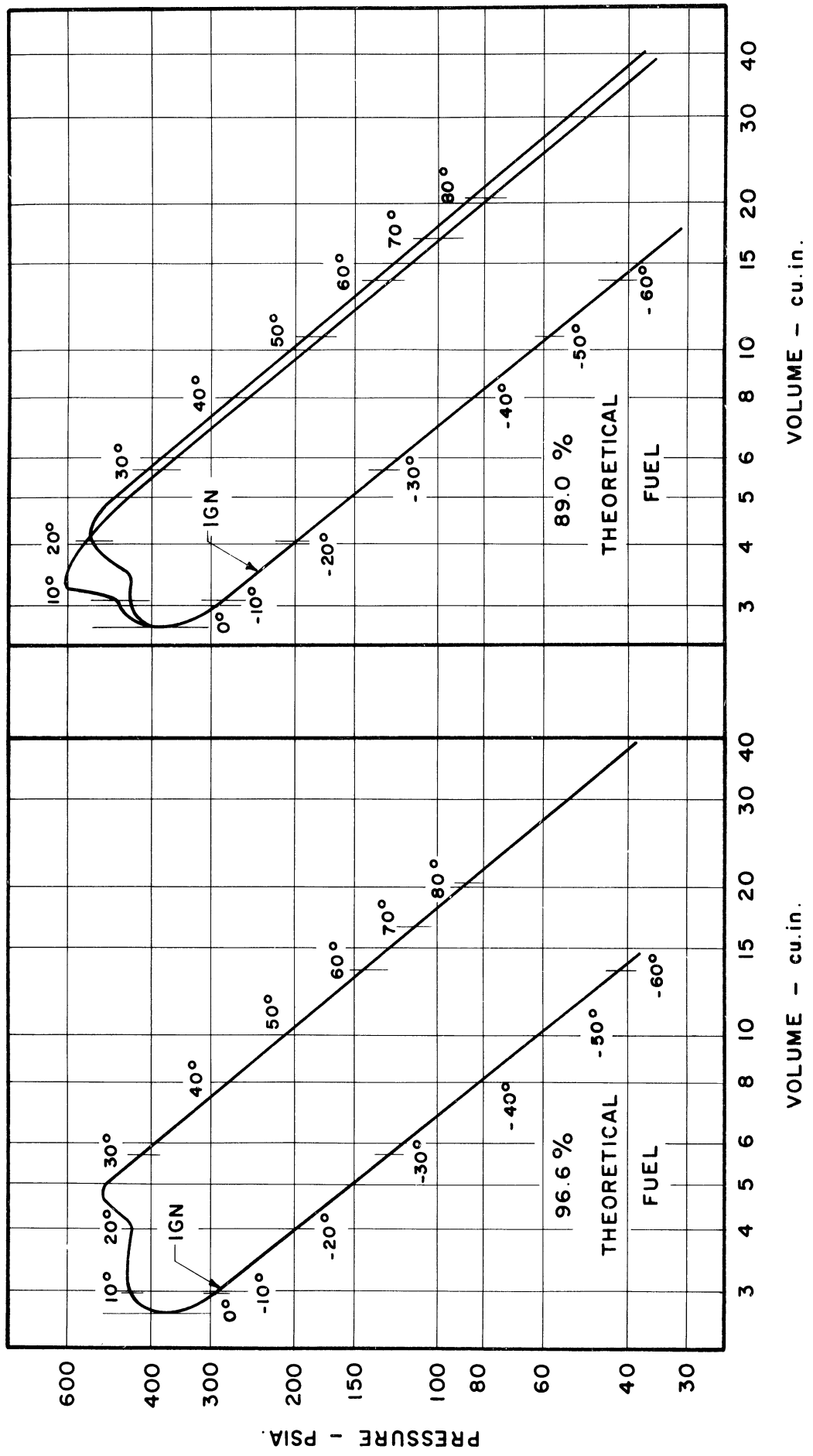

Figure 5.16 Pressure-Volume Diagrams. Compression Ratio = 14.9
Operating conditions same as in Figure 5.1.

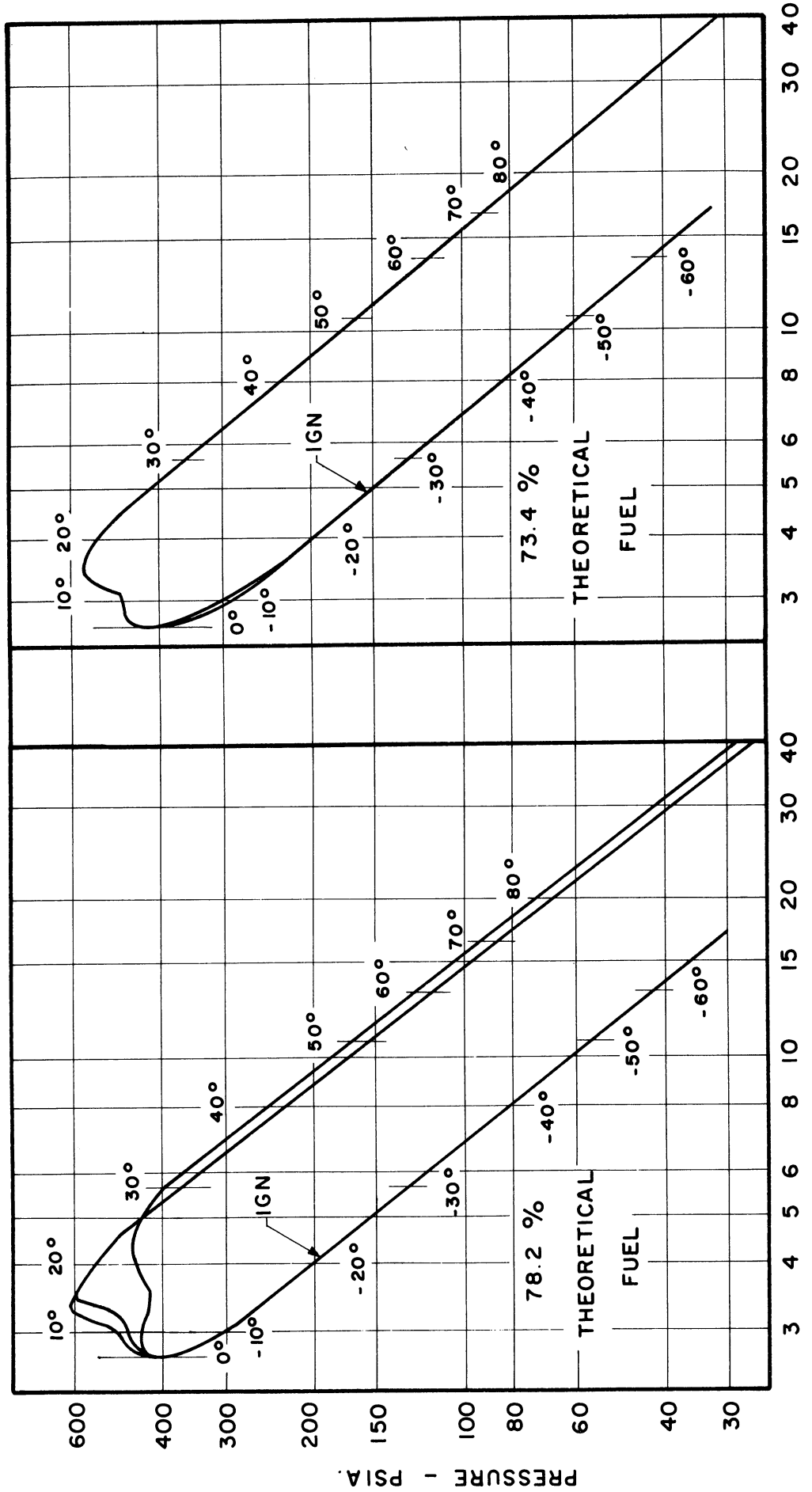

Figure 5.17 Pressure-Volume Diagrams. Compression Ratio = 14.9
Operating conditions same as in Figure 5.1.

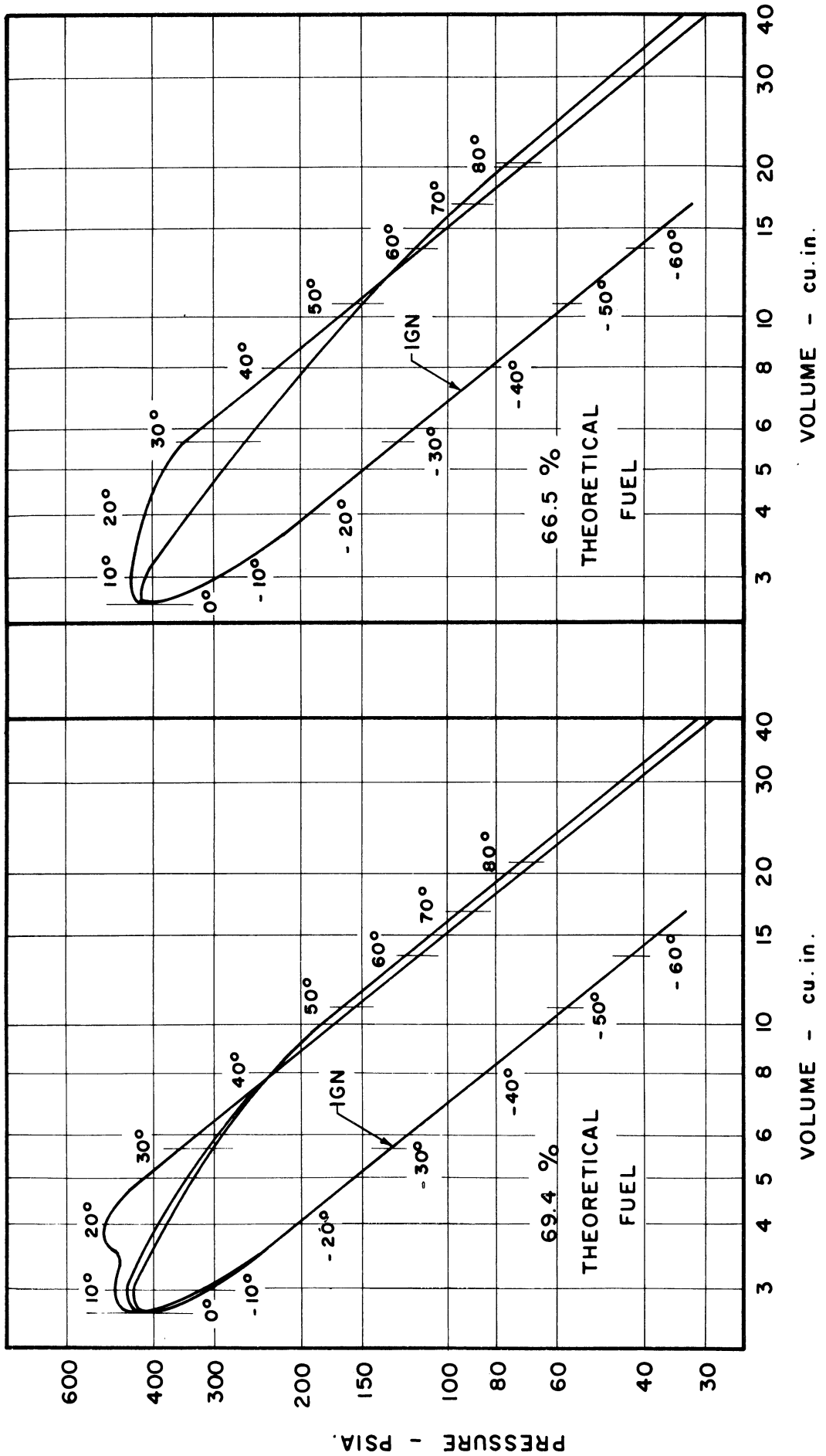

Figure 5.18 Pressure-Volume Diagrams. Compression Ratio = 14.9
Operating conditions same as in Figure 5.1.

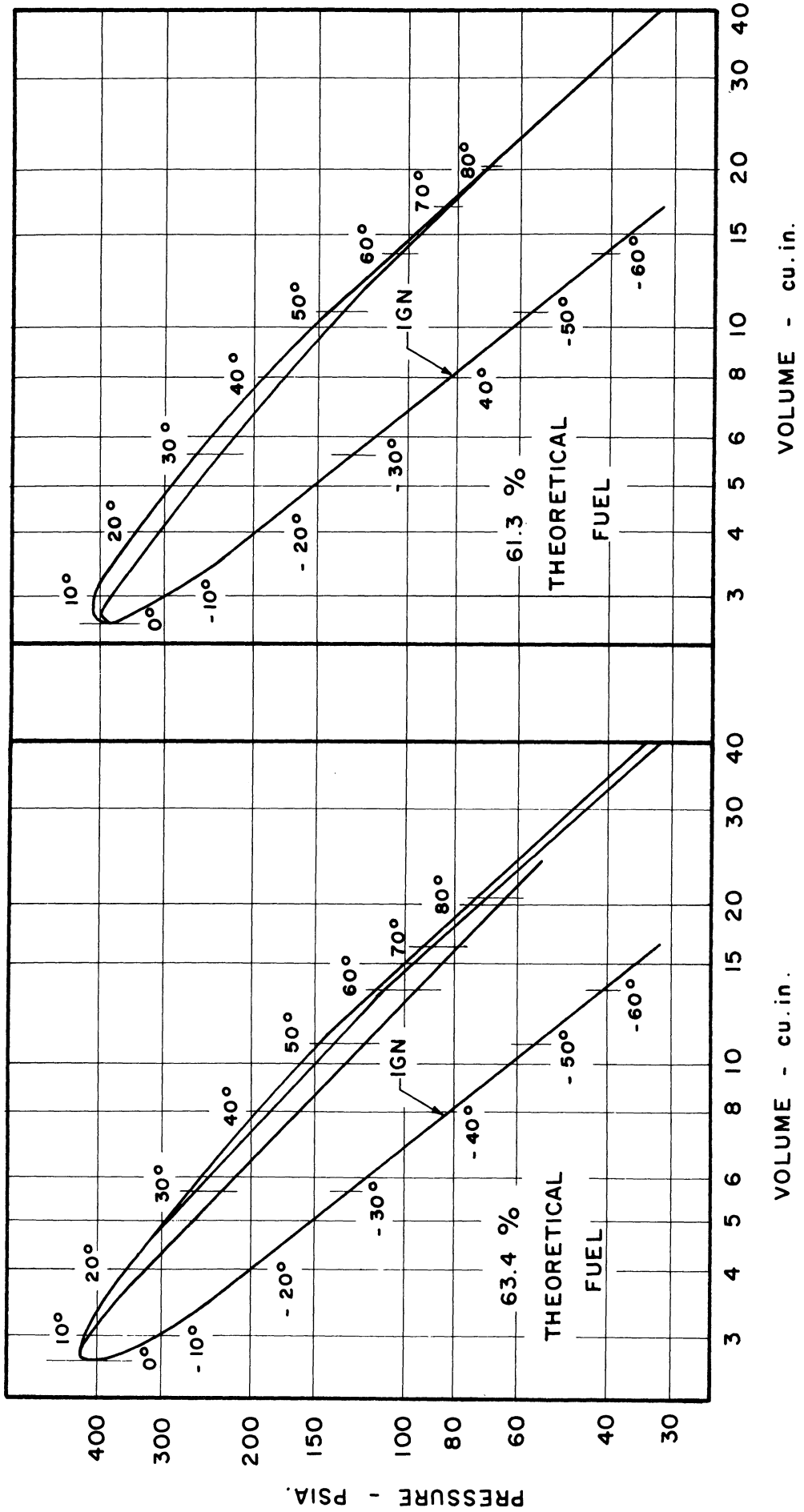

Figure 5.19 Pressure-Volume Diagrams. Compression Ratio = 14.9
Operating conditions same as in Figure 5.1.

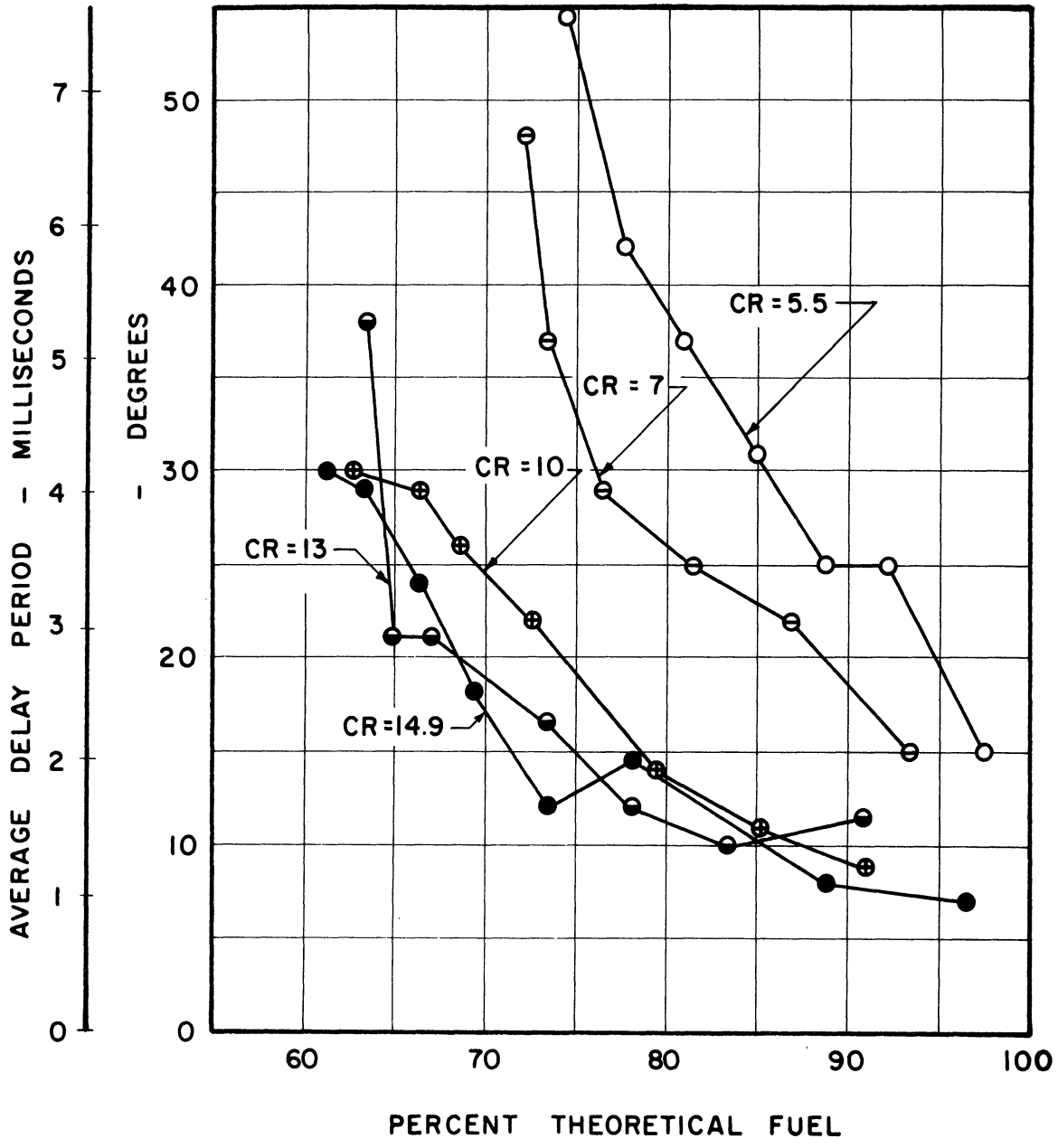

Figure 5.20 Average Duration of Delay Period.
Operating conditions same as in Figure 5.1.

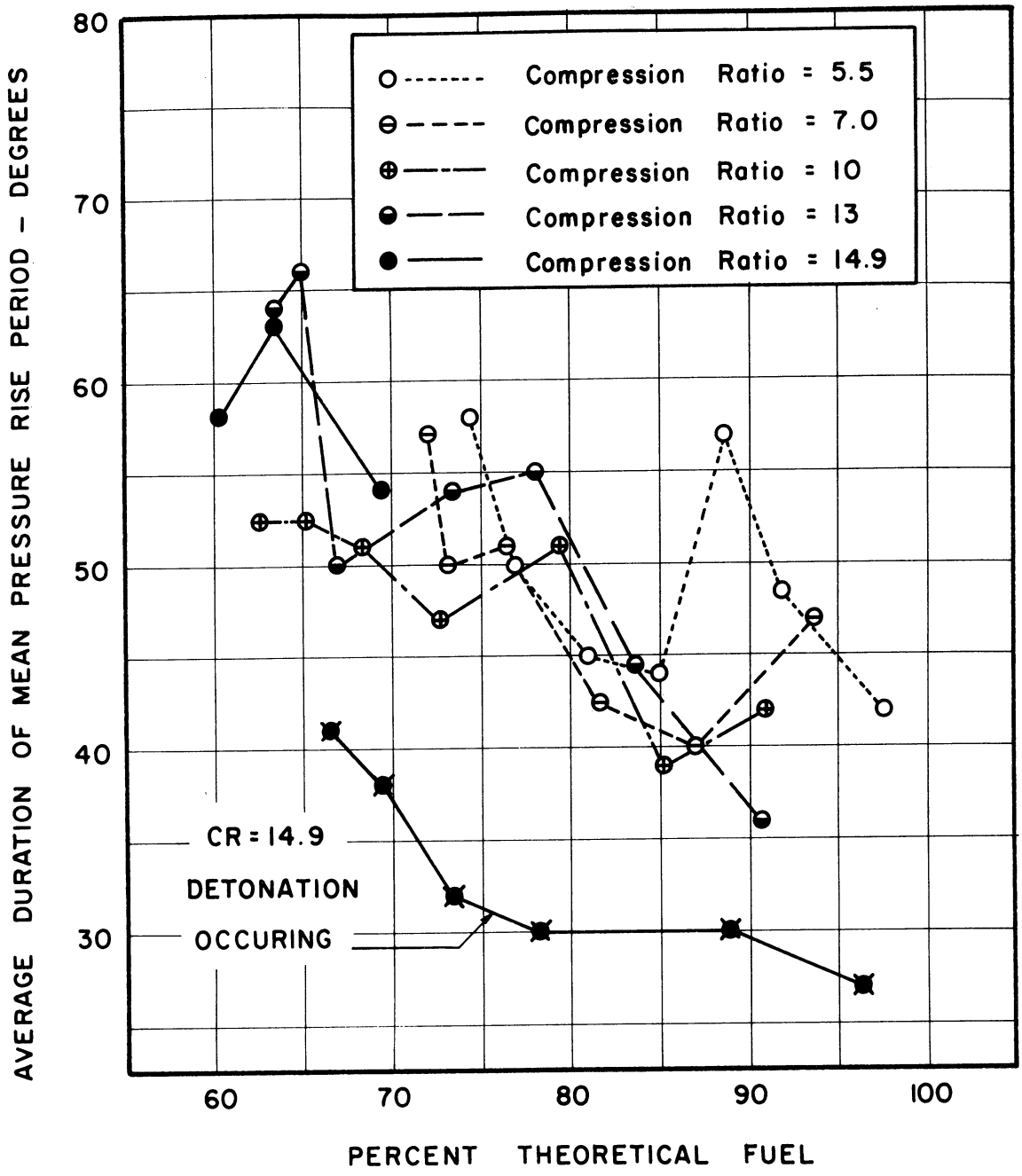

Figure 5.21 Average Duration of Pressure Rise Period. Operating conditions same as in Figure 5.1.

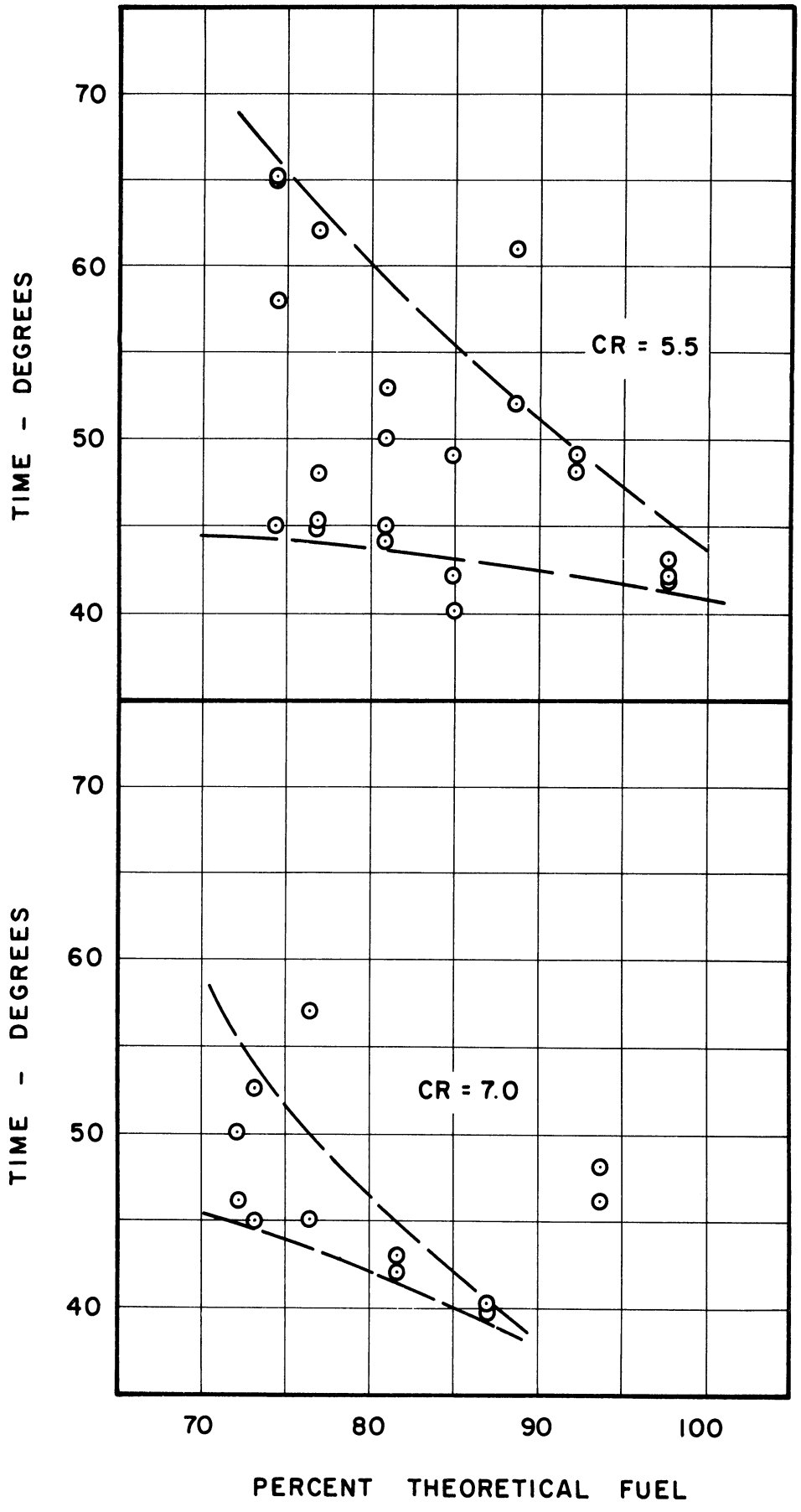

Figure 5.22 Duration of Pressure Rise Period.
Operating conditions same as in Figure 5.1.

TABLE XIII

FUEL ORIFICE CALIBRATION

Orifice Constant = $\dot{W}_f \sqrt{\frac{T}{Ph}}$

Date of Test	Weight of Fuel Used	Flow Time	Flow Rate	Average Fuel Pressure	Average Pressure Difference at Orifice	Average Fuel Temp.	Orifice Constant K_o
	lb.	min.	lb/hr.	psia.	in. H_2O	°R.	
10-19-59	.905	36.3	1.493	45.76	9.27	616	1.80
1- 3-60	1.00	35.4	1.695	46.54	11.94	618.5	1.785
1-19-60	1.00	39.9	1.505	44.5	9.95	619	1.78
2- 1-60	1.20	46.5	1.55	46.5	10.08	619.2	1.79
3-15-60	.40	15.75	1.524	44.4	10.05	615	1.785

TABLE XIV

FREE ENERGY OF COMBUSTION OF PROPANE-AIR MIXTURES

ϕ		1.0	0.9	0.8	0.7	0.6
y		0	2.81	6.32	10.9	16.9
Mole Fractions of Reactants	C_3H_8	.0403	.0362	.0321	.0280	.0240
	O_2	.2015	.2024	.2034	.2041	.2050
	N_2	.7582	.7614	.7645	.7679	.7710
Free Energy of Reactants kcal. per Mole Fuel		-15.34	-16.25	-17.39	-18.86	-20.77
Mole Fractions of Products	CO_2	.1163	.1048	.0934	.0817	.0703
	H_2O	.1550	.1398	.1253	.1090	.0937
	O_2	.0000	.0206	.0413	.0624	.0831
	N_2	.7287	.7348	.7400	.7469	.7529
Free Energy of Products kcal. per Mole Fuel		-513.0	-515.0	-517.2	-519.6	-522.3
Change in Free Energy kcal. per Mole Fuel		-497.7	-498.7	-499.8	-500.8	-501.5
Change in Free Energy BTU. per lb. Fuel		-20,360	-20,403	-20,444	-20,488	-20,514

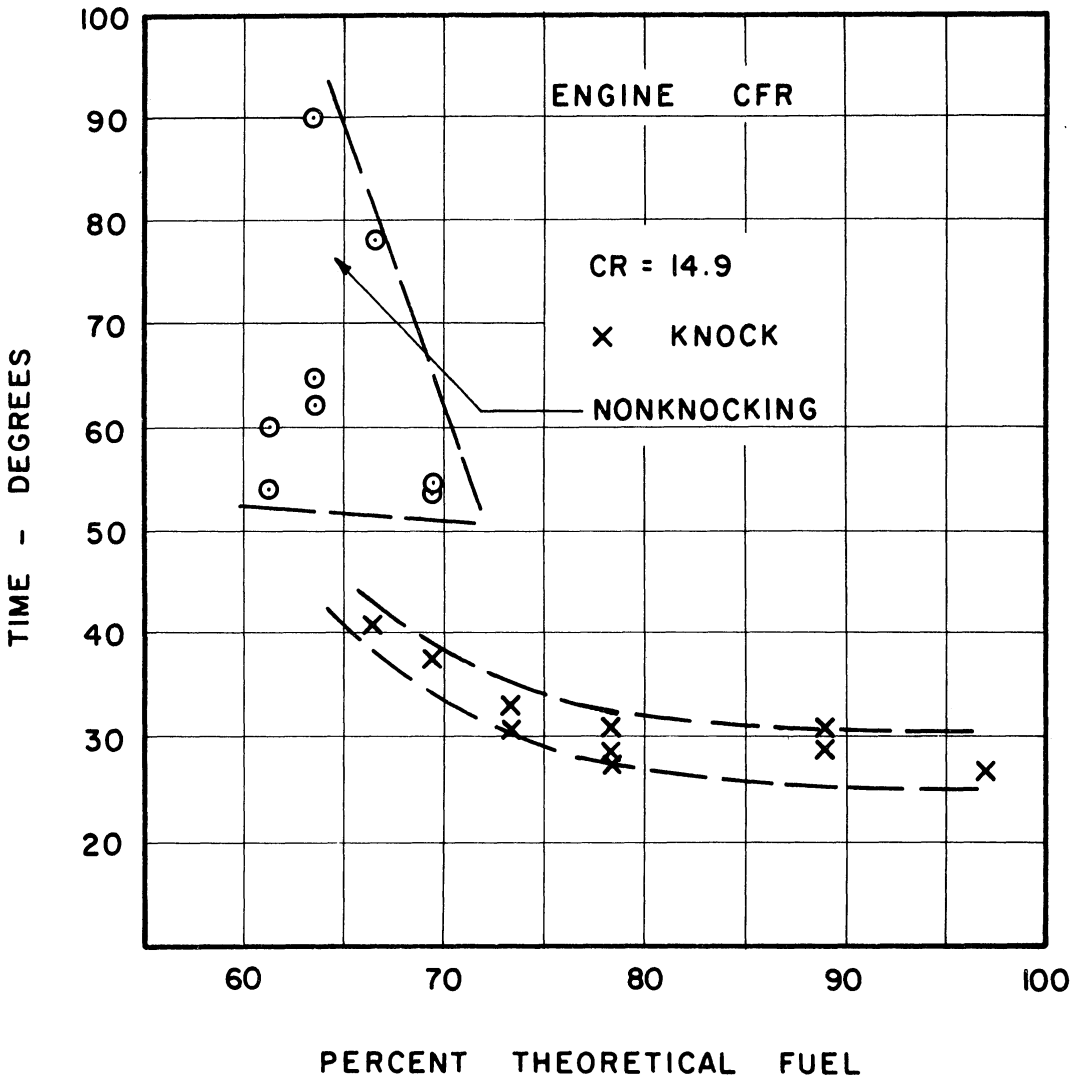

Figure 5.24 Duration of Pressure Rise Period.
Operating conditions same as in Figure 5.1.

CHAPTER VI

CONCLUSIONS AND RECOMMENDATIONS

A. Conclusions

1. The lean limits of flammability of light paraffin hydrocarbons in an engine are functions of the temperature of the reactants, as predicted by the lean limit equation.
2. The lean limits of light paraffins in an engine are not appreciably affected by changes in pressure.
3. The predicted lean limit fuel-air ratio was about 35 percent leaner than the point at which the engine began to misfire.
4. An increase in the inlet temperature or compression ratio of a spark-ignition engine results in the ability to burn a leaner mixture. The fuel-air ratio at the point of misfiring correlates with the compression temperature.
5. Conventional spark plug electrodes appear to quench very lean mixtures at ordinary gap settings.
6. The maximum thermal efficiency was obtained with a mixture containing 70 percent to 80 percent theoretical fuel, depending on the compression ratio. As the compression ratio was raised, the point of maximum efficiency was shifted toward leaner mixtures.
7. The maximum thermal efficiency at a given compression ratio was five percent higher than the thermal efficiency obtained with a stoichiometric mixture.
8. Combustion of lean mixtures in an engine is accompanied by a time delay of one to seven milliseconds between the occurence of the spark and the beginning of the pressure rise. The length

of the delay period increases when the mixture is made leaner, especially at low compression ratios.

9. The pressure rise following the delay period occurs in approximately seven to nine milliseconds, depending on the fuel-air ratio, in this type of engine at a speed of 1200 rpm.
10. The increased ignition advance required with lean mixtures is due principally to the increase in the delay period which occurs as the mixture is made leaner.
11. Cycle-to-cycle variations in pressure increase as the mixture is made leaner.
12. The exhaust temperature decreases as the mixture is made leaner.

B. Recommendations

1. The processes occurring during the pre-pressure or delay period should be studied. Observation of flame propagation in a quartz head engine and spectrographic analysis of the gases in the vicinity of the spark plug are suggested as techniques for this investigation.
2. Further study of the threshold temperature and its relationship to the mechanism of oxidation of hydrocarbons should be made.
3. Information on engine efficiency and other operating characteristics should be extended further into the lean mixture range by the use of hydrogen or hydrogen-propane mixtures as fuels.
4. The effect of lean mixtures on the amount of unburned hydrocarbon components in the exhaust should be investigated.
5. A method of cycle analysis that does not presuppose that the combustion process occurs instantaneously and at constant

volume should be developed and applied in high compression engines.

6. Cycle-to-cycle variations in the pattern of pressure development should be studied with respect to the effect of these variations on the thermal efficiency of the engine, and the factors causing these variations.

7. The effects of engine speed and charge turbulence on the lean limit should be studied.

APPENDIX A

RESIDUAL EXHAUST GAS

In order to calculate the amount of residual exhaust gas present in the charge and the temperature of the charge after mixing with the residual exhaust gas, the following assumptions will be made:

(1) Residual exhaust gas at exhaust temperature T_e and pressure P_e fills the clearance volume V_c at the beginning of the intake stroke.

(2) During the first part of the intake stroke, the residual exhaust gas expands isentropically to the intake pressure P_i, and a temperature T_r.

(3) Fresh mixture is drawn into the cylinder and mixed with the residual gas at constant pressure P_i for the remainder of the intake stroke.

(4) The gases involved are ideal, and have equal molecular weights and specific heats.

(5) All processes are adiabatic.

Under these assumptions, the expansion of the residual gas at the beginning of the intake stroke will follow the law

$$V_r = V_c \left(\frac{P_e}{P_i}\right)^{1/k} = V_c r_P^{1/k} \qquad (A.1)$$

The residual gases will then mix with the fresh mixture, as follows:

$$P_i = \frac{m_r \bar{R} T_r}{M V_r} = \frac{m_i \bar{R} T_i}{M V_i} = \frac{(m_r + m_i)\bar{R} T_c}{M r_V V_c} \qquad (A.2)$$

$$m_r C_P T_r + m_i C_P T_i = (m_r + m_i) C_P T_c \qquad (A.3)$$

By combining these equations,

$$V_i = V_c (r_V - r_P^{1/k}) \qquad (A.4)$$

The fraction of residual exhaust gas is

$$f = \frac{m_r}{m_r + m_i} = \frac{1}{1 + m_i/m_r} \qquad (A.5)$$

But

$$m_i = \frac{P_i V_i M}{\bar{R} T_i}, \qquad m_r = \frac{P_e V_c M}{\bar{R} T_e} \qquad (A.6)$$

$$\frac{m_i}{m_r} = \frac{P_i T_e V_i}{P_e T_i V_c} = \frac{r_T}{r_P}\left(\frac{V_i}{V_c}\right) \qquad (A.7)$$

From Equation (A.4):

$$\frac{m_i}{m_r} = \frac{r_T}{r_P}(r_V - r_P^{1/k}) = r_T\left(\frac{r_V}{r_P} - \frac{1}{r_p^{(k-1)/k}}\right) \qquad (A.8)$$

$$f = \frac{1}{1 + r_T\left(\frac{r_V}{r_P} - \frac{1}{r_p^{(k-1)/k}}\right)} \qquad (A.9)$$

The temperature of the charge T_c can be computed also.

$$m_r = \frac{P_e V_c M}{\bar{R} T_e} \qquad (A.10)$$

$$m_r + m_i = \frac{P_i r_V V_c M}{\bar{R} T_c} \qquad (A.11)$$

$$f = \frac{m_r}{m_r + m_i} = \frac{P_e T_c}{r_V P_i T_e} \qquad (A.12)$$

$$T = f r_V \frac{P_i}{P_e} T_e = \frac{r_V}{r_P} T_e \qquad (A.13)$$

APPENDIX B

THE FREE ENERGY OF COMBUSTION

1. Free Energy of Formation of Components at 25°C and 1 atm.;

   Data taken from Reference 108.

Compound	Phase	Free Energy ($\bar{g}°$) kcal./mole
CO_2	gas	-94.2598
C_3H_8	gas	-5.614
H_2O	gas	-54.6351
N_2	gas	0.0
O_2	gas	0.0

2. Free Energy of Components in a Mixture of Reactants or Products at 25°C and 1 atm.[107,109]:

   For the nth component:

$$\bar{g}_n = \bar{g}_n^{o} + \bar{R}T \ln x_n .$$

   The free energy of the mixture as a whole is

$$\bar{g} = \sum_n x_n \bar{g}_n .$$

3. Mole Fractions of Components in Mixtures of Reactants or Products:

$$C_3H_8 + (y + 23.8)\ \text{Air} \rightarrow 3CO_2 + 4H_2O + 18.8N_2 + y\ \text{Air}$$

$$4.76\ \text{Air} = O_2 + 3.76N_2$$

   y = a constant depending on fuel-air ratio.

   Molecular weight of C_3H_8 = 44.0

   Molecular weight of Air = 29.0

   The fraction of theoretical fuel is

$$\phi = \frac{44}{44 + 29(y + 23.8)} \doteq \frac{44}{44 + 29(23.8)}$$

Therefore, the constant y is

$$y = \left(\frac{29}{44} + 23.8\right)\left(\frac{1}{\phi} - 1\right).$$

Mole Fractions of Reactants:

$$C_3H_8 \qquad x = \frac{1}{y + 24.8}$$

$$O_2 \qquad x = \frac{y + 23.8}{4.76(y + 24.8)}$$

$$N_2 \qquad x = \frac{3.76(y + 23.8)}{4.76(y + 24.8)}$$

Mole Fractions of Products:

$$CO_2 \qquad x = \frac{3}{y + 25.8}$$

$$H_2O \qquad x = \frac{4}{y + 25.8}$$

$$O_2 \qquad x = \frac{y}{4.76(y + 25.8)}$$

$$N_2 \qquad x = \frac{18.8 + \frac{3.76}{4.76}\, y}{y + 25.8}$$

4. Total Number of Moles per Mole of Fuel:

Moles of Reactants = $y + 24.8$

Moles of Products = $y + 25.8$

TABLE IV

LEAN-LIMIT DATA FOR SEVERAL HYDROCARBONS

Fuel	% Fuel by Volume	Mixture Temperature T_R	Weight Fraction of Fuel F_L	Dimensionless Temperature T_R/T_T	Dimensionless Heating Value $-F_L h_{RP}/C_P T_T$	Reference
	%	°R	-	-	-	
CH_4	6.3	522.6	.0357	.185	.790	47
	6.2	582	.0352	.188	.780	
	5.95	672	.0338	.217	.749	
	5.75	762	.0326	.246	.722	
	5.50	852	.0312	.275	.691	
	5.30	942	.0299	.302	.662	
	5.10	1032	.0289	.333	.640	
	4.90	1122	.0277	.361	.614	
	4.80	1212	.0271	.391	.600	
CH_4	6.0	528	.0340	.1705	.754	42
	5.45	672	.0308	.217	.720	
	5.05	852	.0286	.275	.633	
	3.65	1392	.0204	.449	.452	
	3.25	1752	.0182	.566	.403	
CH_4	5.5	528	.0312	.1705	.691	30
	5.3	672	.0299	.217	.662	
	5.0	852	.0282	.275	.625	
	4.9	1032	.0277	.333	.613	
	4.7	1212	.0256	.391	.567	
	3.9	1392	.0219	.449	.485	
C_5H_{12}	1.53	522.6	.0372	.1685	.841	47
	1.50	582	.0365	.188	.825	
	1.44	672	.0351	.217	.794	
	1.39	762	.0339	.246	.767	
	1.34	852	.0327	.275	.739	
	1.30	942	.0318	.302	.709	
	1.22	1032	.0298	.333	.624	
C_6H_{14}	1.26	538.8	.0365	.174	.817	48
	1.22	672	.0353	.217	.788	
	1.18	762	.0342	.246	.764	
	1.14	852	.0331	.275	.740	
C_7H_{16}	1.05	538.8	.0354	.174	.790	48
	1.02	672	.0345	.217	.770	
	.99	762	.0334	.246	.747	
	.95	852	.0322	.275	.719	
C_8H_{18}	.96	538.8	.0368	.174	.821	48
	.93	672	.0357	.217	.796	
	.90	762	.0345	.246	.770	
	.86	852	.0330	.275	.735	
C_9H_{20}	.81	672	.0348	.217	.776	48
	.76	762	.0327	.246	.730	
	.71	852	.0316	.275	.704	

TABLE V

EFFECT OF ENGINE VARIABLES
ON LEAN LIMIT IN A CFR ENGINE

Split Head CFR Engine
Commercial Propane Fuel
Ignition Timing 19° B.T.C.
Exhaust Pressure 16 psia.

Run	r_V	T_i	T_e	rpm.	$\dot{W}_f$	$\dot{W}_a$	FA	P_i	f	F	T_c	T_R	T_R/T_T	$\frac{-FhRP}{CPTT}$
		°R.	°R.		lb/hr.	lb/hr.		psia.			°R.	°R.		
295	7	561	1814	1187	1.22	29.4	.0415	11.5	.0701	.0371	641	1320	.426	.834
296	10	561	1725	1214	1.15	29.4	.0392	11.7	.0482	.0361	611	1430	.462	.812
297	13	560	1375	1197	1.09	29.4	.0370	11.5	.0462	.0341	592	1525	.492	.767
298	16	560	873	1214	1.02	29.4	.0346	11.3	.0583	.0315	573	1600	.516	.707
280	7	610	1796	1205	1.20	29.4	.0410	12.0	.0740	.0366	688	1415	.452	.824
299	10	611	1678	1198	1.115	29.4	.0379	12.0	.0523	.0347	658	1540	.497	.781
281	13	613	1240	1207	1.03	29.4	.0352	12.0	.0532	.0322	644	1660	.535	.725
282	16	612	851	1183	.968	29.4	.0329	11.7	.0625	.0298	625	1745	.563	.671
286	7	648	1815	1211	1.15	29.4	.0393	12.3	.0740	.0352	722	1485	.479	.792
285	10	648	1712	1197	1.09	29.4	.0372	12.3	.0529	.0340	697	1630	.526	.765
288	10	648	1428	1218	1.06	29.5	.0359	11.7	.0667	.0324	695	1625	.524	.730
289	13	648	1036	1190	.987	29.5	.0334	11.7	.0681	.0301	667	1725	.555	.678
284	13	646	1124	1205	.995	29.4	.0338	12.3	.0595	.0308	667	1725	.555	.694
283	16	646	857	1218	.915	29.4	.0311	12.3	.0617	.0284	653	1820	.587	.640
294	7	762	1662	1194	1.065	29.5	.0361	13.3	.0862	.0319	835	1800	.581	.718
293	10	760	1219	1192	.975	29.5	.0330	13.3	.0778	.0295	790	1990	.642	.664
292	13	762	1002	1199	.883	29.5	.0299	13.3	.0719	.0270	779	2170	.700	.608
306	9.2	559	1750	1196	.87	21.4	.0407	7.0	.0908	.0358	638			
302	9.2	558	1830	1204	1.16	29.1	.0399	9.8	.0603	.0362	624			
303	9.2	561	1700	1200	1.545	40.3	.0383	13.1	.0477	.0353	612			
304	9.2	564	1520	1190	1.94	51.5	.0377	16.3	.0423	.0349	603			
305	9.2	560	1320	1208	2.37	62.6	.0379	19.4	.0403	.0352	590			

TABLE VI

PERFORMANCE DATA

Split-Head CFR Engine
Commercial Propane Fuel
Compression Ratio = 5.5

Run	IGN	W_f	$\dot{W}_a$	FA	F	T_i	T_e	P_i	rpm.	BHP.	FHP.	IHP.	η_H	η_G
	°B.T.C.	lb/hr.	lb/hr.	-	%	°F	°F	in. Hg abs.	-	-	-	-	%	%
424	34	1.71	29.0	.0589	92.6	99	1432	19.4	1204	1.95	1.99	3.94	29.3	28.8
425	40	1.60	29.0	.0552	87.1	100	1383	19.3	1199	1.75	1.99	3.74	29.7	29.2
427	41	1.635	29.0	.0560	88.3	101	1400	19.1	1199	1.80	2.00	3.80	29.6	29.0
428	35	1.82	29.0	.0624	97.7	101	1458	19.2	1201	2.14	2.00	4.14	28.9	28.6
429	37	1.71	29.0	.0586	92.2	100	1405	19.2	1200	1.94	2.00	3.94	29.3	28.8
430	47	1.57	29.0	.0538	84.9	101	1350	19.2	1202	1.72	2.00	3.72	30.1	29.6
431	51	1.49	29.0	.0511	80.9	100	1323	19.1	1200	1.52	2.00	3.52	30.0	29.5
432	65	1.415	29.0	.0485	77.0	100	1280	19.0	1200	1.32	2.00	3.32	29.8	29.2
433	65	1.365	29.0	.0468	74.5	100	1205	19.0	1200	1.08	2.00	3.08	28.7	27.9

TABLE VII

PERFORMANCE DATA

Split-Head CFR Engine
Commercial Propane Fuel
Compression Ratio = 7.0

Run	IGN.	$\dot{W}_f$	$\dot{W}_a$	FA	F	T_i	T_e	P_i	rpm.	BHP.	FHP.	IHP.	η_H	η_G
	°B.T.C.	lb/hr.	lb/hr.		%	°F	°F	in. Hg abs.					%	%
417	36	1.60	29.0	.0551	87.0	100	1291	19.0	1200	2.00	2.08	4.08	32.5	31.9
418	41	1.495	29.0	.0516	81.7	100	1250	19.0	1202	1.76	2.09	3.85	32.8	32.1
419	28	1.73	29.0	.0597	93.8	100	1362	19.2	1200	2.30	2.10	4.40	32.4	31.9
420	43	1.395	29.0	.0481	76.4	100	1226	18.9	1200	1.52	2.10	3.62	33.1	32.4
421	53	1.355	29.0	.0460	73.2	100	1183	18.9	1200	1.42	2.10	3.52	33.1	32.3
422	60	1.315	29.0	.0454	72.3	100	1170	18.9	1200	1.26	2.10	3.36	32.5	31.7
423	62	1.275	29.0	.0440	70.2	100	1192	18.9	1202	1.08	2.10	3.18	31.7	30.9

TABLE VIII

PERFORMANCE DATA

Split-Head CFR Engine
Commercial Propane Fuel
Compression Ratio = 10

Run	IGN	$\dot{W}_f$	$\dot{W}_a$	FA	F	T_i	T_e	P_i	rpm.	BHP.	FHP.	IHP.	η_H	η_G
	°B.T.C.	lb/hr.	lb/hr.	-	%	°F	°F	in. Hg abs.	-	-	-	-	%	%
400	28	1.47	29.35	.0501	79.4	99	1167	19.4	1200	2.04	2.16	4.20	36.2	35.4
401	24	1.70	29.35	.0579	91.1	100	1244	19.5	1199	2.62	2.16	4.78	35.7	35.5
402	50	1.15	29.35	.0392	62.8	101	1086	19.1	1200	.80	2.18	2.98	32.9	32.0
403	48	1.21	29.35	.0412	65.9	100	1047	19.2	1203	1.22	2.19	3.41	35.8	35.0
404	45	1.25	29.35	.0426	68.0	100	1050	19.2	1202	1.40	2.19	3.59	36.5	35.7
405	37	1.34	29.35	.0457	72.8	100	1087	19.1	1199	1.66	2.18	3.84	36.4	35.7
406	25	1.58	29.35	.0539	85.2	100	1200	19.4	1200	2.32	2.16	4.48	36.1	35.4

TABLE IX

PERFORMANCE DATA

Split-Head CFR Engine
Commercial Propane Fuel
Compression Ratio = 13

Run	IGN	$\dot{W}_f$	$\dot{W}_a$	FA	F	T_i	T_e	P_i	rpm.	BHP.	FHP.	IHP.	η_H	η_G
	°B.T.C.	lb/hr.	lb/hr.	-	%	°F	°F	in. Hg abs.	-	-	-	-	%	%
407	31	1.35	29.35	.0461	73.4	100	1047	19.2	1200	1.82	2.32	4.14	39.0	38.1
408	43	1.135	29.35	.0387	62.0	100	1044	19.0	1202	.74	2.32	3.06	34.3	33.5
409	45	1.20	29.35	.0409	65.4	100	981	19.2	1199	1.22	2.32	3.64	38.6	37.5
410	41	1.24	29.35	.0423	67.6	100	993	19.2	1198	1.48	2.30	3.78	38.8	37.8
411	24.5	1.445	29.35	.0493	78.2	100	1112	19.4	1199	2.12	2.28	4.40	38.8	38.0
412	20	1.555	29.35	.0530	83.8	100	1159	19.6	1200	2.40	2.28	4.68	38.3	37.7
413	16.5	1.69	29.35	.0577	90.8	100	1221	19.7	1200	2.70	2.26	4.96	37.3	36.6
414	41	1.22	29.0	.0421	67.2	101	994	18.9	1201	1.40	2.30	3.70	38.7	37.6
415	47	1.18	29.0	.0407	65.1	100	960	18.9	1201	1.30	2.28	3.58	38.2	37.6
416	56	1.15	29.0	.0397	63.6	100	930	18.9	1204	1.13	2.29	3.42	37.9	36.9

TABLE X

PERFORMANCE DATA

Split-Head CFR Engine
Commercial Propane Fuel
Compression Ratio = 14.9

Run	IGN	$\dot{W}_f$	$\dot{W}_a$	FA	F	T_i	T_e	P_i	rpm.	BHP.	FHP.	IHP.	η_H	η_G
	°B.T.C.	lb/hr.	lb/hr.	-	%	°F	°F	in. Hg abs.	-	-	-	-	%	%
357	11	1.80	29.2	.0616	96.6	102	1238	-	1199	3.14	2.18	5.32	38.4	37.7
358	40	1.115	29.2	.0382	61.3	101	998	-	1200	.72	2.18	2.90	34.5	33.6
359	14	1.65	29.2	.0565	89.0	101	1149	-	1201	2.76	2.16	4.92	38.9	38.1
360	41	1.155	29.2	.0396	63.4	101	950	18.8	1202	1.20	2.19	3.39	38.7	37.7
362	37	1.215	29.2	.0416	66.5	100	960	18.8	1199	1.50	2.20	3.70	40.0	38.8
363	30	1.27	29.2	.0435	69.4	100	991	18.8	1198	1.68	2.22	3.90	40.3	39.3
364	25	1.36	29.2	.0461	73.4	100	991	19.0	1202	1.99	2.22	4.21	40.5	39.6
365	20.5	1.44	29.2	.0493	78.2	99	1055	19.1	1202	2.21	2.22	4.43	40.2	39.2

TABLE XI

COMBUSTION PRESSURE DELAY AND RISE TIME
DATA FROM PRESSURE INDICATOR DIAGRAMS

Split-Head CFR Engine
Speed.....1200 rpm.
Intake Pressure .....10 psia.
Intake Temperature.....100°F.
Ignition Timing.....M.B.T.
Fuel.....Commercial Propane

θ_I Time of Spark - Degrees from T.D.C.
θ_1 Time of Occurence of 4% Pressure Rise - Degrees from T.D.C.
θ_2 Time of Occurence of 96% Pressure Rise - Degrees from T.D.C.
θ_D Pressure Delay Period ($\theta_1 - \theta_I$) - Degrees
θ_R Pressure Rise Period ($\theta_2 - \theta_1$) - Degrees

Compression Ratio = 5.5

Run	F. %	θ_I	θ_1	θ_2	θ_D	θ_R
428	97.7	-35	-25	18	10	43
		-35	-20	22	15	42
		-35	-15	27	20	42
				Av.	15	42
429	92.2	-37	-15	34	22	49
		-37	-10	38	27	48
				Av.	25	48.5
427	88.8	-41	-20	32	21	52
		-41	-12	50	28	62
				Av.	25	57
430	84.9	-47	-22	27	25	49
		-47	-15	27	32	42
		-47	-10	30	37	40
				Av.	31	44
431	80.9	-51	-19	25	32	44
		-51	-18	27	33	45
		-51	- 5	35	46	40
		-51	- 5	45	46	50
				Av.	39	45

TABLE XI (continued)

COMBUSTION PRESSURE DELAY AND RISE TIME
DATA FROM PRESSURE INDICATOR DIAGRAMS

Compression Ratio = 5.5

Run	F, %	θ_I	θ_1	θ_2	θ_D	θ_R
432	77.0	-65	-25	20	40	45
		-65	-25	23	40	48
		-65	-22	23	43	45
		-65	-22	40	43	62
				Av.	42	50
433	74.5	-65	-15	30	50	45
		-65	-15	43	50	58
		-65	- 5	60	60	65
		-65	- 5	60	60	65
				Av.	55	58
Compression Ratio = 7.0						
419	93.8	-28	-13	33	15	46
		-28	-13	35	15	48
				Av.	15	47
417	87.0	-36	-14	26	22	40
		-36	-14	26	22	40
				Av.	22	40
418	81.7	-41	-20	22	21	42
		-41	-13	30	28	43
				Av.	25	42.5
420	76.4	-43	-23	22	20	45
		-43	- 5	52	38	57
				Av.	29	51
421	73.2	-52	-20	35	33	55
		-52	- 8	37	41	45
				Av.	37	50
422	72.3	-60	-18	28	42	46
		-60	-12	38	48	50
		-60	- 5	70	55	75
				Av.	48	57

TABLE XI (continued)

COMBUSTION PRESSURE DELAY AND RISE TIME
DATA FROM PRESSURE INDICATOR DIAGRAMS

Run	F %	θ_I	θ_1	θ_2	θ_D	θ_R
Compression Ratio = 10						
401	91.1	-24	-15	23	9	38
		-24	-15	28	9	43
		-24	-15	29	9	44
				Av.	9	42
406	85.2	-25	-14	23	11	37
		-25	-14	27	11	41
				Av.	11	39
400	79.4	-28	-16	30	12	46
		-28	-13	40	15	53
		-28	-13	40	15	53
				Av.	14	51
405	72.8	-37	-17	30	20	47
		-37	-14	33	23	47
				Av.	22	47
404	68.0	-45	-22	32	23	54
		-45	-15	33	30	48
				Av.	27	51
403	65.9	-48	-23	23	25	46
		-48	-15	43	33	58
				Av.	29	52
402	62.8	-50	-24	22	26	46
		-50	-15	43	35	58
				Av.	30	52
Compression Ratio = 13						
413	90.8	-16.5	- 5	30	11.5	35
		-16.5	- 5	31	11.5	36
		-16.5	- 5	32	11.5	37
				Av.	11.5	36

TABLE XI (continued)

COMBUSTION PRESSURE DELAY AND RISE TIME
DATA FROM PRESSURE INDICATOR DIAGRAMS

Compression Ratio = 13

Run	F %	θ_I	θ_1	θ_2	θ_D	θ_R
412	83.8	-20	-10	30	10	40
		-20	-10	39	10	49
				Av.	10	44.5
411	78.2	-24.5	-13	22*	11.5	35*
		-24.5	-13	42	11.5	55
				Av.	11.5	
407	73.4	-31	-12	42	19	54
		-31	-17	30*	14	47*
				Av.	16.5	
414	67.2	-41	-20	20*	21	40*
		-41	-20	30	21	50
				Av.	21	
415	65.1	-47	-26	35	21	61
		-47	-26	45	21	71
				Av.	21	66
416	63.6	-56	-22	25	34	65
		-56	-13	50	43	63
				Av.	38	64

Compression Ratio = 14.9

357	96.6	-11	- 4	23*	7	27*
359	89.0	-14	- 6	23*	8	29*
		-14	- 6	25*	8	31*
				Av.	8	
365	78.2	-20.5	- 6	22*	14.5	28*
		-20.5	- 6	22*	14.5	28*
		-20.5	- 6	27*	14.5	33*
				Av.	14.5	

* Detonation occurred

TABLE XI (continued)

COMBUSTION PRESSURE DELAY AND RISE TIME
DATA FROM PRESSURE INDICATOR DIAGRAMS

Compression Ratio = 14.9

Run	F %	θ_I	θ_1	θ_2	θ_D	θ_R
364	73.4	-25	-12	19*	13	31*
		-25	-14	19*	11	33*
				Av.	12	
363	69.4	-30	-14	24*	16	38*
		-30	-12	42	18	54
		-30	-12	42	18	54
				Av.	18	
362	66.5	-37	-13	28*	24	41*
		-37	-13	65	24	78
				Av.	24	
360	63.4	-41	-12	50	29	62
		-41	-12	53	29	65
		-41	-12	180(?)	29	?
				Av.	29	63
358	61.3	-40	-10	44	30	54
		-40	-10	50	30	60
				Av.	30	57

* Detonation occurred

TABLE XII

AIR METER CALIBRATION

Room Temperature-at air tank 74°F.
Barometric Pressure 14.22 psia.
Tank Capacity 9.80 cu. ft.
or .706 lb. air at 74°F.
Air Temperature at Nozzle 72°F.
Nozzle Constant = $\frac{W_a\sqrt{T}}{P}$ $\frac{\text{lb/hr.}}{\text{psia.}}$ $(°R)^{1/2}$

Nozzle Number	Time	Nozzle Pressure	Flow Rate	Nozzle Constant	Nozzle Constant
-	Min.	psia.	lb/hr.	-	Avg.
1	4.335	54.22	9.69	4.13	4.15
1	2.496	94.22	17.0	4.17	
2	2.997	39.2	14.13	8.33	
2	1.834	64.0	23.10	8.34	8.33
2	1.837	64.0	23.06	8.33	
2	1.268	94.0	33.41	8.22	
2	1.260	94.0	33.62	8.27	
3	1.459	39.2	29.03	17.11	17.1
3	1.456	39.2	29.09	17.15	
3	.893	64.2	47.44	17.08	
3	.893	64.1	47.44	17.10	
3	.679	84.3	62.38	17.10	
3	.679	84.3	62.38	17.10	
4	.755	39.7	56.11	32.66	32.6
4	.756	39.7	56.03	32.62	
4	.610	49.2	69.44	32.62	
4	.611	49.2	69.33	32.57	
4	.508	59.2	83.38	32.55	
4	.506	59.3	83.72	32.63	
4	.355	84.1	119.3	32.78	
4	.354	84.1	119.7	32.89	
5	.369	39.0	114.8	68.02	67.6
5	.328	44.1	129.1	67.65	
5	.268	54.2	158.1	67.41	
5	.226	64.1	187.4	67.56	

TABLE XIII

FUEL ORIFICE CALIBRATION

Orifice Constant = $\dot{W}_f \sqrt{\frac{T}{Ph}}$

Date of Test	Weight of Fuel Used	Flow Time	Flow Rate	Average Fuel Pressure	Average Pressure Difference at Orifice	Average Fuel Temp.	Orifice Constant K_o
	lb.	min.	lb/hr.	psia.	in. H_2O	°R.	
10-19-59	.905	36.3	1.493	45.76	9.27	616	1.80
1- 3-60	1.00	35.4	1.695	46.54	11.94	618.5	1.785
1-19-60	1.00	39.9	1.505	44.5	9.95	619	1.78
2- 1-60	1.20	46.5	1.55	46.5	10.08	619.2	1.79
3-15-60	.40	15.75	1.524	44.4	10.05	615	1.785

TABLE XIV

FREE ENERGY OF COMBUSTION OF PROPANE-AIR MIXTURES

ϕ		1.0	0.9	0.8	0.7	0.6
y		0	2.81	6.32	10.9	16.9
Mole Fractions of Reactants	C_3H_8	.0403	.0362	.0321	.0280	.0240
	O_2	.2015	.2024	.2034	.2041	.2050
	N_2	.7582	.7614	.7645	.7679	.7710
Free Energy of Reactants kcal. per Mole Fuel		-15.34	-16.25	-17.39	-18.86	-20.77
Mole Fractions of Products	CO_2	.1163	.1048	.0934	.0817	.0703
	H_2O	.1550	.1398	.1253	.1090	.0937
	O_2	.0000	.0206	.0413	.0624	.0831
	N_2	.7287	.7348	.7400	.7469	.7529
Free Energy of Products kcal. per Mole Fuel		-513.0	-515.0	-517.2	-519.6	-522.3
Change in Free Energy kcal. per Mole Fuel		-497.7	-498.7	-499.8	-500.8	-501.5
Change in Free Energy BTU. per lb. Fuel		-20,360	-20,403	-20,444	-20,488	-20,514

BIBLIOGRAPHY

Engine Characteristics

1. Burstall, A. F., "Experiments on the Behavior of Various Fuels in a High Speed Internal Combustion Engine," Proc. Inst. Auto. Engr. 22:358, 1927.

2. Burstall, A. F., "Experiments on the Power and Efficiency of the High Speed Gas Engine," Proc. Inst. Auto. Engr., 19:620, 1930.

3. Caris, D. F., and Nelson, E. E., "A New Look at High Compression Engines," SAE Trans. 67:112, 1959.

4. David, W. T., and Leah, A. S., "Fuel Economy in Petrol Engines," Jour. and Proc. Inst. Mech. Engr. 143:289, 1940.

5. Gish, R. E.; McCullough, J. D.; Retzloff, J. B.; and Mueller, H. T., "Determination of True Engine Friction," SAE Trans. 66:649, 1958.

6. Goodenough, G. A., and Baker, J. B., A Thermodynamic Analysis of Internal Combustion Cycles, University of Illinois Experiment Station, Bulletin No. 160, 1927.

7. Hopkinson, B., "The Effect of Mixture Strength and Scavenging on Thermal Efficiency," Proc. Inst. Mech. Engr., 1908, p. 417.

8. Hottel, H. C., and Eberhardt, J. E., "A Mollier Diagram for the Internal-Combustion Engine," Chem. Rev. 21:439, 1937.

9. Hottel, H. C.; Williams, G. C.; and Satterfield, C. N., Thermodynamic Charts for Combustion Processes, John Wiley and Sons, Inc., New York, 1949.

10. Hottel, H. C., and Williams, G. C., Charts of Thermodynamic Properties of Fluids Encountered in Calculations of Internal Combustion Engine Cycles, NACA TN-1026, 1946.

11. Kettering, C. F., "More Efficient Utilization of Fuels," SAE Quarterly Trans. 1:669, 1947.

12. Leah, A. S., "Ideal Efficiencies of Otto-Cycle Engines," The Engineer 188:665, 1949.

13. Livengood, J. C.; Rona, J. P.; and Baruch, J. J., "Ultrasonic Temperature Measurement in Internal Combustion Engine Chamber," Jour. Acoust. Soc. Amer. 26:824, 1954.

14. Livengood, J. C.; Taylor, C. F.; and Wu, P. C., "Measurement of Gas Temperature in an Engine by the Velocity of Sound Method," SAE Trans. 66:683, 1958.

15. McCann, W. J., Thermodynamic Charts for Internal Combustion Engine Fluids, NACA TN-1883, 1949.

16. Marvin, C. F., Combustion Time in the Engine Cylinder and Its Effect on Engine Performance, NACA TR-276, 1927.

17. Obert, E. F., Internal Combustion Engines, International Textbook Co., Scranton, Pa., 1952.

18. Paul, W. H., and Humphreys, I. B., "Humphreys Constant-Compression Engine," SAE Quarterly Trans. 6:259, 1952.

19. Rassweiler, G. M.; Withrow, L.; and Cornelius, W., "Engine Combustion and Pressure Development," SAE Jour. 46:275, 1946.

20. Ricardo, H. R., "The Influence of Various Fuels on the Performance of Internal Combustion Engines," Proc. Inst. Auto. Engr., 18, part 1, 51, (1929).

21. Schmidt, F. A. F., Verbrennungsmotoren, Julius Springer, Berlin, 1939.

22. Streeter, R. L., and Lichty, L. C., Internal Combustion Engines, McGraw-Hill, Inc., New York, 1933, 4th ed.

23. Taylor, C. F., The Internal Combustion Engine In Theory and Practice, Wiley and Sons, Inc., New York, 1960.

24. Tizard, H. T., and Pye, D. R., "The Character of Various Fuels for Internal Combustion Engines," The Automobile Engineer 11:55, 99, 134; 1921.

25. von Bennigsen, G., "Einfluss von Anlasshilfen beim Klein-Dieselmotor mit ungeteiler Brennkammer," Motortechnische Zeitschrift 19:175, 1958.

Limits of Flammability

26. Belles, F. E., and Swett, C. C., "Ignition and Flammability Limits of Hydrocarbons," Basic Considerations in the Combustion of Hydrocarbon Fuels with Air, NACA Report No. 1300, 83, (1957).

27. Berl, E., and Fischer, H., "Unsuchungen an Explosibilen Gas-und Dampf-Luft-Gemischen," Zeitschrift für Electrochemie 30:29, 1924.

28. Bone, W. A., and Townend, D. T. A., Flames and Combustion in Gases, Longmans, Green, and Co., London, 1927.

29. Briand, M.; Dumanois, P.; and Lafitte, P., "The Influence of Temperature on the Limits of Inflammability of Some Combustible Vapors," Compte Rendus de Academie des Science 197:322, 1933.

30. Burrell, G. A., and Robertson, I. W., "Effects of Temperature and Pressure on the Explosibility of Methane-Air Mixtures," U.S. Bur. Mines, Tech. Paper 126, 1916.

31. Burgess, M. J., and Wheeler, R. V., "The Lower Limit of Inflammability of Mixtures of the Paraffin Hydrocarbons with Air," Jour. Chem. Soc. 99:2013, 1911.

32. Burgoyne, J. H., and Williams-Leir, G., "Limits of Inflammability of Gases," Fuel 27-28:118, 1948-49.

33. Coward, H. F., and Jones, G. W., "Limits of Inflammability of Gases and Vapors," U.S. Bureau of Mines Bulletin 503, 1952.

34. Crussard, L., "Limites d'inflammabilite et retard specifique d'inflammation," Compte Rendus de Academie des Science 158:340, 1914.

35. Davy, H., "On the Fire-damp of Coal Mines," Phil. Trans. Royal Soc. London, 1816, p. 1.

36. Davy, H., "Some Researches on Flame," Phil. Trans. Royal Soc. London 107:45, 1817.

37. Egerton, A. C., "Limits of Inflammability," Fourth International Symposium on Combustion, Williams and Wilkins, Baltimore, 1953.

38. Egerton, A., and Powling, J., "The Limits of Flame Propagation at Atmospheric Pressure: 2. The Influence of Changes in the Physical Properties," Proc. of the Royal Soc. of London A 193:190, 1948.

39. Egerton, A. C., and Thabet, S. K., "Flame Propagation: the Measurement of Burning Velocities of Slow Flames and the Determination of Limits of Combustion," Proc. Royal Soc. London A 211:445, 1952.

40. LeChatelier, H., and Boudouard, O., "Sur les limities d'inflammabilite de l'oxyde de carbone," Compte Rendus de Acadamie des Science 126:1344, 1898.

41. LeChatelier, H., and Boudouard, O., "Sur les limities d'inflammabilite des vapours combustibles," Compte Rendus de Academie des Science 126:1510, 1898.

42. Mason, W., and Wheeler, V. W., "The Effect of Temperature and of Pressure on the Limits of Inflammability of Mixtures of Methane and Air," Jour. Chem. Soc. 113:45, 1918.

43. Matson, A. F., and Dufour, R. E., The Lower Limit of Inflammability and the Autogenous Ignition Temperature of Certain Common Solvent Vapors Encountered in Ovens, Underwriters Laboratories Bulletin of Research No. 43, 1950.

44. Nagai, Y., "The Effect of Pressure on the Limits of Inflammability and the Average Life-Period of Activated Molecules in Combustion," Jour. Faculty of Engr., Tokyo Imp. Univ., 17:89, 1927.

45. Roszkowski, J., "Ueber die Einwirkung der Temperatur auf die Explosionsgrenzen brenbarer Gasmischen," Jour. für Gasbeleuchten und Wasserversorgung 33:491, 527, 535, 553; 1890.

46. Terres, E., and Plentz, F., "Über den Einfluss des Druckes auf die Verbrennung explosiver Gas-Luftmischung," Jour. für Gasbeleuchtung und Wasserversorgung 57:990, 1016, 1024; 1914.

47. White, A. G., "Limits for the Propagation of Flame in Inflammable Gas-Air Mixtures: Part III: The Effect of Temperature on the Limits," Jour. Chem. Soc. 127:672, 1925.

48. Zabetakis, M. G.; Scott, G. S.; and Jones, G. W., "Limits of Flammability of Paraffin Hydrocarbons in Air," Ind. and Engr. Chem. 43:2120, 1951.

Flame Propagation

49. Anderson, J. W., and Fein, R. S., "Measurement of Normal Burning Velocities and Flame Temperatures of Bunsen Flames," Jour. Chem. Phys. 17:1268, 1949.

50. Burgess, M. J., and Wheeler, R. V., "The Lower Limit of Inflammability of Mixtures of the Paraffin Hydrocarbons with Air," Jour. Chem. Soc. 99:2013, 1911.

51. Daniell, P. J., "The Theory of Flame Motion," Proc. Royal Soc. London A 193:393, 1930.

52. Dixon, H. B., and Coward, H. F., "The Ignition Temperatures of Gases," Jour. Chem. Soc. 95:515, 1909.

53. Dixon-Lewis, G., "Temperature Distribution in Flame Reaction Zones," Fourth International Symposium on Combustion, p. 263, Williams and Wilkins, Baltimore, 1953.

54. Dugger, G. L.; Simon, D. M.; and Gerstein, M., "Laminar Flame Propagation," Basic Considerations in the Combustion of Hydrocarbon Fuels with Air, NACA Report No. 1300, p. 127, 1957.

55. Friedman, R., "Measurement of the Temperature Profile in a Laminar Flame," Fourth International Symposium on Combustion, 259, Williams and Wilkins, Baltimore, 1953.

56. Friedman, R., and Burke, E., "Measurement of Temperature Distribution in a Low-Pressure Flat Flame," Jour. Chem. Phys. 22:824, 1954.

57. Fristrom, R. M.; Prescott, R.; Neumann, R. K.; and Avery, W. H., "Temperature Profiles in Propane-Air Flame Fronts," Fourth International Symposium on Combustion, 267, Williams and Wilkins, Baltimore, (1953).

58. Jost, W., Explosion and Combustion Processes in Gases, McGraw-Hill, Inc., New York, 1946.

59. Lewis, B., and von Elbe, G., Combustion, Flames, and Explosions of Gases, Academic Press, Inc., New York, 1951.

60. Linnet, J. W., "Some Experimental Results Relating to Laminar Flame Propagation," Selected Combustion Problems, Butterworths Scientific Publications, London, 1954.

61. McDavid, J. W., "The Temperature of Ignition of Gaseous Substances," Trans. Chem. Soc. 111:1003, 1917.

62. Mallard, M. E., "De la vistesse d'inflammation I'un melange d'air et de grisou," Annales des mines, ser. 7, 7:355, 1875.

63. Mallard, M. E., and LeChatelier, H., ("Experimental and Theoretical Researches on the Combustion of Explosive Gas Mixtures,") Annales des mines, ser 8, 4:274, 1883.

64. Nusselt, W., "Die Zundgeschwindigkeit brennbarer Gasgemische," Zeitschrift dis Vereines deutscher Ingeneer 59:892, 1915.

65. Silver, R. S., "The Ignition of Gaseous Mixtures by Hot Particles," Phil. Mag., Ser. 7, 23:633, 1937.

66. Weir, A.; Morrison, R. B.; and Adamson, T. C., Combustion, University of Michigan, 1956.

67. Wheeler, R. V., "The Propagation of Flame in Mixtures of Methane and Air. The 'Uniform Motion,'" Jour. Chem. Soc. 105:2607, 1914.

Spark Ignition

68. Belles, F. E., and Swett, C. C., "Ignition and Flammability Limits of Hydrocarbons," Basic Considerations in the Combustion of Hydrocarbon Fuels with Air, NACA Report No. 1300, 83, (1957).

69. Blanc, M. V.; Guest, P. G.; von Elbe, G.; and Lewis, B., "Ignition of Explosive Gas Mixtures by Electric Sparks," Jour. Chem. Phys. 15:798, 1947.

70. Bone, W. A., and Townend, D. T. A., Flames and Combustion in Gases, Longmans, Green, and Co., London, 1927.

71. Calcote, H. F., Gregory, C. A.; Barnett, C. M.; and Gilmer, R. B., "Spark Ignition. Effect of Molecular Structure," Ind. and Engr. Chem. 44:2656, 1952.

72. Fenn, John B., "Lean Flammability Limits and Minimum Spark Energy," Ind. and Engr. Chem. 43:2865, 1951.

73. Holm, J. M., "On the Initiation of Gaseous Explosions by Small Flames," Phil. Mag., Ser. 7, 14:18, 1932; 15:331, 1933.

74. Jost, W., Explosion and Combustion Processes in Gases, McGraw-Hill, Inc., New York, 1946.

75. Landau, H. G., "The Ignition of Gases by Local Sources," Chem. Rev. 21:245, 1937.

76. Metzler, A. J., Minimum Spark-Ignition Energies of 12 Pure Fuels at Atmospheric Pressure and Reduced Pressure, NACA RM-E53H31, 1953.

77. Morgan, J. D., Principles of Ignition, Pitman and Sons, Ltd., London, 1942.

78. Potter, A. E., and Berlad, A. L., A Relationship Between Burning Velocity and Quenching Distance, NACA TN-3882, 1956.

79. Potter, A. E., and Berlad, A. L., A Thermal Equation for Flame Quenching, NACA TR-1264, 1956.

80. Randolph, D. W., and Silsbee, F. B., Flame Speed and Spark Intensity, NACA TR-187, 1924.

81. Silsbee, F. B., The Sparking Voltage of Spark Plugs, NACA TR-202, 1925.

82. Swett, C. C., Investigation of Spark Gaps Subjected to Altitude and Air-Velocity Conditions, NACA RM-E9E17, 1949.

83. Swett, C. C., Spark Ignition of Flowing Gases: Part 1. Energies to Ignite Propane-Air Mixtures, NACA RM-E9E17, 1949.

84. Swett, C. C., Spark Ignition of Flowing Gases: Part 2. Effect of Electrode Parameters on Energy Required to Ignite a Propane-Air Mixture, NACA RM E51J12, 1951.

85. Swett, C. C., Spark Ignition of Flowing Gases: Part 5. Application of Fuel-Air Ratio and Initial Temperature Data to Ignition Theory, NACA RM-E55I16, 1955.

86. Swett, C. C., Spark Ignition of Flowing Gases, NACA TR-1287, 1956.

87. Taylor-Jones, E.; Morgan, J. D.; and Wheeler, R. V., "On the Form of the Temperature Wave Spreading by Conduction from Point and Spherical Sources," Lond. Phil. Mag., Ser. 6, 43:359, 1923.

88. von Elbe, G., "The Problem of Ignition," Fourth International Symposium on Combustion, 13, Williams and Wilkins, Baltimore, 1953.

"Pre-Pressure" Period

89. Bouchard, C. L.; Taylor, C. F.; and Taylor, E. S., "Variables Affecting Flame Speed in the Otto-Cycle Engine," SAE Trans. 41:514, 1937.

90. Brokaw, R. S., and Jackson, J. L., "Effect of Temperature, Pressure, and Composition on Ignition Delays for Propane Flames," Fifth International Symposium on Combustion, Rheinhold Pub. Corp., New York, 1955.

91. Burstall, A. F., "Experiments on the Power and Efficiency of the High Speed Gas Engine," Proc. Inst. Auto. Engr. 19:620, 1930.

92. David, W. T., "Turbulence in Internal Combustion Engines," The Engineer 164:733, 1937.

93. David, W. T., "The Process of Combustion in Spark Ignition Engines," The Engineer 169:509, 1940.

94. Ellis, O. C., and Wheeler, R. V., "The Movement of Flame in Closed Vessels: Afterburning," Jour. Chem. Soc., Feb. 1927, p. 310.

95. Judge, A. W., Modern Petrol Engines, Chapman and Hall, Ltd., London, 1955.

96. Maleev, V. L., Internal Combustion Engines, McGraw-Hill, Inc., New York, 1945.

97. Marvin, C. F., Combustion Time in the Engine Cylinder and Its Effect on Engine Performance, NACA TR-276, 1927.

98. Pye, D. R., The Internal Combustion Engine, Oxford University Press, London, 1931.

99. Ricardo, H. R., "Combustion in Diesel Engines," Proc. Inst. Auto. Engr. 24:645, 1930.

100. Shinn, J. N., Factors Affecting Unburned Hydrocarbons in Combustion Products, Ph.D. Dissertation, Yale University, 1956.

101. Withrow, L., and Boyd, T. A., "Photographic Flame Studies in an Engine," Ind. and Engr. Chem. 23:539, 1931.

102. Woodbury, C. A.; Lewis, H. A.; and Canby, A. J., "The Nature of Flame Movement in a Closed Cylinder," SAE Trans. 16, part 1, 465, (1921).

Measurement of Air Consumption

103. American Society of Mechanical Engineers, "Flow Measurement by Means of Standard Nozzles and Orifice Plates," ASME Power Test Code, Supplement on Instruments and Apparatus, Part 5, Chapter 4, 1959.

104. Buckland, B. O., "Fluid Meter Nozzles," ASME Trans. 56:827, 1934; 57:251, 1935.

105. Cornelius, W., and Caplan, J. D., "An Improved System for Control and Measurement of Air Consumption of a Single Cylinder Engine," SAE Quarterly Trans. 6:666, 1952.

106. Grace, H. P., and Lapple, C. E., "Discharge Coefficients of Small-Diameter Orifices and Flow Nozzles," Trans. ASME 73:639, 1951.

Miscellaneous References

107. Keenan, J. C., Thermodynamics, John Wiley and Sons, Inc., New York, 1941, p. 264 ff.

108. National Bureau of Standards, Selected Properties of Hydrocarbons, National Bureau of Standards Circular C461, 1947.

109. Van Wylen, G. J., Thermodynamics, John Wiley and Sons, Inc., New York, 1959.

110. Robison, J. A.; Behrens, M. D.; Mosher, R. G.; and Chandler, J. M., "New Research Tool Aids Combustion Analysis," SAE Jour. 66:53, Jan., 1958.